INVESTIGATING MITOCHONDRIAL DEOXYRIBONUCLEOTIDE METABOLISM AND ITS ROLE IN A FAMILY OF GENETIC DISEASES

By

VISHAL GANDHI

Dissertation

Submitted to the Faculty of the

Graduate School of Vanderbilt University

in partial fulfillment of the requirements

for the degree of

DOCTOR OF PHILOSOPHY

in

Human Genetics

December, 2011

Nashville, Tennessee

Approved:

Professor Scott Williams

Professor Tricia Thornton-Wells

Professor David Samuels

Professor Todd Hulgan

Professor Emmanuele DiBenedetto

ACKNOWLEDGEMENTS

Dr. David Samuels – research advisor. For his support and mentorship.

NIH – funding agency. For their research grant.

Mark, Song, and Passorn – current and former members of the lab. For their friendship.

Drs. Emmanuele DiBenedetto, Todd Hulgan, Tricia Thornton-Wells, and Scott Williams – my committee. For their support and guidance.

Students and members of the Vanderbilt University Center for Human Genetics Research and Program in Human Genetics; and of Virginia Bioinformatics Institute and Program in Genetics, Bioinformatics, and Computational Biology. For their support and friendship.

Yan.

My parents.

TABLE OF CONTENTS

LIST OF TABLES

LIST OF FIGURES

CHAPTER I

INTRODUCTION

I.1. Mitochondrial biology

Mitochondria are semi-autonomous, double membrane-bound sub-cellular organelles present in nearly all eukaryotic cells. Cells typically contain numerous mitochondria. The space between the two membranes that bound each mitochondrion is referred to as the mitochondrial intermembrane space and that which is contained within the inner membrane is referred to as the mitochondrial matrix space. Mitochondria are very dynamic structures. They grow, divide, fuse, and are degraded. Mitochondria cannot be created *de novo* by the cell, but must be formed by the growth and division of existing mitochondria, a process called mitochondrial biogenesis.

Mitochondria are the predominant source of cellular energy. As the sites of oxidative phosphorylation, mitochondria generate most of the cellular ATP, the energy currency of the cell. Each mitochondrion possesses a number of copies of a small circular genome (16.6 kbp in humans). The compact mitochondrial DNA (mtDNA) molecule only includes protein encoding genes for 13 essential subunits of the respiratory chain (and genes for translation of those 13 genes). The other 72 subunits of the respiratory chain, as well as the much larger number of proteins that function in mitochondrial biogenesis and maintenance and in mtDNA replication and maintenance, are encoded in the nuclear genome (nDNA). The nDNA-encoded proteins with mitochondrial localization are

translated by the ribosomes in the cytoplasm and then transported as unfolded peptide chains into the mitochondria through special protein channels called TOM-TIM complexes [1].

Besides ATP production, mitochondria are important players in many key cellular functions. These include metabolism of amino acids and fatty acids, the citric acid cycle, and apoptosis to name a few. Mitochondria are essential for life – and this is probably due to their role in the assembly of iron-sulfur clusters [2], rather than their more famous identity as the powerhouses of the cell. Because of their substantial contribution to the proper functioning of cells, mitochondrial dysfunction has been implicated in an array of important human pathologies, including, but not limited to, cancer, neurodegenerative disorders, and a family of genetic diseases called mitochondrial DNA depletion syndromes (MDS) [3]. Mitochondrial DNA depletion syndromes are characterized by a reduction in the cellular amount of mitochondrial DNA and result from mutations in at least nine known nuclear genes (Table 1). Eight of these nine genes code for proteins with functions either in the apparatus that replicates mtDNA or in the production of the deoxyribonucleoside triphosphates required for mtDNA replication.

Table 1: Mitochondrial DNA depletion syndromes.

Gene	OMIM ID	OMIM name
TK2	609560	MTDPS2 (Myopathic type)
DGUOK	251880	MTDPS3 (Hepatocerebral type)
MPV17	256810	MTDPS6 (Hepatocerebral type)
C10ORF2	271245	MTDPS7 (Hepatocerebral type)
POLG	203700, 613662	MTDPS4A (Alpers type), MTDPS4B (MNGIE type)
SUCLG1	245400	MTDPS9 (Encephalomyopathic type with methylmalonic aciduria)
SUCLA2	612073	MTDPS5 (Encephalomyopathic with methylmalonic aciduria)
TYMP	603041	MTDPS1 (MNGIE type)
RRM2B	612075	MTDPS8A (Encephalomyopathic type with renal tubulopathy), MTDPS8B (MNGIE type)

I.2. Nucleotide metabolism

Nucleotide metabolism can be broadly defined as the set of anabolic and catabolic conversions of nucleotides.

Let us briefly review some terminology associated with nucleotide metabolism. A nucleoside consists of a sugar molecule attached to a base. The common bases are adenine (A), cytosine (C), guanine (G), thymine (T), and uracil (U).

Nucleosides can be divided into two classes, ribonucleosides and deoxyribonucleosides. The difference is in the sugar molecule, which is ribose in the former and deoxyribose in the latter. Thus, the common deoxyribonucleosides (dN) are deoxyadenosine, deoxycytidine, deoxyguanosine, deoxythymidine (also referred to as thymidine), and deoxyuridine; while the common ribonucleosides (rN) are adenosine, cytidine, guanosine, and uridine.

A nucleoside can undergo as many as three enzyme-catalyzed phosphorylations. Nucleotide is the term for a phosphorylated nucleoside. Thus for each deoxyribo- as well as ribo- nucleoside, three corresponding nucleotides are possible. For deoxyribonucleosides, these are deoxyribonucleoside monophosphate (dNMP), deoxyribonucleoside diphosphate (dNDP), and deoxyribonucleoside triphosphate (dNTP).

dNTPs and rNTPs are essential for the replication, maintenance, and repair of DNA and RNA, respectively. dNTPs are generated via two routes, the *de novo* pathway and the salvage pathway. In the *de novo* pathway, after small molecules are converted to ribonucleoside diphosphates, a cytoplasmic enzyme called ribonucleotide reductase (RRM) converts the ribonucleoside diphosphates to the corresponding deoxyribonucleoside diphosphates [4]. These resulting deoxyribonucleoside diphosphates can then be phosphorylated to generate the dNTPs. Additionally, dNTPs can also be synthesized through three successive phosphorylations of deoxyribonucleosides. This pathway of dNTP generation is referred to as the salvage pathway.

In the cell, DNA resides in two places, the nucleus and the mitochondria, and therefore dNTPs are required in both compartments. In the cytoplasm, the majority of dNTPs are generated via the *de novo* pathway. The existence of the *de novo* route in the mitochondria has not been established, and therefore, dNTP production in the mitochondria is thought to occur solely through the salvage route. The primary focus of the remainder of this dissertation is on mitochondrial dNTP pools. All of the genes discussed in this dissertation are encoded in the nuclear genome.

I.3. Generating mitochondrial dNTP pools

Mitochondrial salvage: Deoxyribonucleotide metabolism for generating dNTPs within mitochondria occurs through the salvage pathway (Figure 1), though other sources may also exist. This metabolism within the mitochondrion is separate from the corresponding metabolism that provides dNTPs for nuclear DNA replication. There exists one report of

a mitochondrial ribonucleotide reductase, thus suggesting the presence of a mitochondrial *de novo* pathway, but that finding remains uncorroborated [5]. In the mitochondrial salvage pathway, the canonical A, C, G, and T deoxyribonucleosides, after entering the mitochondrion through equilibrative nucleoside transporters (ENTs), are converted to the corresponding deoxyribonucleoside triphosphates through three successive phosphorylations. This is a complex process with some reactions occurring in parallel for the four deoxyribonucleosides, and some reactions using the same enzyme (for example, the first phosphorylation of dT and dC are both catalyzed by thymidine kinase 2) in addition to the presence (not shown in Figure 1A) of feedback mechanisms (for example, dTTP and dCTP inhibition on thymidine kinase 2 [6]).

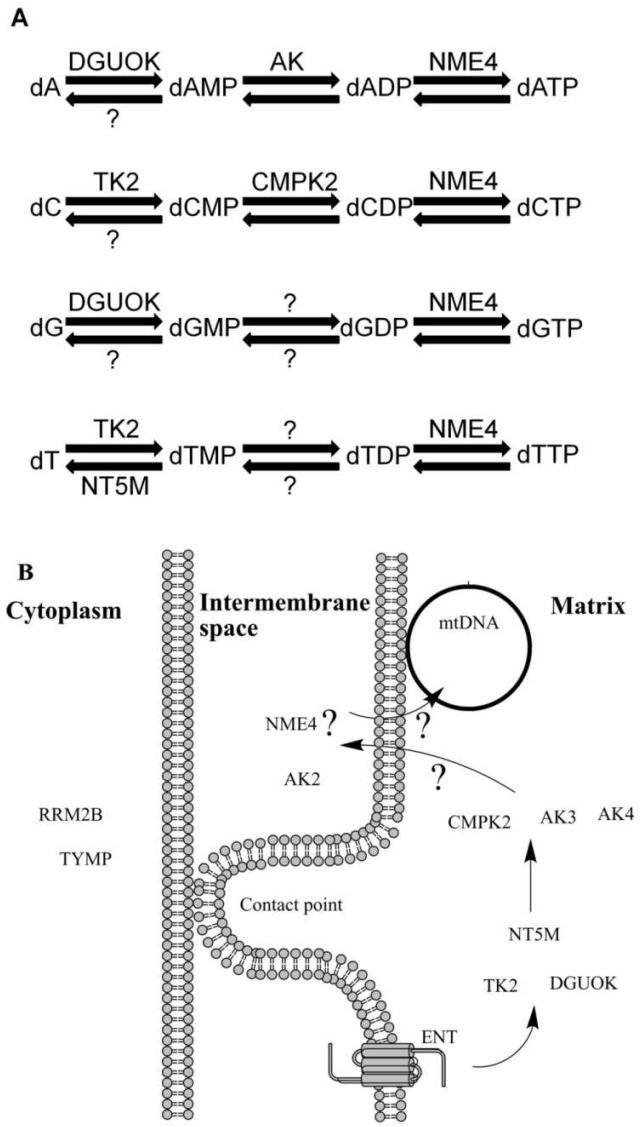

Figure 1: Mitochondrial deoxyribonucleoside salvage metabolism. (A) Biochemical pathway representation of the mitochondrial deoxyribonucleoside salvage metabolism. Deoxyribonucleosides undergo a series of reversible phosphorylations to become deoxyribonucleoside triphosphates (substrates for mtDNA replication). Enzymes that are yet to be identified are represented by question marks. (B) Subcellular localizations of some enzymes important for the production of intra-mitochondrial dNTPs. Arrows denote the flow of substrates between the enzymes. The question marks denote substrate flows that appear to be required by the enzyme localization data, but which seem unreasonable. Reproduced from Gandhi and Samuels (2011) [7].

The known elements of the mitochondrial salvage pathway are as follows. Deoxyguanosine kinase (DGUOK) and thymidine kinase 2 (TK2) are the purine and pyrimidine deoxyribonucleoside kinases, respectively. Apart from these deoxyribonucleoside kinases, other elements of this pathway are relatively less studied. Mitochondria possess a pyrimidine 5',3'-deoxyribonucleotidase (NT5M) which can dephosphorylate dTMP. The existence of additional deoxyribonucleotidases as well as the extent of NT5M's contribution towards opposing dAMP, dCMP, and dGMP production is not established. For monophosphate kinase activity, candidates include adenylate kinase (AK) isoforms, cytidine monophosphate kinase 2 (CMPK2), and thymidine monophosphate kinase 2 (TMPK2) acting on dAMP, dCMP, and dTMP respectively. It is unclear which AK isoform has the most contribution towards producing mitochondrial dADP. Regarding CMPK2, its kinetics with dUMP as a substrate were far more favorable than the kinetics with dCMP which is its second-most preferred substrate [8]. Additionally, CMPK2 might be dispensable in dCTP synthesis given that its expression is restricted and was not detected in tissues with high energetic demand such as heart and muscle [8]. Following putative identification, attempts at characterizing the enzyme activity of TMPK2 have been unsuccessful both *in vitro* and in cell extracts [9]. No candidates exist for dGMP phosphorylation activity in the mitochondria. Assuming that mitochondria possess a complete salvage pathway, the lack of knowledge of the monophosphate kinases is a fundamental gap in our understanding. NME4 is a candidate for the mitochondrial nucleoside diphosphate kinase activity. Again, knowledge about mitochondrial nucleoside diphosphate kinase activity is scarce, and multiple NME isoforms have been reported.

The physical structure of the mitochondrion provides another complication that is rarely considered in this context. The mitochondrion has an intermembrane space (between the inner and outer membranes) and a matrix compartment within the inner membrane (Figure 1B). Several contact sites exist between the inner and outer membranes. mtDNA is tethered to the inside of the inner membrane, within the matrix, so it would be expected that the enzymes of the salvage pathway also would be located within the matrix. In the simplest picture of the mitochondrial salvage pathway, deoxyribonucleosides are transported through the inner membrane by the equilibrative nucleoside transporter and then phosphorylated to dNTPs within the matrix. However, evidence exists to suggest that the AK2 adenylate kinase as well as NME4 nucleoside diphosphate kinase might actually be localized to the mitochondrial intermembrane space [10, 11], not in the matrix. It is possible that other isoforms of these enzymes might localize to the mitochondrial matrix [10, 11]. If so, which versions are more crucial to intra-mitochondrial dNTP pools? If it is not the matrix versions, it is hard to understand how the salvage pathway would function without an unnecessarily complicated transport of deoxyribonucleotides back and forth across the inner membrane (arrows marked with question marks in Figure 1B).

In a recent report, in addition to its presence in mitochondria, a cytosolic form of TK2 was detected in multiple rat tissues [12]. This is in addition to the well-studied thymidine kinase 1 (TK1) which is the distinct cytoplasmic counterpart of mitochondrial TK2. In summary, it is possible that despite intensive study we currently might know only a

fraction of the components that participate in the pathways of mitochondrial dNTP pool generation.

Deoxyribonucleotide flow between the cytoplasm and mitochondria: Older evidence supported the view that mitochondrial nucleotides may be isolated from the corresponding cytoplasmic pools [13], but several more recent studies exist to support the transport of deoxyribonucleotides between the cytoplasm and mitochondria [14-18] and show that nucleotide import from the cytosol very likely contributes to mitochondrial dNTP pools in both cycling and quiescent cells [17, 18] (Figure 2). dCTP transport activity in proteoliposomes containing the mitochondrial protein fraction of human acute lymphocytic leukemia cells has been observed [14]. Because the orientation of the insertion of proteins in lipid vesicles is not controlled, we cannot conclude whether the dCTP transport was unidirectional or bidirectional [14]. Other ribonucleoside and deoxyribonucleoside triphosphates were able to inhibit the dCTP transport, thus raising the possibility of a more general, non-specific transport function for this protein. A mitochondrial transporter (pyrimidine nucleotide carrier, PNC1) with a preference for UTP has also been described [16]. Again, PNC1 was also able to transport a variety of other molecules, including other ribonucleoside and deoxyribonucleoside triphosphates. Transport of dTMP into and out of isolated mitochondria also has been reported [15]. In that experiment, a fraction of dTMP was converted to thymidine, dTDP, and dTTP both in the medium and in the mitochondria. Thus, interpretation of the exact nature of that transport is complicated. Using isotope experiments, Bianchi and colleagues have established the importance of cytoplasmic enzymes in the maintenance of mitochondrial

dTTP and dGTP pools [17, 18]. By following the flux of radioactivity, they identified two-way transport of thymidine and deoxyguanosine nucleotides between the cytoplasm and mitochondria, and determined that while the cytoplasmic de novo pathway is the predominant source of mitochondrial dTTP in proliferating cells, even non-proliferating cells depend on ribonucleotide reduction in the cytoplasm. Details of the transport, such as the identities of the transporter and the transport substrate, and the kinetics of transport remain unresolved. It is also unknown if the behavior of deoxyadenosine and deoxycytidine nucleotides is similar to what has been observed regarding thymidine and deoxyguanosine nucleotides. Thus, even though solid evidence has accumulated to support the transport of deoxyribonucleotides between the cytoplasm and mitochondria, in the end we know little about the molecular mechanisms of this transport process.

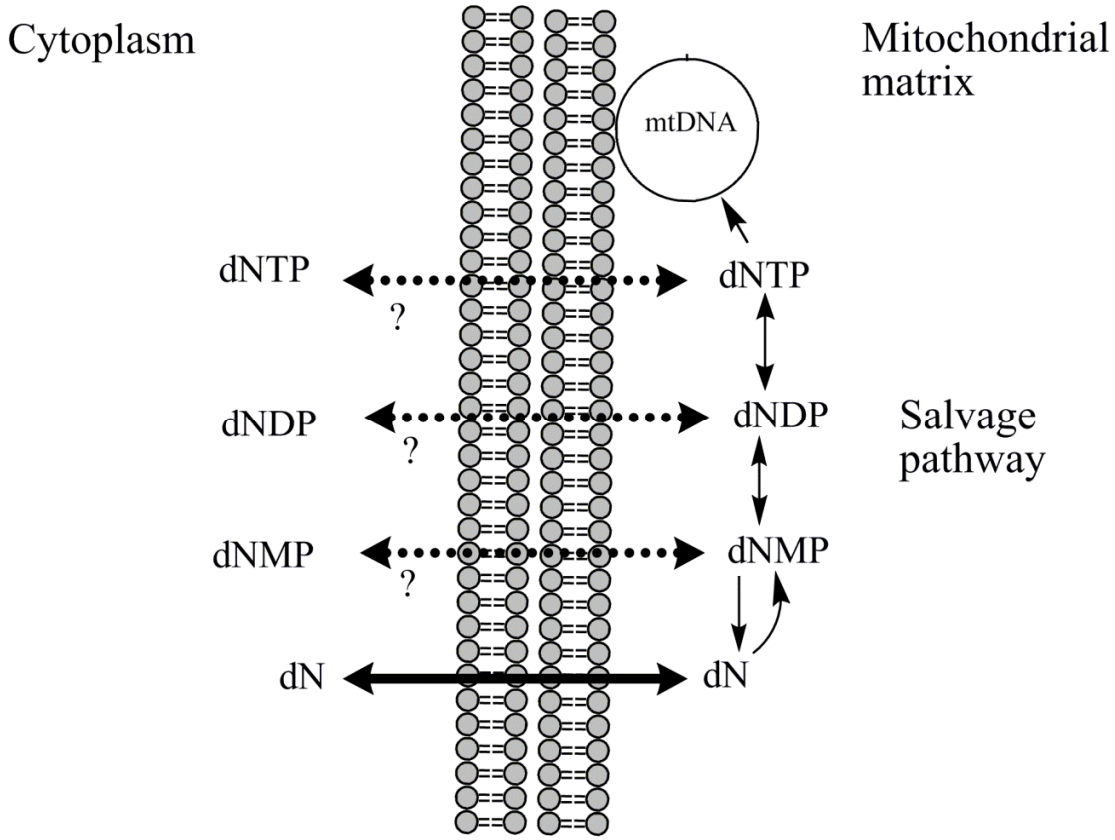

Figure 2: The origin of intra-mitochondrial dNTPs. dN = deoxyribonucleoside, dNMP, dNDP and dNTP = mono, di, or tri phosphorylated deoxyribonucleoside respectively. The solid arrow denotes the identified deoxyribonucleoside transport mechanism. Dotted arrows represent possible but unidentified deoxyribonucleotide transport mechanisms. The conversions between nucleosides and dNMPs are irreversible and carried out in the forward and reverse direction by separate enzymes. Reproduced from Gandhi and Samuels (2011) [19].

I.4. The importance of mitochondrial dNTP pools

Mitochondrial DNA depletion syndromes: Mitochondrial DNA depletion syndromes are a set of genetic diseases commonly defined as a reduction in the amount of cellular mitochondrial DNA without other defects such as deletions or point mutations [20]. However, underlying this definition is a clinically and genetically complex set of diseases (Table 1). Genetic and allelic heterogeneity; variable penetrance, severity of symptoms, and ages of onset; and gene-dependent tissue-specificity of phenotype are all characteristics of mtDNA depletion syndromes. Another complication in the characterization of mtDNA depletion syndromes is that depletion of mtDNA is not always exclusive of other genomic defects. For example, in mitochondrial neurogastrointestinal encephalomyopathy (MNGIE), deletions may accompany the depletion of mtDNA [21]. Mutations in the mitochondrial DNA polymerase (POLG) may lead to any of a diverse set of disorders, including progressive external opthalmoplegia (PEO). Also in PEO, mutations, deletions, and depletion of mitochondrial DNA may not necessarily be mutually exclusive [21], and the inheritance may be sporadic, dominant, or recessive [22]. Thus, while the inheritance of mtDNA depletion syndromes is usually deemed to be autosomal recessive [23], features of the mtDNA depletion syndrome phenotype also follow other inheritance patterns. The diseases that make up the mtDNA depletion syndrome family are shown in Table 1, along with their OMIM IDs. MDS is nearly always severely debilitating and often lethal in infancy or early childhood for homozygous patients [23]. The prevalence of these diseases is not yet well determined. However, quantification of mtDNA in the liver or muscle tissue of 100 children with unexplained respiratory chain deficiency showed mtDNA depletion to be less than 35%

of the control values in 50% of these cases, indicating that depletion of mtDNA is a common cause of respiratory chain deficiency in childhood [24]. Mutations in nine nuclear-encoded genes are known to cause mtDNA depletion syndrome. Eight of the nine genes code for enzymes that contribute to generating mitochondrial deoxyribonucleoside triphosphates or that participate in mtDNA replication. The function of the ninth gene, MPV17, which encodes a mitochondrial inner membrane protein, remains to be determined.

The discoveries of a mutated p53-inducible small ribonucleotide reductase subunit (RRM2B) [25] and a mutated thymidine phosphorylase (TYMP) [26] as causes of mtDNA depletion syndrome highlight the importance of cytoplasmic nucleotide metabolism in maintaining mtDNA. Both RRM2B and TYMP are cytoplasmic enzymes of nucleotide metabolism (Figure 1B). RRM2B is a subunit of cytoplasmic ribonucleotide reductase, the key enzyme of the *de novo* pathway which reduces ribonucleoside diphosphates to deoxyribonucleoside diphosphates. TYMP converts deoxythymidine to thymine, and thus a lack of TYMP activity can result in excess deoxythymidine. This association between DNA depletion in the mitochondria and defects in cytoplasmic nucleotide metabolism implies that cytoplasmic nucleotides influence and contribute significantly to intra-mitochondrial pools of deoxyribonucleotides. We can therefore speculate that defects in other enzymes of cytoplasmic nucleotide metabolism, in addition to RRM2B and TYMP, could also lead to mtDNA depletion.

On a side note, the intermembrane localization of NME4 is interesting considering the importance of RRM2B-catalyzed ribonucleotide reduction in the cytoplasm for maintaining mitochondrial DNA. In the presence of active production of deoxyribonucleoside diphosphates in the cytoplasm, terminal phosphorylation of those dNDPs by NME4 and the subsequent entry of the resulting dNTPs into the mitochondrial matrix would appear to be a logical benefit of NME4's localization to the intermembrane space.

Mitochondrial dNTP pools in patient cells: Experiments with patient cells have demonstrated the effects of pathogenic mutations on mitochondrial dNTP pools. In fibroblasts from a patient with deoxyguanosine kinase deficiency where quiescence was induced through serum starvation, reduced mitochondrial dGTP led to an imbalance between the four dNTPs compared to controls [27]. In fibroblasts from patients with TK2 deficiency, mitochondrial dTTP, dCTP, and dATP pools were all decreased while dGTP was slightly increased in one patient and slightly decreased in another patient [28]. The fact that externally supplied deoxyribonucleosides and deoxyribonucleoside monophosphates are able to rescue mtDNA depletion provides further evidence that limited substrate availability can cause mtDNA depletion [27, 29, 30]. Experiments from cellular and animal models have also reported disruptions in mitochondrial dNTP pool homeostasis [31-33]. TK2 H126N (c.378–379CG>AA) knockin mice had unbalanced mitochondrial dNTP pools due to reduced dTTP in brain and reduced dCTP in liver [31]. Culturing HeLa cells in the presence of high levels of thymidine (50 μM) to mimic the conditions leading to MNGIE (caused by mutations in TYMP), led to an expansion of

mitochondrial dTTP and dGTP pools and a reduction of the mitochondrial dCTP pool [33]. In another cellular model of MNGIE, incubation of quiescent fibroblasts in the presence of high levels of deoxythymidine or deoxyuridine led to an expansion of mitochondrial dTTP, but mitochondrial dCTP was unaffected [32].

In conclusion, the availability and balance of the intra-mitochondrial dNTP pools are major determinants of the rate and fidelity of mtDNA replication and thus of the integrity of the mitochondrial genome [34]. Besides mtDNA depletion syndromes, mitochondrial dNTP pools are important in other human pathologies. Mitochondrial toxicity induced by HIV/AIDS therapy can manifest as severe clinical phenotypes and increased mortality [35, 36]. This toxicity is likely the result of interference with mtDNA replication and intra-mitochondrial nucleotide metabolism brought about by nucleoside analogs [37-40]. To advance our understanding of these numerous human disorders, to elucidate the role of mtDNA mutations in aging and cancer [3, 41-46], and to devise suitable therapies, it is critical that we understand the formation and regulation of intra-mitochondrial dNTP concentrations. Because mitochondrial dNTP levels are disrupted in mtDNA depletion syndromes, a thorough understanding of the maintenance of mitochondrial dNTPs is a necessary step towards insights on the mechanisms and the potentials therapies of mtDNA depletion syndromes.

Considering that mitochondrial dNTP pools are crucial for normal functioning of cells, what are the features of wild-type mitochondrial dNTP pools? We know that flow of deoxyribonucleotides between the cytoplasm and mitochondria is possible.

What is the influence of this flow on the relationship between wild-type mitochondrial dNTP pools and cytoplasmic dNTP pools?

I.5. Regulation of dNTP pools and DNA replication

The fidelity of nDNA replication and cell-cycle progression are influenced by the concentrations of the DNA precursors, the substrate dNTPs [47]. S-phase specific activities of the cytoplasmic *de novo* ribonucleotide reductase and the salvage thymidine kinase 1 enzymes lead to a many-fold difference in dNTP levels between S-phase and non-S phase cells [48, 49]. This mechanism prevents an out-of-phase excess or imbalance of DNA precursors, thus also preventing unscheduled or erroneous DNA replication. Ribonucleotide reductase reduces ribonucleotides to the corresponding deoxyribonucleotides and has an important role in cell proliferation. Increased ribonucleotide reductase activity has a role in cancerous transformation as well as metastasis [50]. It is also known that oncogenically transformed mammalian cells contain much higher dNTP pools than normal cells [34]. Recently, it was shown that nucleotide deficiency results in DNA damage in early stages of oncogenesis as cells are forced to proliferate despite low nucleotide pools [51]. A mitochondrial transporter (PNC1) with the ability to transport a variety of substrates including ribonucleoside and deoxyribonucleoside triphosphates but a preference for UTP has been reported [16, 52]. It is interesting that the PNC1 gene had higher expression in transformed cells and primary prostate cancers and that enhanced expression of PNC1 was reported to have a role in transformation and in the invasive potential of tumor cells.

In summary, it is well-acknowledged that the process of carcinogenic transformation is often connected to impaired nucleotide homeostasis. Combined with the fact that a cross-talk between cytoplasmic and mitochondrial deoxyribonucleotides is possible, what are the features of mitochondrial dNTP pools in transformed cells? How do their features relate to those of the cytoplasmic dNTP pools in such cells?

Mitochondrial DNA replication [53], and the mitochondrial nucleoside salvage pathway that generates the precursor deoxyribonucleoside triphosphates for mitochondrial DNA replication, generally have been believed to function independently of nuclear DNA replication and cytoplasmic nucleotide metabolism. The mitochondrial DNA molecule has a half-life of 10-30 days [54]. To maintain the mtDNA content of the cell, mtDNA must replicate even in postmitotic cells [53]. Synthesis of mtDNA and mitochondrial biogenesis, therefore, must be able to proceed independently of nuclear DNA synthesis and cellular division [53]. However, mtDNA and nDNA synthesis cannot be completely decoupled since mtDNA replication must be increased at some point in cell division to provide sufficient mtDNA for the two daughter cells. Clearly there must be a flexible system of control linking these two parallel metabolic pathways that allows them to work together sometimes and independently at other times. The observation associating mutated RRM2B (a p53-inducible ribonucleotide reductase subunit) with mtDNA depletion and at least one observation of mtDNA replication restricted to S-phase in deoxyguanosine kinase deficient cells further make it clear that mtDNA replication and maintenance are not always completely independent of the cytoplasmic state [25, 30].

How does the expression of genes coding for mitochondrial enzymes of deoxyribonucleotide metabolism relate to the expression of genes of the corresponding cytoplasmic enzymes? Can we reconcile these gene expression patterns with the patterns in the dNTP pools that result from the activities of the enzymes encoded by the genes?

I.6. The difficulty of studying mitochondrial dNTP pools

Due to the small physical scale of mitochondria and relatively rapid dynamics of the pathways, it is very difficult to study the dynamics of mitochondrial dNTPs through traditional wet-lab methods. Owing to the complexity of the pathways that generate mitochondrial dNTP pools for the maintenance of mitochondrial DNA, there exist many open questions in the field, as we have seen. I outline some more below.

Although we know deoxyribonucleotide transport between the cytoplasm and mitochondria occurs, what is the identity of the transported substrate? Is it the mono-, di-, or the tri-phosphate? What is the implication of a lack of transport? Which pathway components represent major bottlenecks in the generation of mitochondrial dNTP pools?

I.7. Research summary and significance

The unifying objective of this dissertation was to increase our understanding of the features of mitochondrial dNTP pools.

The extent of the association between cytoplasmic and mitochondrial dNTP pools was not clear prior to my research. Chapter II shows that mitochondrial and cytoplasmic dNTP concentrations are correlated in normal cells but not in transformed cells. In the research presented in Chapter II, although the raw data was not produced in our laboratory, I generated a usable resource out of it. I converted, analyzed, and summarized all relevant published data to a more comprehensive form, thus substantially adding to the usefulness of the data. It can be misleading to compare previously published results as they were originally reported because of the units that are used to report such data. My work of converting all relevant data to biochemically meaningful micromolar concentrations allows for comparisons of published dNTP pool measurements between published experiments; sub-cellular compartments; and normal and transformed cell lines. An additional significant contribution of the analysis presented in Chapter II is the suggestion of specific experiments furthering the field. The highly significant association between cytoplasmic and mitochondrial dNTP concentrations that I discovered would indicate the existence of regulatory mechanisms that synchronize the respective dNTP pools. Finally, for publication of these results, I incorporated my analysis into the context of an overall review of the field and pointed out both the state of our understanding as well as key areas where knowledge is lacking.

What mechanism might give rise to the strong and highly statistically significant correlation between cytoplasmic and mitochondrial dNTP pools in normal cells but not in transformed cells? I offer one mechanism through the research presented in Chapter III. I hypothesized that coordinated gene expression could be one mechanism to explain the

correlation between cytoplasmic and mitochondrial dNTP pools. At the time I commenced my research, the enzymes that generate dNTP pools in the mitochondria were not considered to be carefully regulated. In fact, it was not uncommon for them to be perceived as housekeeping enzymes. I also tested this perception in my research presented in Chapter III. I obtained tissue-expression data for a selected set of genes from the NCBI Unigene database and conducted an *in silico* gene expression analysis. My results showed that in normal tissues, the expression of genes encoding proteins of mitochondrial salvage varies in coordination with the expression of the corresponding genes of cytoplasmic salvage. However, in transformed tissues, consistent with the disruption in the correlation in dNTP concentrations I found in Chapter II, the coordination in the gene expression is also disrupted. Unlike in normal tissues, the expression of mitochondrial genes is negatively associated with the expression of cytoplasmic genes. To my knowledge, such a systematic investigation into the expression network of genes important for cytoplasmic and mitochondrial dNTP pools has not been carried out apart from my research.

By discovering the results in Chapters II and III that have implications for transformed tissues and by highlighting mitochondrial deoxyguanosine kinase expression as potentially a significant factor for transformed tissues, my research highlighted the possibility of important connections between mitochondrial dNTP pools and cancer.

Chapter IV presents a comprehensive analysis of enzyme kinetics of the mitochondrial deoxyribonucleoside salvage pathway enzymes. The complexity of the homeostasis of

mitochondrial dNTP pools makes it extremely difficult to understand the processes in their entirety using traditional laboratory techniques. For developing novel approaches for therapy, it is important to first improve our understanding of the mitochondrial salvage pathway. I attacked this using a logical, objective, and systematic approach, and my work is the only computational model incorporating all available relevant knowledge regarding this complex biological process. While it was accepted that deoxyribonucleotide import from the cytoplasm to the mitochondria is possible, my results showed that it is in fact essential for mtDNA maintenance in most circumstances. I also discovered that import would need to occur at the diphosphate or triphosphate levels; import at the monophosphate level does not satisfy the rate at which dNTP substrates are required for mtDNA replication in cycling cells.

The content in this dissertation was reproduced with revisions from published papers on which I am first author [7, 19]. A paper describing the work presented in Chapter III is in preparation.

CHAPTER II

A REVIEW COMPARING DEOXYRIBONUCLEOSIDE TRIPHOSPHATE CONCENTRATIONS IN THE MITOCHONDRIAL AND CYTOPLASMIC COMPARTMENTS OF NORMAL AND TRANSFORMED CELLS

II.1. Introduction

Although mitochondrial dNTP generation is an important pathway, much about the origin of mitochondrial dNTPs remains unclear. Since the etiology of mtDNA depletion syndromes can be traced to altered mitochondrial dNTP pools, it is critical to understand how the mitochondrial dNTP pools relate to the corresponding cytoplasmic pools. The evidence reviewed in Chapter I repeatedly points toward a significant amount of interaction between the mitochondrial and cytoplasmic dNTP pools. What data exists concerning the relationship between the dNTP concentrations in these two subcellular compartments, and is the existing data consistent with the increasing evidence of communication between the cytoplasm and mitochondria with respect to deoxyribonucleotides? In this chapter we focus on these questions. We reviewed the available data on simultaneous measurements of cytoplasmic and mitochondrial dNTP pools in wild-type cells [27, 32, 33, 55-59].

The content of this chapter has been reproduced with revisions from a published paper on which I was first author [19].

II.2. Overview

The deoxyribonucleoside triphosphate pools that support the replication of mitochondrial DNA are physically separated from the rest of the cell by the double membrane of the mitochondria. Perturbed homeostasis of mitochondrial dNTP pools is associated with a set of severe diseases collectively termed mitochondrial DNA depletion syndromes. It is important to determine the degree of interaction of the mitochondrial dNTP pools with the corresponding dNTP pools in the cytoplasm. We reviewed the literature on previously reported simultaneous measurements of mitochondrial and cytoplasmic deoxyribonucleoside triphosphate pools to investigate and quantify the extent of the influence of the cytoplasmic nucleotide metabolism on mitochondrial dNTP pools. We converted the reported measurements to concentrations creating a catalog of paired mitochondrial and cytoplasmic dNTP concentration measurements. We found that over experiments from multiple laboratories, dNTP concentrations in the mitochondria are highly correlated with dNTP concentrations in the cytoplasm in normal cells in culture (Pearson $R = 0.79$, $p = 3 \times 10^{-7}$) but not in transformed cells. For dTTP and dATP, there was a strong linear relationship between the cytoplasmic and mitochondrial concentrations in normal cells. From this linear model we hypothesize that the salvage pathway within the mitochondrion is only capable of forming a concentration of approximately 2 μM of dTTP and dATP, and that higher concentrations require transport of deoxyribonucleotides from the cytoplasm.

II.3. Methods

Conversion to correct concentration units: With the goal of investigating whether concentrations calculated from previously measured dNTP pools are consistent with the biochemical evidence of deoxyribonucleotide flow between the cytoplasm and mitochondria, we converted the reported data to molar concentrations. This conversion requires the estimation of several parameters. Enzyme activities, kinetics, and the rate and fidelity of mtDNA replication are all influenced by the local dNTP concentrations. These concentrations are maintained by metabolic pathways that function in two subcellular compartments with very different volumes. Although concentrations are indeed the true biochemical driving factors, dNTP data is instead generally reported as amounts per million cells in culture. Per cell amounts can be misleading, since the conversion from these experimentally convenient units to the actual units of concentration in subcellular compartments can vary radically between different cell types. Paradoxically, the justification for using units such as the amount per million cells is to make comparisons possible; but, all the while, the cell lines and culture conditions in different experiments are different in the critical parameters needed to convert these units to actual concentration units. For reporting dNTP pools, the most commonly used units in the literature are picomoles per million cells for both subcellular compartments, or picomoles per milligram mitochondrial protein. In the following section we give estimates to convert these units to true concentration units.

To obtain concentrations from data reported as amount dNTP (picomoles) per cell, we must use estimates of cell and subcellular compartment volumes (for details see Table 2).

Bestwick *et al.* [55] reported dNTP amounts in subcellular fractions of asynchronously growing HeLa cells. For cellular and mitochondrial volumes of HeLa cells, we referred to a publication from Posakony *et al.* [60] who followed cellular and mitochondrial volume at different times along the cell cycle of HeLa cells. We combined nuclear and cytoplasmic amounts reported by Bestwick *et al.* [55], and converted these to molar concentrations using averaged cellular volume subtracted for mitochondrial volume. We calculated mitochondrial concentrations by using the average mitochondrial volume from different cell cycle phases.

Song *et al.* [33] reported mitochondrial dNTP pools in HeLa cells as the amount dNTP (in picomoles) per milligram mitochondrial protein. To calculate the corresponding concentrations, we used a factor of 0.82 microliters water space per milligram rat heart mitochondrial protein [61]. For converting whole-cell amounts from picomoles per million cells, we first used the calculated mitochondrial concentrations and the mitochondrial volume measure for HeLa cells in G1 phase [60] to estimate the picomole amounts of dNTPs in mitochondria per million HeLa cells. After subtracting mitochondrial amounts and volume from corresponding whole-cell values for HeLa cells in G1 phase [60], we arrived at an approximation of cytoplasmic concentrations of Song *et al.*'s data for confluent HeLa cultures.

Rampazzo *et al*. [59] measured dNTP amounts in exponentially growing human osteosarcoma line (HOS) cells and mouse fibroblasts (3T3) cell lines. Since we did not find a publication that provides the required conversion factors for the HOS cells, as an

estimate we used the measurements from HeLa cells. We averaged cellular and mitochondrial volumes measured in different cell cycle phases of HeLa cells [60] and obtained cytoplasmic and mitochondrial dNTP concentrations. For the cytoplasmic volume, we subtracted the total mitochondrial volume from the cellular volume to account for the fact that Rampazzo *et al.* combined nuclear and cytosolic dNTP pools. We did not find the mitochondrial volume measure for 3T3 cells. As an estimate, we averaged the mitochondrial volumes reported for HeLa and Chinese hamster cells [60, 62] and obtained the cytoplasmic volume after correcting whole-cell volume [63] for the total mitochondrial volume. We then converted dNTP amounts for 3T3 cells to concentrations using these volume measures.

Ferraro *et al.* [57] and Pontarin *et al.* [32] reported dNTP amounts measured in human lung and skin fibroblasts. We used the human skin fibroblast volume reported by Imaizumi *et al*. [64]; and after correcting this whole-cell measure by subtracting mitochondrial volume, we transformed the reported cytoplasmic picomole amounts to cytoplasmic concentrations. We obtained the averaged mitochondrial volume from HeLa cells [60]. We used the cytoplasmic volume of fibroblast cells obtained by subtracting mitochondrial volume from fibroblast cell volume to account for the fact that Ferraro *et al.* [57] and Pontarin *et al*. [32] combined nuclear and cytosolic dNTP pools. The parameters used for these conversions were also used to convert the data from Saada [27] and Frangini *et al.* [58].

Finally, to convert dNTP amounts reported by Desler *et al.* [56] for HeLa cells, we used parameters from HeLa cells [60] for average cellular and mitochondrial volumes. We subtracted mitochondrial amounts and volume from corresponding whole-cell measures and obtained cytoplasmic and mitochondrial concentrations.

The conversion parameter values are listed in Table 2. There exist reports of mitochondrial dNTP pool measurements that are not discussed here [15, 28, 65-67]. In these experiments, because the corresponding cytoplasmic dNTP pools were not also reported, the mitochondrial dNTP measurements were not useful for the purposes of answering the questions posed in this chapter. It should be clear from the preceding paragraphs that the conversion of the traditionally used units to the actual units of concentration is not trivial. Ideally, each experiment should take care to measure and report the additional information needed for this conversion to true concentration units. The missing parameter values, which we estimated as described above, may have introduced noise into the following analysis potentially obscuring any relationship between the cytoplasmic and mitochondrial pools.

Table 2: Parameter values used to calculate subcellular dNTP concentrations. Not all parameters were available for all cell lines.

Reference	Parameter	Estimate
[60]	Cellular volume per HeLa cell	1766 ± 55 fL
[60]	Cytoplasmic volume per HeLa cell	1611 ± 62 fL
[60]	Number of mitochondria per HeLa cell	545 ± 31
[60]	Volume of a mitochondrion in HeLa cells	0.285 ± 0.005 fL
[60]	Mitochondrial volume per HeLa cell	155 ± 29 fL
[60]	Cellular volume per HeLa cell (G1 phase only)	1353 ± 54 fL
[60]	Cytoplasmic volume per HeLa cell (G1 phase only)	1235 ± 55 fL
[60]	Number of mitochondria per HeLa cell (G1 phase only)	417 ± 39
[60]	Volume of a mitochondrion in HeLa cells (G1 phase only)	0.283 ± 0.006 fL
[60]	Mitochondrial volume per HeLa cell (G1 phase only)	118 ± 11 fL
[61]	Mitochondrial volume per milligram protein	0.82 µL
[60, 62, 63]	Cytoplasmic volume per 3T3 cell	2622 ± 67 fL
[60, 62]	Mitochondrial volume per 3T3 cell	96 ± 15 fL
[60, 64]	Cytoplasmic volume per fibroblast cell	3252 ± 29 fL

II.4. Results and Discussion

Variation in cytoplasmic and mitochondrial dNTP concentrations: Paired measurements of dNTP levels in mitochondria and cytoplasm, converted to concentration units as described above, are given in Tables 3-5 and shown in Figures 3 and 4. The variation in dNTP concentrations in both compartments is striking. Even for cells within each particular category, the range of dNTP concentrations in both compartments spans an order of magnitude. This argues for measuring dNTP levels in a wide variety of cell lines, especially those cell types that are affected in mitochondrial DNA depletion syndromes. Also, given these characteristics of the distribution of dNTP concentrations, the usefulness of calculating a mean value across cell types is diminished. Nevertheless, the mean dNTP concentrations that we calculated in both cellular compartments are higher in cycling cells than in quiescent cells (fold difference of ~10 in the cytoplasm and ~4 in the mitochondria). It is interesting that mitochondrial dNTP pools vary proportionally with the cytoplasmic pools and cycling state of cells. This observation is consistent with deoxyribonucleotide flow between the cytoplasm and mitochondria and is indicative of mitochondrial dNTP pools being regulated in a similar manner as the cytoplasmic pools. Mean cytoplasmic dNTP micromolar concentrations in postmitotic, mitotic, and transformed cells were approximately 1, 12, and 21 respectively; and mean mitochondrial micromolar concentrations were about 2, 8, and 10 respectively. These calculated mean concentrations hint that perhaps the equilibrium between the cytoplasm and mitochondria with respect to dNTP concentrations could be qualitatively and quantitatively different for the three cell categories, since the calculated mean

mitochondrial concentration is lower than the mean cytoplasmic concentration in normal mitotic and transformed cells, and higher in postmitotic cells.

Table 3: dNTP concentrations in the cytoplasm and mitochondria of normal mitotic cells.

Cell line (Reference)	**dNTP**	**Cytoplasmic concentration (micromolar)**	**Mitochondrial concentration (micromolar)**
Cycling skin fibroblasts [32]	T	26 ±0.2	12±2.2
Cycling skin fibroblasts [32]	C	20±0.2	13±2.3
Cycling lung fibroblasts [57]	T	18±2.0	10±1.9
Cycling lung fibroblasts [57]	A	3.9±1.0	1.9±0.3
Cycling lung fibroblasts [57]	C	6±1	4±1
Cycling lung fibroblasts [57]	G	2.2±0.2	1.3±0.3
Cycling skin fibroblasts [57]	T	26±0.2	12±2.2
Cycling skin fibroblasts [57]	A	18±0.2	9.0±1.6
Cycling skin fibroblasts [57]	C	20±0.2	13±2.3
Cycling skin fibroblasts [57]	G	3.7±0.03	2.6±0.5
Cycling skin fibroblasts [27]	T	8.2±1.5	7.2±2.0
Cycling skin fibroblasts [27]	A	3.8±0.5	4.8±1.2
Cycling skin fibroblasts [27]	C	3.7±1.1	7.4±2.1
Cycling skin fibroblasts [27]	G	3.8±1.7	14±3.3

Table 4: dNTP concentrations in the cytoplasm and mitochondria of normal postmitotic cells.

Cell line (Reference)	dNTP	Cytoplasmic concentration (micromolar)	Mitochondrial concentration (micromolar)
Quiescent skin fibroblasts [32]	T	0.30±0.002	1.4±0.3
Quiescent skin fibroblasts [32]	C	0.980±0.008	2.1±0.4
Quiescent lung fibroblasts [57]	T	0.760±0.006	0.8±0.2
Quiescent lung fibroblasts [57]	A	3.5±0.3	1.9±0.3
Quiescent lung fibroblasts [57]	C	2.46±0.61	1.28±0.23
Quiescent lung fibroblasts [57]	G	1.1±0.3	0.25±0.05
Quiescent skin fibroblasts [57]	T	0.92±0.01	0.96±0.17
Quiescent skin fibroblasts [57]	A	1.07±0.01	3.5±0.6
Quiescent skin fibroblasts [57]	C	2.15±0.01	1.4±0.3
Quiescent skin fibroblasts [57]	G	1.23±0.01	0.8±0.1
Quiescent skin fibroblasts [27]	T	0.6±0.3	4.2±1.1
Quiescent skin fibroblasts [27]	A	1.7±0.3	3.1±1.7
Quiescent skin fibroblasts [27]	C	0.3±0.2	2.6±0.8
Quiescent skin fibroblasts [27]	G	0.8±0.3	8.5±1.9
Quiescent skin fibroblasts [58]	T	0.5±0.1	0.7±0.2

Table 5: dNTP concentrations in the cytoplasm and mitochondria of transformed cells.

Cell line (Reference)	**dNTP**	**Cytoplasmic concentration (micromolar)**	**Mitochondrial concentration (micromolar)**
HOS [59]	T	27±5.5	4.4±0.8
HOS [59]	A	6.8±0.3	2.9±0.5
HOS [59]	C	12±0.4	4.8±0.9
HOS [59]	G	3.6±0.1	1.7±0.3
3T3 [59]	T	7.2±0.2	5.4±0.8
3T3 [59]	A	4.2±0.1	4.7±0.7
3T3 [59]	C	7.6±0.2	5.8±0.9
3T3 [59]	G	2.09±0.05	4.0±0.6
HeLa [33]	T	26±5.3	35±6.1
HeLa [33]	A	23±2.3	15±0.3
HeLa [33]	C	11±0.6	7.9±1.2
HeLa [33]	G	3.3±0.9	29±1.2
HeLa [56]	T	57±9.6	5.5±2.7
HeLa [56]	A	28±6.2	6.4±2.2
HeLa [56]	C	17±2.8	14±2.8
HeLa [56]	G	20±2.0	7.1±3.3
HeLa [55]	T	79±3.0	17±3.1
HeLa [55]	A	74±2.8	11±2.0
HeLa [55]	C	14±0.5	15±2.8
HeLa [55]	G	6.1±0.2	6.4±1.2

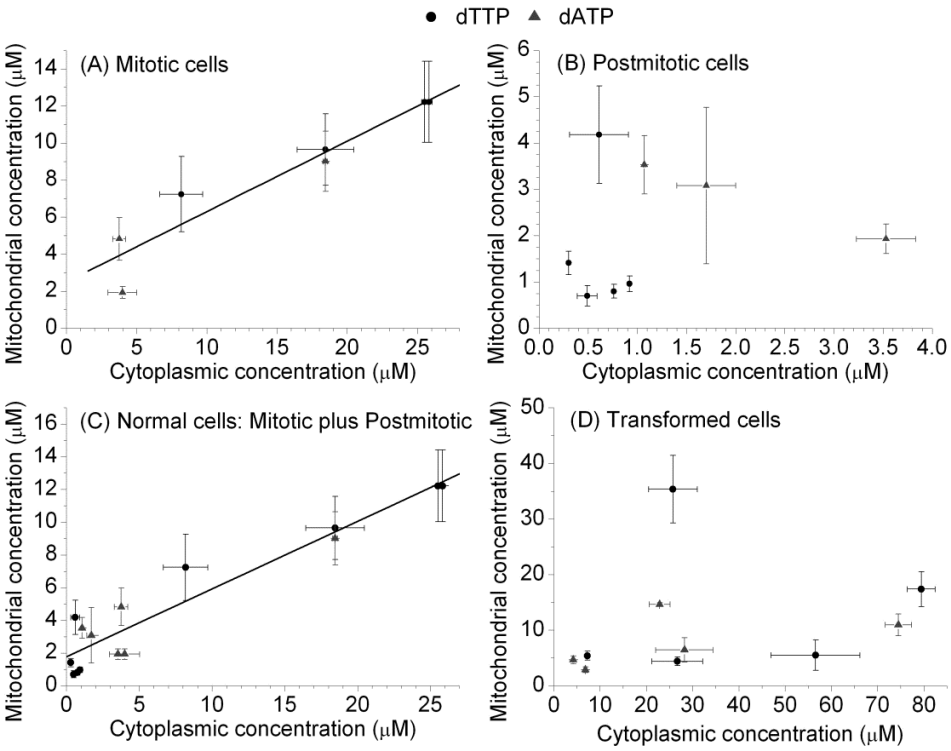

Figure 3: Cytoplasmic and mitochondrial concentrations compiled from the literature of dTTP and dATP from (A) mitotic cells data, (B) postmitotic cell data, (C) mitotic and postmitotic data combined, and (D) transformed cells. The error bars were calculated by statistically propagating the uncertainties in the original measurements. Lines are linear fits to the data, shown when statistically significant.

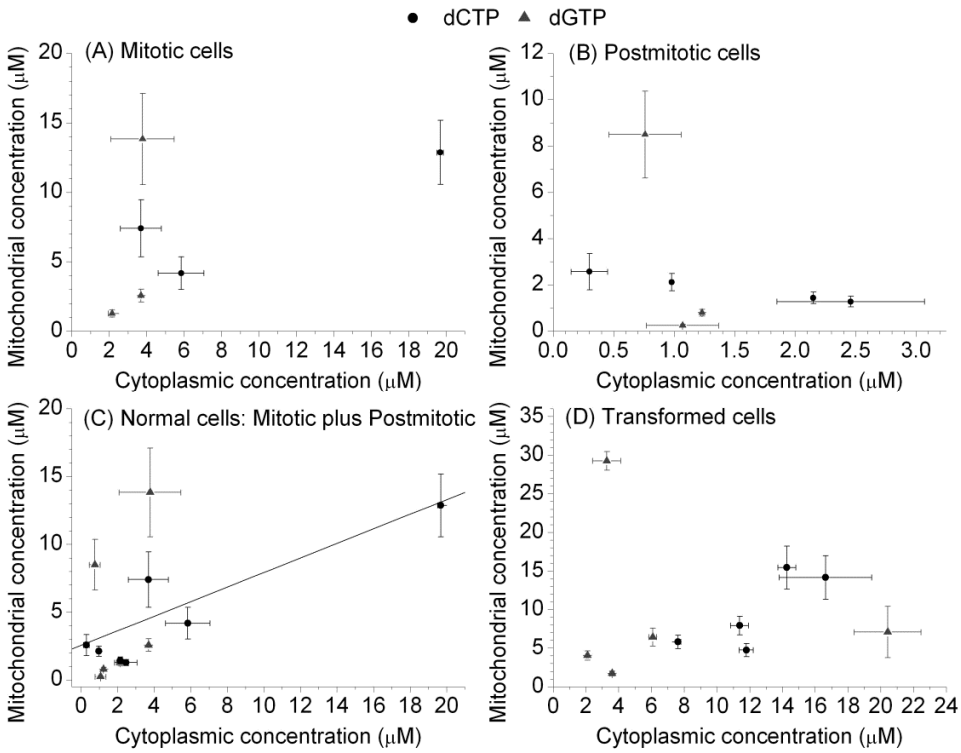

Figure 4: Cytoplasmic and mitochondrial concentrations compiled from the literature of dCTP and dGTP from (A) mitotic cells data, (B) postmitotic cell data, (C) mitotic and postmitotic data combined, and (D) transformed cells. The error bars were calculated by statistically propagating the uncertainties in the original measurements. Lines are linear fits to the data, shown when statistically significant.

A suggested problem with dNTP assays: It is possible that some of the reported dNTP measurements are overestimates. In a recent paper, Ferraro *et al.* [68] concluded that reported dNTP measurements can be contaminated by ribonucleotide triphosphates. This contamination is a consequence of the low discrimination power of the Klenow DNA polymerase fragment that is widely used to measure dNTP amounts by means of a polymerase assay. It was suggested that these assay complications might have resulted in overestimates of dNTPs, including the very high values reported for mitochondrial dGTP levels in rat tissues [67]. When Ferraro *et al*. extracted and measured dNTPs from cycling and confluent human fibroblasts, the original Klenow assay did not result in any overestimation of dTTP. The deoxyribonucleotides dATP, dGTP, and dCTP were all overestimated, and the severity of this complication seemed to most affect dGTP and, to a lesser extent, dCTP. From our interpretation of the Ferraro *et al.* analysis we judged that the dATP measurements analyzed here may not have significant contamination from ATP competition for incorporation. At an ATP/dATP ratio of 350 in cycling cells, the overestimation in Ferraro et al's results for dATP was about 21% compared to their modified assay and about 26% compared to HPLC. At an ATP/dATP ratio of 1450 in confluent cells, the overestimation in dATP was slightly more than 100% compared to their modified assay. Ferraro *et al.* could not use HPLC for measuring dNTP pools in confluent cells. Since we did not have paired rNTP measurements for our dNTP data and since Ferraro *et al.*'s paper did not provide a spectrum of overestimation effects over a broad enough range of Klenow concentrations and ATP/dATP ratios, we cannot quantitatively determine the true effects of this complication on the dATP concentrations, although at a low ATP/dATP ratio, the observed overestimation was not substantial.

Ferraro *et al.* concluded that the Klenow enzyme is unsuitable for measuring dGTP and dCTP pools, but the assay can be used with modifications to measure dTTP and dATP pools. We took these concerns into account by reviewing the data on dTTP and dATP concentrations separately from the data on dGTP and dCTP concentrations. Accordingly, we have split our data discussion into two groups; the dTTP and dATP group and the dGTP and dCTP group.

Analyzing simultaneous data on cytoplasmic and mitochondrial dNTP concentrations: dTTP and dATP observations: Figures 3 and 4 (and Tables 3-5) show the comparison of paired measurements of dNTP concentrations in the cytoplasm and in the mitochondrial compartments of the cell. Despite the relatively low number of available observations and the potential for additional noise due to the need for some parameter estimations, these data show highly significant correlations. In addition, the pattern of which correlations are highly significant and which are non-significant is interesting. For the combined dTTP and dATP measurements in the mitotic cells (Figure 3A) the mitochondrial and cytoplasmic concentrations had a very highly significant correlation (p-value = 0.0009) while the postmitotic cell measurements alone (Figure 3B) had no significant correlation. However, when the postmitotic cell and mitotic cell measurements were analyzed together (Figure 3C) the correlation became extremely significant ($p = 5 \times 10^{-8}$). The concentrations were highly correlated ($R^2 = 0.9$ in both cases, Figure 3A and Figure 3C). Such a strong and highly significant correlation over the broad range of concentrations, in data from multiple independent experiments from different laboratories, is extremely compelling evidence for a tight connection between

the cytoplasmic and mitochondrial dTTP and dATP pools. Correlations, of course, cannot prove which of these two pools is controlling the other. However, considering the relatively small total cellular volume of the mitochondria compared to the cytoplasm, it is reasonable to assume that it is the larger cytoplasmic dNTP pool that is controlling the much smaller mitochondrial pool.

We label the combined mitotic and postmitotic cells as ‘normal’ to contrast them with the final category which is transformed cells (Figure 3D) consisting of HeLa, HOS, and 3T3 cells. The transformed cells show no significant correlation between the mitochondrial and cytoplasmic concentrations for dTTP and dATP. This is in stark contrast to the normal cycling cells (Figure 3A) which had a very strong correlation. The statistics are summarized in Table 6.

Table 6: Statistics for correlations between mitochondrial and cytoplasmic dNTP concentrations. NS = not significant.

Cell Type	**dNTP Type**	**Number of Observations**	**Pearson R^2**	**p-value**	**Slope**
Mitotic	dTTP and dATP	7	0.90	9×10^{-4}	0.37 ± 0.05
Postmitotic	dTTP and dATP	8	0.01	0.77	NS
Normal (Mitotic + postmitotic)	dTTP and dATP	15	0.90	5×10^{-8}	0.41 ± 0.04
Normal (Mitotic + postmitotic)	dTTP	9	0.92	3×10^{-5}	0.42 ± 0.04
Normal (Mitotic + postmitotic)	dATP	6	0.77	0.01	0.36 ± 0.09
Transformed	dTTP and dATP	10	0.05	0.53	NS
Mitotic	dCTP and dGTP	7	0.42	0.11	NS
Postmitotic	dCTP and dGTP	7	0.14	0.39	NS
Normal (Mitotic + postmitotic)	dCTP and dGTP	14	0.49	0.005	0.53 ± 0.15
Normal (Mitotic + postmitotic)	dCTP	8	0.88	0.0005	0.56 ± 0.08
Normal (Mitotic + postmitotic)	dGTP	6	0.16	0.42	NS
Transformed	dCTP and dGTP	10	1×10^{-5}	0.99	NS
Normal (Mitotic + postmitotic)	All dNTPs	29	0.62	3×10^{-7}	0.43 ± 0.06
Transformed	All dNTPs	20	0.03	0.45	NS

In Figure 3 the two different deoxyribonucleotides dTTP and dATP are plotted with different symbols. Although the amount of data for each deoxyribonucleotide separately is quite small, both dTTP and dATP appear to be following the same relationship between cytoplasmic and mitochondrial concentrations in mitotic cells and in the combined 'normal cell' category. There are enough measurements in the normal cell category (Figure 3C) to allow an analysis of dTTP and dATP separately, and they are independently statistically significant ($p = 3 \times 10^{-5}$ for dTTP and $p = 0.01$ for dATP). More importantly, the slopes on the linear regressions for dTTP and dATP analyzed separately are consistent with each other (0.42 ± 0.04 and 0.36 ± 0.09 respectively) (Table 6). The simplest interpretation of this is that a common mechanism is acting on both dATP and dTTP.

We fit a linear model of mitochondrial dTTP and dATP concentrations as a function of their cytoplasmic concentrations in normal cells obtaining the following equation:

$$[dNTP]_{mito} = (0.41 \pm 0.04)[dNTP]_{cyto} + (1.8 \pm 0.4)\,\mu M \quad \textbf{.....Eq. 1}$$

where dNTP is either dTTP or dATP and concentrations are measured in micromolar. The R^2 of this model was 0.9 and the p-value of the F-statistic was 5×10^{-8}. The model indicates that in normal cells, mitochondrial dTTP and dATP concentrations are slightly less than half the cytoplasmic dNTP concentration plus about 1.8 micromolar. If we assume that the mitochondrial salvage pathway is independent of the cytoplasm dNTP concentrations, then one simple interpretation of this model is that the slope represents the transport function between these two subcellular compartments and the intercept represents the production of the mitochondrial salvage pathway, independent of the

cytoplasmic pathways. Based on this linear model fit to the experimental data, we speculate that the mitochondrial salvage pathway alone is sufficient to support a concentration of roughly 2 micromolar of dATP and dTTP within the mitochondria. In postmitotic cells, the mitochondrial concentrations are in general higher than the cytoplasmic concentrations (Figure 3B). In these cells, because of low cytoplasmic concentrations, the intercept term of the model has increased influence on the mitochondrial concentrations compared to its influence in mitotic cells.

dCTP and dGTP observations: For dGTP and dCTP the connection between the mitochondrial and cytoplasmic concentrations is far less clear (Figure 4). No significant correlations exist for the mitotic and postmitotic cells analyzed separately (Figures 4A and 4B). When these data are combined into the normal cell category (Figure 4C) the correlation is significant ($p = 0.005$). As was seen with dTTP and dATP, dGTP and dCTP were not significantly correlated in the transformed cell data. When dCTP and dGTP were analyzed separately for the normal cell category the dCTP concentrations were significantly correlated ($p = 0.0005$) but the dGTP concentrations were not significant. The slope for the dCTP concentration correlation in normal cells was slightly larger (0.56 ± 0.08) than that obtained for dTTP and dATP (Table 6). The primary difference between the dNTP concentrations in the mitochondrial and cytoplasmic compartments occurs in dGTP, which is consistent with the concerns raised by Ferraro et al [68], and discussed above, about the validity of measured dGTP levels using current standard methods.

Interpreting the correlations in normal cells: The data show that in normal cells in culture, dTTP, dATP, and dCTP concentrations in the mitochondria are correlated with those in the cytoplasm with very highly significant p-values. While the mitochondrial dNTP concentrations within the quiescent cells when taken alone are not significantly correlated with the cytoplasmic dNTP concentrations, these values fit into the statistically significant linear correlation in the normal cycling cells. The lack of significant correlation within the quiescent cell data may be simply due to the small dynamic range of the concentrations within the quiescent cells, compared to the noise level in the measurements. dNTPs in mitochondria can in principle originate from two routes: import of cytoplasmic deoxynucleosides and subsequent phosphorylation within the mitochondria (the standard salvage pathway), and/or an import of phosphorylated deoxyribonucleotides from the cytoplasm (Figure 2). If the primary source of dNTPs within the mitochondrion was the salvage pathway then one would expect that the mitochondrial and cytoplasmic dNTP concentrations would be independent, since the salvage pathway could produce mitochondrial dNTPs completely independently of the cytoplasmic dNTPs. Our analysis of the available data shows this is not the case in normal cells and is in agreement with conclusions made by the researchers who produced the data. Our description of the original interpretation of the data is focused just on those conclusions that relate to our own, and we refer the readers to the original papers for the complete interpretations. Rampazzo *et al*. [59] in their study of transformed cells concluded that while dNTP levels were lower in the mitochondrial compartment than in the cytoplasmic compartment, the difference might be explained by different patterns of the concentrations in the three phosphorylation states, so that the summed

deoxyribonucleotide concentrations may be roughly equivalent in the two compartments. Since the deoxyribonucleotides other than dNTP were not measured in these experiments, their conclusion cannot be directly tested. In that paper Rampazzo *et al*. also reported that the mitochondrial dTTP level in the transformed cells varies with the cell cycle. In the later experiment by the same group Ferraro *et al.* [57] measured dNTP levels in non-transformed cells and concluded that the proportions of mitochondrial to cytoplasmic dNTP levels in non-transformed cells was similar to that in their previous experiment on transformed cells [59]. In contrast to these interpretations, we have chosen to concentrate just on the reported dNTP levels, instead of attempting to extrapolate to the mono-phosphate and di-phosphate levels. Also in contrast to these papers, we have determined that there is a very significant difference between the results from the non-transformed and the transformed cells.

The association between cytoplasmic and mitochondrial dNTP concentrations suggests a strong cytoplasmic control on the pathways that give rise to the mitochondrial dNTPs. The simplest form of this control would be the transport of deoxyribonucleotides from the cytoplasm to the mitochondrion with only a small amount of dNTP production from the mitochondrial salvage pathway. An alternative, but less parsimonious mechanism would involve a coordinated modulation of nucleotide metabolism in the two subcellular compartments. One caveat of our review is that the available data is based on cell cultures from a limited range of cell types, primarily lung and skin fibroblasts. Quiescent fibroblasts may not be a good general model for all non-cycling cells, in particular for neurons and muscle fibers. This data indicates the need to carry out similar experiments

simultaneously measuring the cytoplasmic and mitochondrial dNTP concentrations in these postmitotic cell types that are directly relevant to the genetic diseases involving altered mitochondrial dNTP production. Measuring the compartmental volumes in the same experiment in addition to measuring dNTP levels would allow for a direct comparison of dNTP concentration measurements from different labs and between cell lines, avoiding the parameter assumptions that were necessary here.

Since the mitochondrial dNTP levels are strongly affected by the cytoplasmic dNTP levels, alterations in many of the other genes of the cytoplasmic deoxyribonucleotide metabolism may also have phenotypes involving failure to properly maintain mitochondrial DNA. The hypothetical transport mechanism that shuttles deoxyribonucleotides into the mitochondria would also be a candidate for mtDNA depletion syndromes, and its expression pattern would be a factor in determining the vulnerability of tissues to mutations in the transporter. These results, showing that the mitochondrial and cytoplasmic dNTP levels are tightly correlated, greatly expand the range of proteins that may lead to mitochondrial dNTP imbalances, and thus to problems with mtDNA replication.

Interpreting the lack of correlations in transformed cells: The correlation between the mitochondrial and cytoplasmic dNTP concentrations, which is strong in normal cycling cells, is lost in this data from transformed cells. A comparison of Figure 3D (transformed cells) to Figure 4A (normal mitotic cells) shows that the range of values for both the mitochondrial and cytoplasmic dTTP and dATP concentrations is increased by roughly a

factor of three in the transformed cells compared to the normal cycling cells. It is possible that the higher percentage of S-phase cells in a transformed cell culture compared to a culture of normal fibroblasts contributes to this increase in dTTP and dATP concentrations. The dNTP metabolism in both pools appears to be altered, though one could argue from the distribution of the data (Figure 3D) that the cytoplasmic values are more systematically increased than are the mitochondrial values. However, there is not enough data currently to make a confident comparison. Certainly, the tight correlation seen in the normal cycling cells is disrupted in the transformed cells by some unknown mechanism. One might reasonably ask whether this disruption of the correlation between the dNTP levels is a minor consequence of the transformation process or is a fundamental (perhaps even necessary) part of the transformation process. The Warburg hypothesis proposes that a shift of energy metabolism from oxidative phosphorylation to glycolysis is intimately involved in the transformation of normal cells to the cancerous state, and not just a side-effect [69]. The Warburg hypothesis has gone in and out of favor over the decades since it was first proposed, though recent experiments support it [70]. Diminished transcription or translation of mtDNA-coded components of oxidative phosphorylation would diminish the ATP production in the mitochondria. The correlation of cytoplasmic and mitochondrial dNTP concentrations in normal cells and its disruption in transformed cells indicates that the transformation process alters the cytoplasmic-mitochondrial communication in dNTP levels. By our analysis, decoupling of dNTP concentrations can be attributed mostly to disproportionately higher dNTP concentrations in the cytoplasm, as the mitochondrial concentrations in such cells are generally not drastically elevated compared to normal cycling cells. One speculative mechanism that

could account for this disruption of the normally tight correlation in dNTP levels between the two compartments would be a limitation in the transport of deoxyribonucleotides from the cytoplasm into the mitochondrion. This could come about simply through the saturation of the transport mechanism as the cytoplasmic dNTP concentrations rise in the transformed cells, or it could come about through the active suppression of the transport mechanism as part of the cell transformation process. Aside from the potential importance of the loss of this correlation in dNTP levels as a feature of transformed cells, there is a great practical importance to this observation. This data supports the conclusion that transformed cells should not be used in studies of the mitochondrial deoxyribonucleotide metabolism, since something fundamental about that metabolism is altered in transformed cells. This would be inconvenient, since transformed cell lines are generally far easier to use in *in vitro* than are primary cell cultures. However, the data in Figures 3 and 4 clearly indicate that something critical is disrupted in the mitochondrial dNTP metabolism pathway, at least in these three transformed cell types. An additional concern is the lack of data on the mitochondrial compartment size in 3T3 and HOS cells, as discussed above. Conceivably, the parameter assumptions needed to convert the reported units to concentrations may introduce enough noise to mask a correlation between the two compartments in the transformed cells. Further work on this question is clearly needed. In particular, an experiment measuring mitochondrial and cytoplasmic dNTP concentrations in both normal cells and their transformed versions would be very valuable.

Our interpretations in the context of the problem with dNTP assays: As described earlier, Ferraro *et al.* [68] recently concluded that the dNTP levels measured by the Klenow polymerase assay could be significantly contaminated by ribonucleotides. Their results indicated that dTTP measurements would have minimal contamination problems. The fact that the dATP correlation slope (Table 6) is consistent with the dTTP correlation slope, and that in general the pattern in the dATP data is indistinguishable from the pattern in the dTTP data (Figure 3) gives us confidence in the dATP measured values. The dCTP measured values also showed a significant correlation between the mitochondrial and cytoplasmic concentrations in normal cells, though with a slightly higher slope than the dTTP or dATP correlations (Table 6). This slightly higher slope could reasonably be due to a ribonucleotide contamination in that assay, or it may reflect slightly different kinetics of the unknown mechanism causing this correlation. Finally the dGTP values in the two compartments showed no correlation and this is consistent with Ferraro *et al.*'s results showing that the dGTP measurements could possibly be strongly contaminated by ribonucleotides, though of course we cannot rule out the possibility that the apparent correlation between cytoplasmic and mitochondrial dNTP concentrations simply does not occur for dGTP.

Conclusion: We have carried out a meta-analysis of the available data on dNTP levels in the cytoplasmic and mitochondrial subcellular compartments. By compiling the data from multiple experiments into a single larger data set, we have been able to make quantitative interpretations and statistically significant tests of the data. Our review of the data showed that in normal cells the concentrations of dTTP and dATP in the mitochondrion

are very strongly correlated with that in the cytoplasm, but that this relationship does not occur in transformed cells. Thus, in terms of the subcellular distribution of dNTPs, transformed cells may not be suitable for studying normal *in vivo* regulation of intra-mitochondrial dNTPs.

The meta-analysis that we have carried out here, combining the results of multiple independent experiments, points the way toward a unified set of experiments carried out under consistent conditions and focused toward testing the hypothesis resulting from this meta-analysis. It would also be valuable to assess whether the extent of the cytoplasmic influence on the mitochondrial levels of dNTPs is different for the individual nucleotides, and if so, how divergent are the origins of the four canonical dNTPs? A suitable next step would be for a research group to simultaneously measure cytoplasmic and mitochondrial dNTPs in a broader set of cell lines including transformed cells, in a controlled, uniform environment. In order for measurement of dNTP levels to be truly useful, the extra effort of converting the experimentally convenient units of amount per million cells to the relevant units of concentration should be done. In many cases in this analysis we had to estimate values for missing information. One side effect of estimating this missing information is the possible introduction of noise into the data. The strong correlations existed despite this unavoidable complication. Fundamental measurements, such as cell volume and total mitochondrial volume, need to be reported in these studies in order to make the data comparable across different studies. While we understand the difficulty of the extra measurements needed to report dNTP levels in actual concentration units, we

would argue that the increased usability of the resulting data makes this effort worthwhile.

CHAPTER III

CORRELATED TISSUE EXPRESSION OF GENES OF CYTOPLASMIC AND MITOCHONDRIAL NUCLEOTIDE METABOLISMS IN NORMAL TISSUES IS DISRUPTED IN TRANSFORMED TISSUES

III.1. Introduction

This analysis was motivated by the following questions. What is the relationship between the expression of corresponding genes of cytoplasmic and mitochondrial nucleotide metabolisms? Can gene expression patterns explain the observed correlation patterns in dNTP concentrations? We also know that the cytoplasmic and mitochondrial compartments are in metabolic communication and can exchange deoxyribonucleotides. Therefore, deoxyribonucleotide levels in the cytoplasm can impact mitochondrial deoxyribonucleotide levels, and vice versa. Since it is well established that transformation is associated with altered cytoplasmic dNTP pools, does the transformation process have an effect on the link between the cytoplasm and mitochondria?

III.2. Overview

We investigated the expression of a set of nuclear genes encoding proteins of the corresponding pathways of cytoplasmic and mitochondrial nucleotide metabolism in normal and cancerous tissues. We also included ribonucleotide reductase in our analysis. We were interested in determining the extent of coordination between these two corresponding metabolisms at the gene expression level in healthy tissues and whether

healthy and cancerous tissues differed in the coordination of gene expression of the two metabolisms. This analysis revealed a large number of highly significant positive correlations between the tissue expression profiles of the genes of the mitochondrial and cytoplasmic pathways in normal tissues indicating that in normal tissues the two metabolisms coordinately generate deoxyribonucleoside triphosphates. In transformed tissues, this correlation structure was disrupted. Multiple correlations involving the mitochondrial nucleoside kinase gene DGUOK were statistically significantly different between normal and transformed tissues suggesting that control of DGUOK expression relative to other cytoplasmic genes is important in transformed tissues.

A paper describing the work presented in this chapter is in preparation.

III.3. Methods

Selection of genes: The list of relevant genes was defined based on Reactome's 'Metabolism of nucleotides' pathway [71]. Within 'Metabolism of nucleotides', the sub-categories of interest to us were the reactions of the cytoplasmic and mitochondrial pathways of 'Purine salvage', 'Purine catabolism', 'Pyrimidine salvage', and 'Pyrimidine catabolism'. These sub-categories are made of reactions of anabolism or catabolism of nucleotides, and contain the reactions of intra-mitochondrial salvage of deoxyribonucleosides, which were the focus of our analysis. Genes coding for enzymes involved in these reactions were chosen for our analysis. Genes coding for enzymes involved in anabolism or catabolism of nucleosides were not included (e.g., thymidine phosphorylase). Genes coding for interconversion of nucleotides were also not included

(eg: thymidylate synthase). Given its importance in maintaining both cytoplasmic and mitochondrial dNTPs, we included ribonucleotide reductase as a special exception although it does not conform to the above criteria. All genes are encoded by the nuclear genome. We refer to them as ‘cytoplasmic’ and ‘mitochondrial’ to refer to the localization of the proteins encoded by the genes.

Obtaining expression values: The NCBI UniGene database provides EST frequencies of UniGene clusters, which are representative of the mRNA frequencies of the gene that corresponds to that cluster. The features of the UniGene database are described in [72]. All of the data is from human tissue samples. We obtained EST profiles for our selected genes from the UniGene database build #228 for the set of UniGene-classified ‘Breakdown by Body Sites’ and ‘Breakdown by Health State’ tissues. The first category is comprised of tissues such as muscle, eye, liver, etc, and the second category is comprised of tumors, carcinomas, cancers, etc. We therefore denote these categories as ‘normal tissues’ and ‘transformed tissues’, respectively. We did not include expression values for the tissues ‘ascites’ in the normal category and ‘normal’, and ‘non-neoplasia’ in the transformed category because of the ambiguity of the classification of those tissues, leaving 44 tissues in the normal category and 24 tissues in the transformed category. For four genes in our target set (TMPK2, AK6, NME2, and NT5C1A) we did not find expression values in UniGene, leaving 25 genes, of which five encoded mitochondrial enzymes. Our final dataset was comprised of expression values (transcripts per million) of 25 selected genes in 44 normal tissues and 24 transformed tissues. EST counts came

from non-subtracted and non-normalized libraries. The list of genes is given in Tables 7 and 8.

Table 7: Cytoplasmic protein genes used in this analysis.

Gene	Protein product
RRM1	ribonucleotide reductase subunit M1
RRM2	ribonucleotide reductase subunit M2
RRM2B	ribonucleotide reductase subunit M2B
TK1	thymidine kinase 1
DCK	deoxycytidine kinase
AK1	adenylate kinase 1
AK5	adenylate kinase 5
GUK1	guanylate kinase 1
CMPK1	cytidine monophosphate kinase 1
DTYMK	deoxythymidylate kinase
NME1	nucleoside diphosphate kinase 1
NME3	nucleoside diphosphate kinase 3
ADK	adenosine kinase
NT5E	5'-nucleotidase, ecto
NT5C2	5'-nucleotidase, cytosolic II
NT5C1B	5'-nucleotidase, cytosolic IB
NT5C	5', 3'-nucleotidase, cytosolic
NT5C3	5'-nucleotidase, cytosolic III
UCK1	uridine-cytidine kinase 1
UCK2	uridine-cytidine kinase 2

Table 8: Mitochondrial protein genes used in this analysis.

Gene	**Protein product**
TK2	thymidine kinase 2
DGUOK	deoxyguanosine kinase
NT5M	5',3'-nucleotidase, mitochondrial
AK2	adenylate kinase 2
NME4	nucleoside diphosphate kinase 4

Statistics: For statistical robustness, we used the non-parametric measure of Spearman rank correlation to measure the strength of pairwise relationships. Correlations that were statistically significantly different between normal and transformed tissues were obtained using Fisher's z transformation.

The full dataset and correlations are presented in Tables 9-11 in the Appendix.

III.4. Results

In a set of 25 genes, 300 gene-pairs are possible. For each of the 300 gene-pairs, we calculated the non-parametric Spearman rank correlation in both normal and transformed tissues. In Figure 1 we give an example of this correlation for the mitochondrial protein gene DGUOK and cytoplasmic protein gene GUK1. In normal tissues, the correlation of the expression levels is 0.46, with the highly significant p-value of 0.001 (Figure 5A). Note that since we are using a non-parametric correlation, any outliers such as can be seen in Figure 5A, have minimal effect on the correlation value. In transformed cells (Figure 5B), the correlation is -0.23 with an insignificant p-value of 0.26.

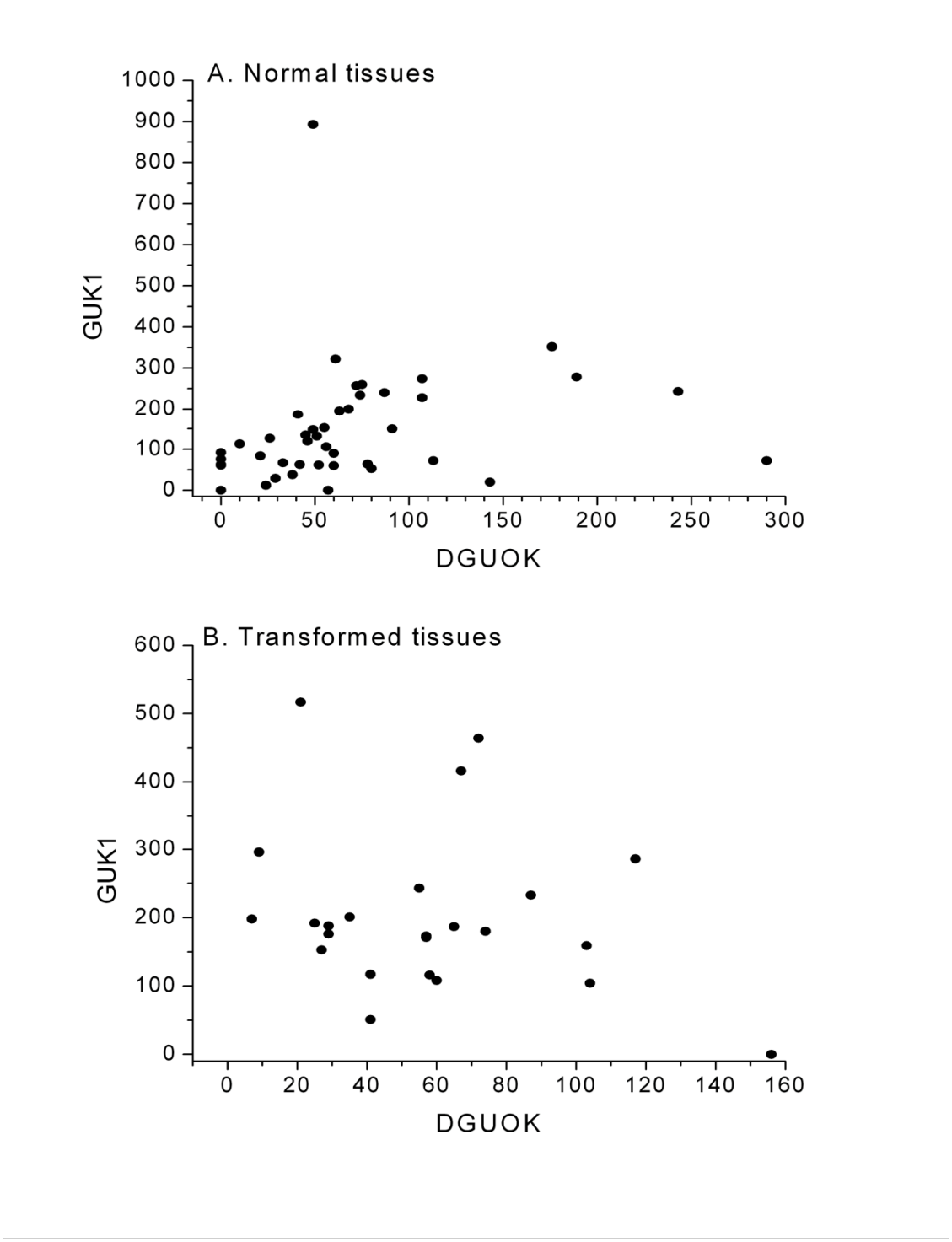

Figure 5: Correlation between DGUOK and GUK1 in (A) normal and (B) transformed tissues. The Spearman correlation Rho in normal tissues is 0.46 and is highly significant (p = 0.001), but is not significant in transformed tissues (Rho = -0.23, p = 0.26).

Correlations in transformed tissues are not independent of the correlations in normal tissues: We investigated the entire set of correlations to test for the presence of any systematic trends. The results are shown in Figure 6. Each point is a pair of genes, and their correlation in normal tissues and transformed tissues is represented by the X axis and Y axis respectively. The Spearman correlation between the correlations within the two tissue categories is 0.52 ($p < 10^{-4}$). Thus, the correlations in transformed tissues are not independent from the correlations in normal tissues. This reproducibility of the general pattern in expression levels between the two data sets lends support for the validity of our analysis of these correlations. However, there is an important difference between the correlations in the transformed tissues compared to the normal tissues. For 176 of the 300 pairs, the correlation in normal tissues was higher than the corresponding correlation in transformed tissues. Note that the line in Figure 6 is the line of equal values, not a fit to the data. The number of gene pairs below this line (176 of the pairs) was statistically significantly different from 150 (50% of 300) with a chi-square p-value of 0.002. In Figure 6, the gene pairs are color-coded based on whether their protein products are cytoplasmic and mitochondrial. However, visually there appears to be no difference in the patterns of the correlations for the three different categories of gene pairs.

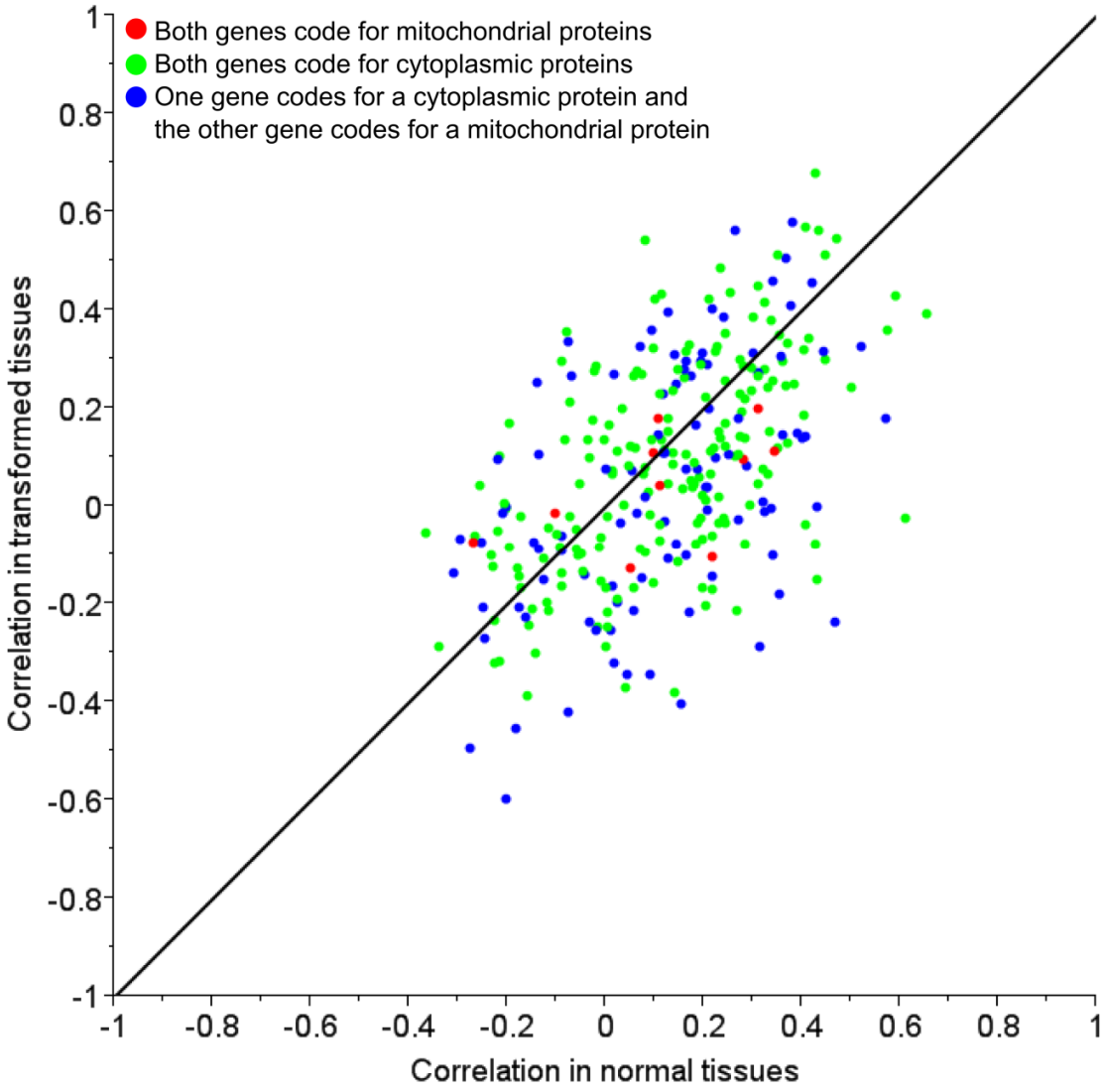

Figure 6: Magnitudes of all 300 correlations in normal and transformed tissues. Each point is the magnitude of the Spearman correlation for a pair of genes. The line of equal values is shown. Red, both genes code for mitochondrial enzymes; green, both genes code for cytoplasmic enzymes; and blue, one gene codes for a cytoplasmic enzyme and the other gene codes for a mitochondrial enzyme. The correlations in transformed tissues are not independent of the correlations in normal tissues (Spearman correlation = 0.52, $p < 10^{-4}$). The number of correlations below the equal value line, 176, is statistically significantly (chi-square test, $p = 0.002$) greater than 150 (50% of 300) indicating a trend of higher magnitudes of correlations in normal tissues.

Differences in normal and transformed tissue correlations are not due to different sample sizes: One possible confounding factor in this analysis is that the number of tissues in the transformed category was only 24, which is a smaller number than the 44 tissues in the normal category. To control for this difference, we investigated the influence of the sample sizes on the number of significant correlations in this set of genes. We hypothesized that even when the sample size of the normal category was artificially made equal to that of the transformed category, the number of significant correlations in the truncated normal dataset would still exceed the number observed in the transformed category. The results are presented in Figure 7. These datasets for normal tissues were truncated by choosing 20 tissues randomly (out of 44) and removing the expression values for all genes for those 20 tissues. This cut the number of normal tissues to be equal to the number of transformed tissues, removing the potential for bias. This procedure was repeated to generate 100 random subsets of the normal dataset. The mean number of significant correlations in the truncated datasets was 43.5 with a standard error of 0.9. The number of significant correlations in none of the 100 truncated datasets was lower than the number observed in the full set of transformed tissues, indicating an empirical p-value of less than 0.01. We can conclude that the smaller number of significant correlations in transformed tissues compared to normal tissues is not simply due to the smaller sample size.

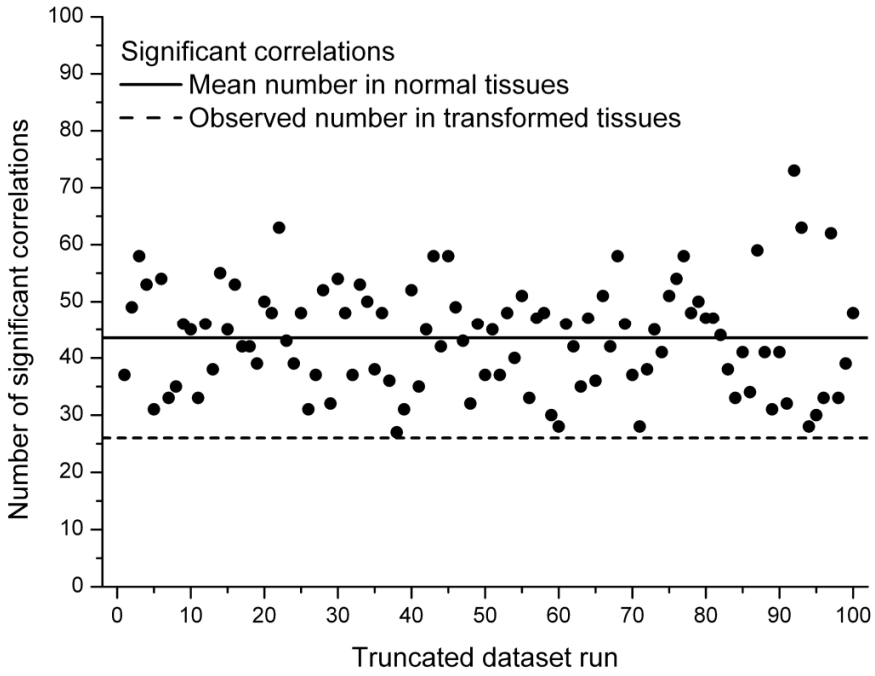

Figure 7: Smaller number of correlations in transformed tissues is not simply due to smaller sample size. We randomly chose 20 tissues and removed all gene expression values in order to truncate the number of tissues in the normal dataset to equal the number in the transformed dataset. This procedure was repeated 100 times, and for each truncated dataset the number of significant correlations was recorded. The mean of the resulting distribution was 43.5 with a standard error of 0.9 in the truncated normal datasets compared to the 26 correlations observed in the transformed tissue dataset containing the same number of tissues.

Transformed tissues have more negative correlations than normal tissues: Out of the 300 gene-pair correlations, 83 were negative in normal tissues while 120 were negative in transformed tissues. Note that these numbers include both significant and non-significant correlations. As the non-significant correlations are by definition not statistically significantly different from 0, there should be no systematic trend in the sign of the correlations. However, that was not the case and the difference in the number of negative correlations was statistically significant (Fisher's one-tailed p-value = 0.0009). Considering just the significant correlations, four out of the 26 correlations in transformed tissues were negative, while three out of the 66 correlations in normal tissues were negative. This difference was not statistically significant, likely due to small scale of the numbers of significant negative correlations.

Cytoplasmic and mitochondrial genes are coordinately expressed in normal tissues and this coordination is disrupted in transformed tissues: Figure 8 shows the significant correlations between genes for cytoplasmic proteins and mitochondrial proteins in normal (A) and transformed (B) tissues. We emphasize that all of these genes are located in the nuclear genome, not the mitochondrial genome. The distinction is between the subcellular localization of the gene products, not the localization of the genes themselves. For the purpose of focusing our analysis, we only plotted here the correlations between cytoplasmic protein and mitochondrial protein genes and disregarded those correlations where either both genes were for cytoplasmic proteins or both genes were for mitochondrial proteins. In Figure 8, red circles are mitochondrial protein genes and blue circles are cytoplasmic protein genes. Genes are further grouped

and aligned by enzyme class, indicating the role of the enzyme within the pathway. Solid lines represent positive correlations between gene expression levels and dashed lines represent negative correlations. The bold lines (greater width) are the correlations with the absolute value of the magnitude greater than 0.5.

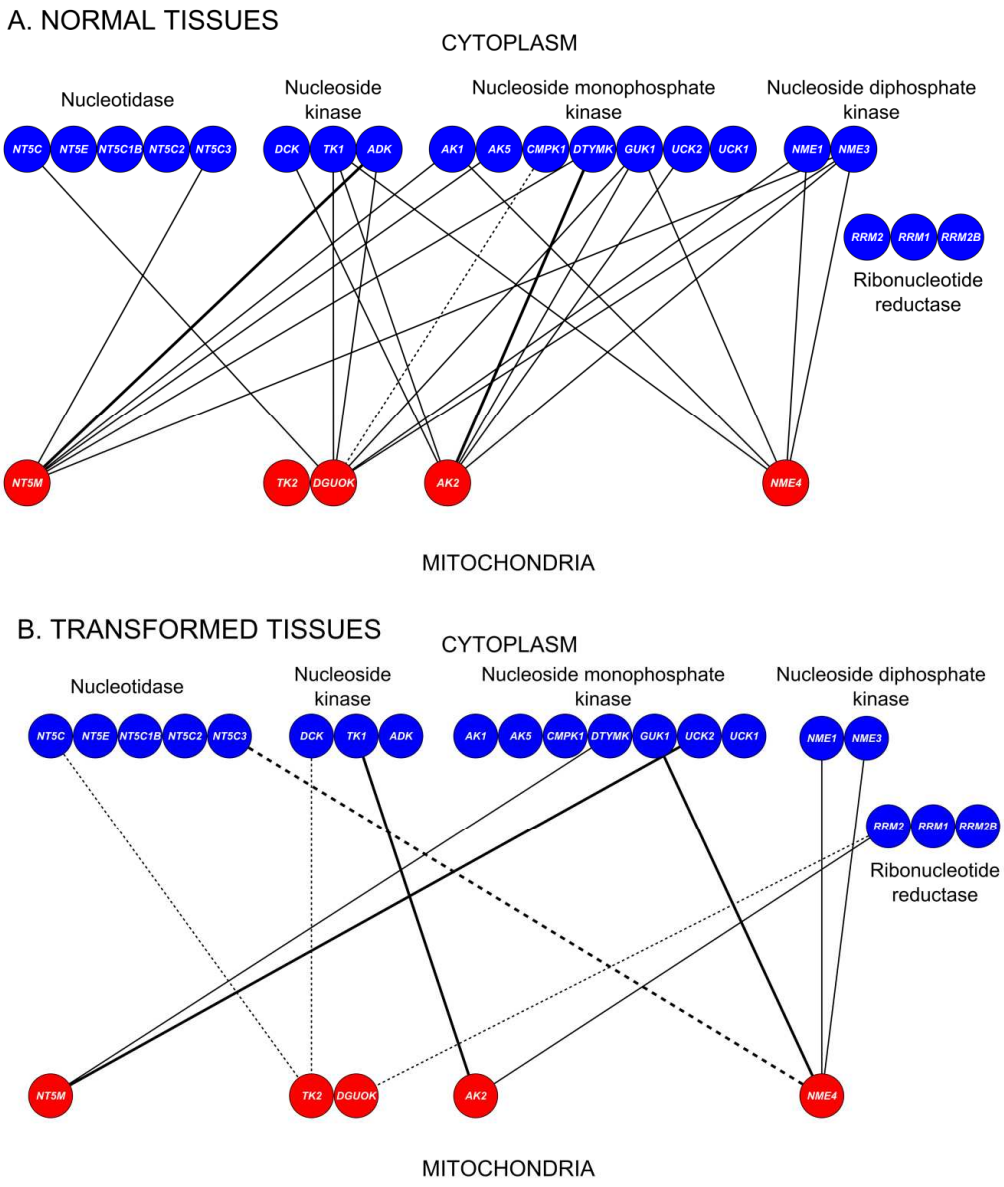

Figure 8: Statistically significant ($p < 0.05$) correlations between cytoplasmic and mitochondrial protein genes in normal and transformed tissues. A, normal tissues; B, transformed tissues; Blue, cytoplasmic protein genes; Red, mitochondrial protein genes; Solid lines, positive correlations; dashed lines, negative correlations. Lines with greater width represent absolute values of correlation magnitudes (Spearman Rho) of more than 0.5. Cytoplasmic and mitochondrial genes are coordinately expressed in normal tissues and this coordination is disrupted in transformed tissues. The complete list of correlations is presented in Table 11 in the Appendix.

As seen in Figure 8A, normal tissues have a large number of significant correlations linking the tissue expression of cytoplasmic and mitochondrial protein genes. Moreover, all but one of the correlations is positive. Mitochondrial protein genes of the different enzyme classes are correlated to the cytoplasmic protein genes not only of the corresponding enzyme classes, but also to the cytoplasmic protein genes of other enzyme classes. Clearly, in normal tissues, the expression of cytoplasmic and mitochondrial proteins of this metabolism is coordinately up-and-down regulated. However, this coordination is disrupted in transformed tissues (Figure 8B). The number of correlations is much smaller in transformed tissues. As shown in Figure 7, this reduction is not simply due to the smaller sample size of the transformed category. The frequency of negative correlations is also higher in the transformed tissues. The correlations between the corresponding cytoplasmic and mitochondrial protein genes of the same enzyme classes, so numerous in normal tissues, are lost in the transformed tissues except within the nucleoside diphosphate kinase group, the final step in the salvage pathway to form nucleoside triphosphates needed to replicate DNA. This is interesting because of the evidence that puts the localization of mitochondrial NME4 protein to the mitochondrial intermembrane space [11]. The mitochondrial intermembrane space is considered to be in equilibrium with the cytoplasm for the small molecules that are the substrates of these enzymes, making the designation of this space as mitochondrial or cytoplasmic somewhat ambiguous. Mitochondrial AK2 also has been reported to localize to the intermembrane space [10]. As seen in Figure 7B, AK2 is positively correlated with cytoplasmic protein genes in the transformed tissues. Thus, genes coding for nucleotide metabolism enzymes located in the mitochondrial intermembrane space are expressed coordinately with the

genes encoding enzymes of cytoplasmic nucleotide metabolism in transformed tissues. On the other hand, DGUOK and TK2, which are nucleoside kinases localized to the mitochondrial matrix, are exclusively negatively correlated with cytoplasmic protein genes. Additionally, the positive correlations of NT5M, a mitochondrial nucleotidase that dephosphorylates nucleoside monophosphates to nucleosides, support the conclusion that the equilibrium of the metabolism in the mitochondrial matrix is shifted towards deoxyribonucleosides rather than phosphorylated deoxyribonucleotides. Together, the correlation structure in transformed tissues indicates that mitochondrial intermembrane space metabolism is coordinately regulated with the cytoplasmic metabolism while the matrix metabolism is negatively regulated.

Genes of cytoplasmic nucleotide metabolism have higher expression in transformed tissues: From Figure 8B, we observed that the expression of mitochondrial protein genes is generally negatively correlated with the expression of the cytoplasmic protein genes. But in which subcellular compartment is expression significantly changed? To answer that question, we tested for statistically significant differences between gene expression in normal tissues compared to the expression in transformed tissues, using the non-parametric Wilcoxon-Mann-Whitney test. The results are shown in Figure 9. Six of our 25 genes had significantly different ($p < 0.05$) expression levels between normal and transformed tissues. Out of these six genes, five are for cytoplasmic proteins. The only mitochondrial protein gene in this group, NME4, codes for the nucleoside diphosphate kinase that has been reported to be localized to the mitochondrial intermembrane space [11]. As mentioned above, the mitochondrial intermembrane space is generally

considered to be in equilibrium with the cytoplasm for small molecules. As seen in Figure 9, genes encoding several critical and highly regulated members of cytoplasmic nucleotide metabolism such as RRM2, TK1, and NME1 have higher expression in transformed tissues. In fact, all of the genes whose expression was significantly different between the two tissue categories had higher expression in the transformed category. Thus, Figure 9 indicates, not surprisingly, that cytoplasmic nucleotide metabolism is upregulated in transformed tissues. None of the genes coding for mitochondrial matrix proteins are significantly different in their expression in normal and transformed tissues. Thus, unlike the cytoplasmic metabolism, the mitochondrial metabolism is not upregulated in transformed tissues. The negative correlations between the two metabolisms seen in Figure 8B additionally indicate that higher expression of the cytoplasmic protein genes is associated with lower expression of the mitochondrial protein genes in the transformed tissues. In Figure 9, we also observe that there is a noticeable overlap between the distributions of expression in normal and transformed tissues. However, in general transformed tissues contain fewer values of zero expression compared to normal tissues indicating that the switch from no expression in normal tissues to detectable expression in transformed tissues is an important driver of the statistically significant differences in expression. It should be mentioned that a statistically significant difference in expression does not necessarily equate to biologically significant difference. We also note the overlap between the distributions of expression values in normal and transformed tissues shown in Figure 9. Although we have used box-plots to capture the data, note that statistical significance was assessed using a non-parametric test.

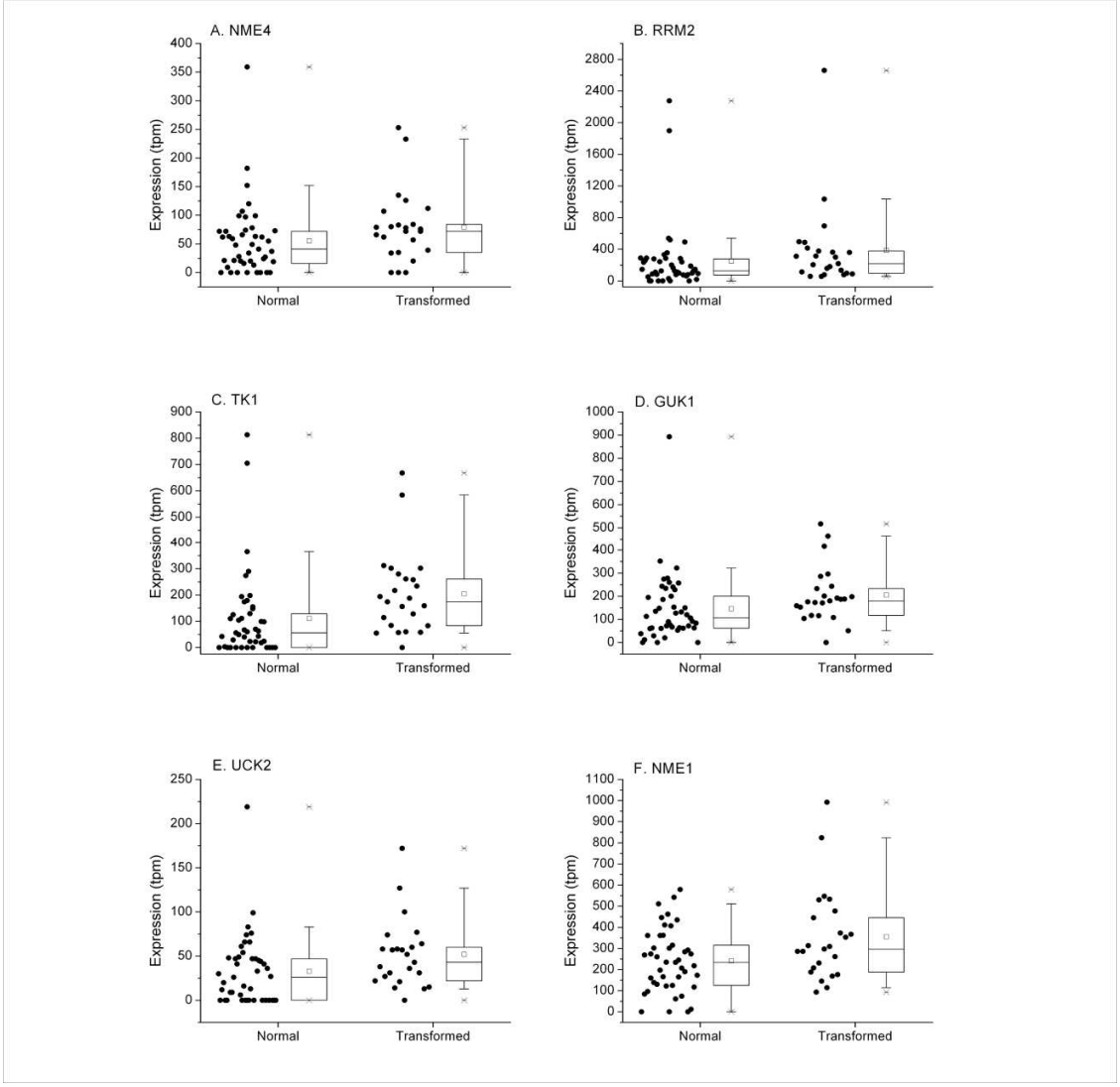

Figure 9: Genes with statistically significantly different expression between normal and transformed tissues based on Wilcoxon-Mann-Whitney test. The expression of all genes is higher ($p < 0.05$) in transformed tissues and except NME4, all genes code for cytoplasmic enzymes. A. NME4, p-value = 0.03. B. RRM2, p-value = 0.03. C. TK1, p-value = 0.0007. D. GUK1 = 0.01. E. UCK2, p-value = 0.01. F. NME1, p-value = 0.03.

DGUOK expression is important for transformed tissues: Which correlations distinguish normal tissues from transformed tissues? We answered this question by using the Fisher r to z transform to find the correlations that are statistically significantly different between normal and transformed tissues. The results are shown in Figure 10. Again, only the correlations connecting mitochondrial genes with cytoplasmic genes are evaluated. All three correlations with significant changes ($p < 0.05$) switched from being positive in normal tissues to being negative in transformed tissues. More importantly, all three correlations involved a single gene for a mitochondrial protein, DGUOK. This suggests that the control on the expression of DGUOK relative to the expression of other genes could be an important characteristic of transformed tissues. DGUOK is a mitochondrial matrix nucleoside kinase acting on deoxyguanosine and deoxyadenosine. Thus, due to its influence on dGTP and dATP synthesis, the expression of DGUOK is important for mtDNA maintenance.

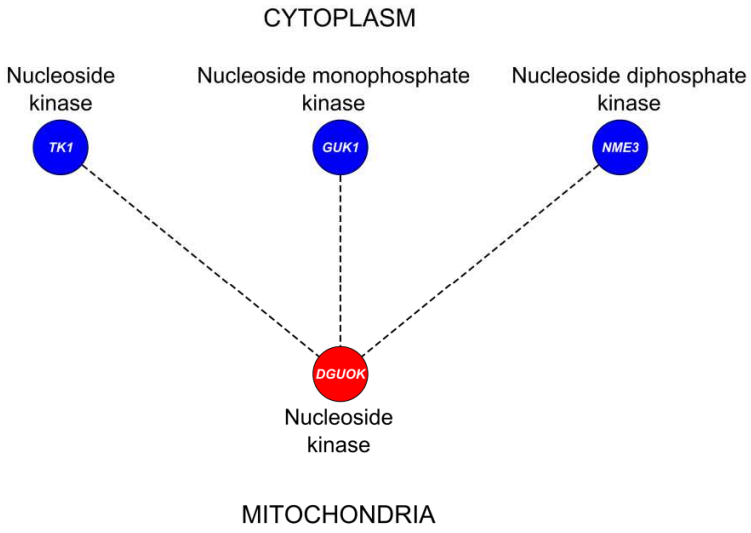

Figure 10: Correlations that are statistically significantly different ($p < 0.05$) between normal and transformed tissues. Only correlations connecting cytoplasmic and mitochondrial protein genes are shown. All correlations changed from positive in normal tissues to negative in transformed tissues and all correlations involved mitochondrial DGUOK.

III.5. Discussion

mRNA levels do not necessarily predict protein levels and protein levels are also controlled by translation rates and degradation rates. A more subtle point is that the strongest or the most significant correlations of any quantities may not necessarily be the most biologically significant. Even considering these warnings, the pattern in the expression levels of this set of genes is consistent and is indicative of a strong relationship between the parallel mitochondrial and cytoplasmic metabolic pathways for dNTPs. Furthermore, it is clear that this strong relationship is disrupted in transformed cells.

Evidence from mammalian cell-culture models [53, 73] supports the paradigm that mitochondrial DNA molecules replicate randomly throughout the cell-cycle and continue replicating in postmitotic cells which do not replicate nDNA. To investigate the relationship between nucleoside salvage in the cytoplasm and mitochondria, we analyzed tissue expression profiles of genes involved in these two processes. The results give a consistent picture of a significant and positive linking between the parallel mitochondrial and cytoplasmic nucleoside salvage pathways that generate some of the substrate dNTPs for DNA replication. We observed that unlike the reported lack of coordination of mtDNA and nDNA replication, the expression profiles of genes encoding proteins that produce dNTPs were coordinated. Our observation suggests that dNTP production in the mitochondria increases correspondingly with increasing dNTP production in the cytoplasm and is consistent with the reports of deoxyribonucleotide transport between the cytoplasm and mitochondria. In further support, metabolic defects in cytoplasmic

nucleotide metabolism that manifest as reduced fidelity of replication of the mitochondrial genome are well-acknowledged [74]. Particularly, altered ribonucleotide reductase activity as a cause of DNA depletion in the mitochondria [25] is also well-established. Ribonucleotide reductase, and more generally the cytoplasmic pathway of *de novo* nucleotide metabolism generate the majority of dNTPs in the cytoplasm and also contribute to mitochondrial dNTP pools.

Figure 8A leads to the clear conclusion that the two parallel deoxyribonucleotide metabolisms collaborate to produce dNTPs in normal tissues. However, in transformed tissues (Figures 6 and 8B), we observed that correlations in the genes of cytoplasmic and mitochondrial nucleoside salvage were weakened, negative correlations were more frequent, and the total number of significant correlations was far smaller. Taken together, our results show that, at the gene expression level, the coordination between cytoplasmic and mitochondrial salvage genes is disrupted in transformed tissues. Dissecting the correlation patterns reveals two interesting insights. First, all correlations involving the mitochondrial nucleoside kinase genes TK2 and DGUOK in transformed tissues were negative. TK2 and DGUOK catalyze the first step of nucleoside salvage in the mitochondrial matrix. It follows that in transformed tissues, when dNTP production in the cytoplasm is high, dNTP production in the mitochondrial matrix through the salvage pathway would be suppressed. The positive correlations of the mitochondrial nucleotidase NT5M with cytoplasmic genes would also indicate that the mitochondrial metabolism is shifted towards deoxyribonucleosides. In this case, mitochondria would act as sources of deoxyribonucleosides via export to the cytoplasm through equilibrative

nucleoside transport. The second insight relates to the positive correlations shared by AK2 and NME4 with cytoplasmic genes. As noted earlier, AK2 and NME4 both localize to the intermembrane space, which is considered to be in equilibrium with the cytoplasm. This implies that the activities of AK2 and NME4 are more closely aligned to the enzymes of cytoplasmic nucleotide metabolism in transformed tissues. It seems that unlike the other mitochondrial enzymes, NME4 and AK2 are probably utilized to support deoxyribonucleotide metabolism in the cytoplasm in transformed tissues.

An interesting transcriptional correspondence between the two metabolisms was observed in serum-starved resting HeLa cells [75] where the cellular response to an siRNA-induced decrease in the mitochondrial nucleoside kinase DGUOK mRNA was an increase in the expression of the cytoplasmic deoxycytidine kinase DCK. In our analysis, we discovered three correlations involving DGUOK that were statistically significantly different between normal and transformed tissues. Moreover, each of the three correlations switched from being positive in normal tissues to being negative in transformed tissues. DGUOK is important for the maintenance of mtDNA. Mutations in DGUOK are associated with mtDNA depletion [76]. Interestingly, it has been shown that lack of mitochondrial DNA (rho^0) can lead to chromosomal instability in the nuclear genome [77]. We hypothesize that control of DGUOK expression is important in transformed cells and would recommend experimental validation of this hypothesis. One possible approach in this regard would be to alter the expression of DGUOK in transformed tissues or cells and investigate whether that affects the transformed state or transformation potential of transformed tissues or cells.

The Warburg Effect connects energy production, a key function of mitochondria, and cancer [69]. Most cancer cells generate cellular ATP through glycolysis even when oxygen is available [78, 79]. Mitochondria do not necessarily shut down in such cells. In fact, certain mitochondrial functions are essential for tumor cell proliferation [52]. We might speculate that by controlling the expression of a small set of nuclear genes encoding proteins of mitochondrial nucleotide metabolism, cancer cells would be able to control mtDNA replication and thus selectively control mitochondrial oxidative phosphorylation.

Our analysis discovered a large number of statistically significant and biological plausible correlations showing that genes of cytoplasmic and mitochondrial nucleotide metabolism are coordinately expressed in normal tissues. In transformed tissues, this relationship is disrupted. It would be valuable for a research group to test either the strongest or the most significant correlations and correlations involving critical genes such as ribonucleotide reductase and deoxyguanosine kinase. It would be particularly illuminating to investigate the same correlations first in a set of normal tissues or cells and then upon induction of transformation of those tissues or cells.

CHAPTER IV

ENZYME KINETICS OF THE MITOCHONDRIAL DEOXYRIBONUCLEOSIDE SALVAGE PATHWAY ARE NOT SUFFICIENT TO SUPPORT RAPID mtDNA REPLICATION

IV.1. Introduction

A considerable amount of data on the mitochondrial deoxyribonucleoside salvage pathway has accumulated over time. Most of this data was gathered from investigating discrete components of this pathway. There is a need for studying this collection of data in its entirety. This chapter presents a computational model for fulfilling this need. The mitochondrial salvage pathway is complex, and a systems analysis of this pathway as a whole is an important companion to the study of the individual enzyme kinetics. Our comprehensive computational model allowed us to investigate the dynamics and origins of mitochondrial dNTPs. Our modeling is based on experimentally measured kinetics and model results enable us to quantitatively track the concentrations as well as the balance of the various deoxynucleosides and deoxynucleotides over time within an individual mitochondrion.

The content of this chapter has been reproduced with revisions from a published paper on which I was first author [7].

IV.2. Overview

Using a computational model, we simulated mitochondrial deoxynucleotide metabolism and mitochondrial DNA replication. Our results indicate that the output from the

mitochondrial salvage enzymes alone is inadequate to support a mitochondrial DNA replication duration of as long as 10 hours. We find that an external source of deoxyribonucleoside diphosphates or triphosphates, in addition to those supplied by mitochondrial salvage, is essential for the replication of mitochondrial DNA to complete in the experimentally observed duration of approximately 1 to 2 hours [80]. For meeting a replication target of 2 hours, we found that almost two-thirds of the dNTP requirements had to be externally supplied as either deoxyribonucleoside di- or triphosphates, at about equal rates for all four dNTPs. Added monophosphates did not suffice. However, for a replication target of 10 hours, mitochondrial salvage was able to provide for most, but not all, of the total substrate requirements. Still, additional dGTPs and dATPs had to be supplied. Our analysis of the enzyme kinetics also revealed that the majority of enzymes of this pathway prefer substrates that are not precursors (canonical deoxyribonucleosides and deoxyribonucleotides) for mitochondrial DNA replication, such as phosphorylated ribonucleotides, instead of the corresponding deoxyribonucleotides. The kinetic constants for reactions between mitochondrial salvage enzymes and deoxyribonucleotide substrates are physiologically unreasonable for achieving efficient catalysis with the expected *in situ* concentrations of deoxyribonucleotides.

IV.3. Methods

As far as possible, we restricted our analysis to data from human enzymes. Exceptions are noted below. We assumed Michaelis-Menten kinetics for all enzymes except TK2 which has negatively cooperative kinetics with Hill coefficient less than 1 with deoxythymidine [6].

k_{cat} / K_m: K_m values were obtained from the literature [6, 8, 81-90] or the BRENDA database [91]. For most enzymes, we could only find a single report of kinetic parameters. For the nucleoside kinases DGUOK and TK2, we did find multiple reports of kinetic parameters. In these cases, we selected the reference providing the most comprehensive information. To compute k_{cat} values, we first obtained reported V_{max} values [6, 8, 81, 83-85, 87-90] and molecular weights [8, 82, 91, 92] of the various enzymes from the literature or the BRENDA database. If the enzyme was reported to be a multimer, we added the molecular weights of the subunits to calculate the molecular weight of the holoenzyme. The quantity k_{cat} / K_m (M^{-1} s^{-1}) was calculated from the reported values of V_{max} / K_m (with units of μmol min^{-1} mg^{-1} μM^{-1}) using the following conversion,

$$\frac{K_{cat}}{K_m} = \frac{V_{\max}}{K_m}(W_{enzyme})\left(\frac{10^6}{60}\right) \quad \textbf{Eq. 2}$$

where W_{enzyme} is the enzyme molecular weight. Reported values for K_m, V_{max}, and the calculated k_{cat} / K_m values are provided in Table 12 in the Appendix.

Substrate concentrations: Values for the concentrations of the deoxyribonucleoside, deoxyribonucleotide, ribonucleoside, and ribonucleotide substrates were used to calculate '(substrate) Concentration / (substrate) K_m' ratios. These values were used for a comparison of activities of the enzyme with different substrates and are not meant to be precise. Instead, rough order-of-magnitude concentration values were used to compare values for this ratio, which often varies by several orders of magnitude within a single

enzyme for different substrates. Literature reports suggest that mitochondrial dNTP pools are higher in actively cycling cells compared to quiescent cells [27, 32, 57, 93]. We assumed a 10-fold lower concentration of deoxyribonucleotides in quiescent cells, and chose 10 µM and 1 µM as reasonable representative estimates of mitochondrial dNTP concentrations in cycling and quiescent cells respectively. The basis of these estimates are the concentrations calculated from published values in HeLa cells [33] and quiescent fibroblasts [58] respectively. We used a value of 0.82 ml/g mitochondrial protein [61] to calculate concentrations from the measured pool sizes in HeLa cells, and we used the value of 92.3 μm^3 for mitochondrial volume per cell [60] to obtain the concentrations from the measured pool size in quiescent fibroblasts. For simplicity, we assumed ribonucleotides and deoxyribonucleotides to be equally concentrated in the three phosphorylation states (mono, di, or tri-phosphorylated). Again for simplicity we assumed all four nucleotides (dAXP, dCXP, dGXP, dTXP where X = phosphorylation state) to have equal concentrations. Nucleoside concentrations were assumed to be equilibrated between plasma, cytoplasm, and mitochondria and set at a constant 0.5 µM using a reported value for plasma concentration [94]. Lower nucleoside concentrations have also recently been reported [95, 96]. We have kept the higher value in our analysis since this is the most conservative choice. Lower nucleoside concentration values would make the problems that we point out in this analysis even more severe. Ribonucleotide concentrations were assumed to be constant and set at 100 µM, that is, one order of magnitude higher in cycling cells and two orders of magnitude higher in quiescent cells compared to deoxyribonucleotide concentrations. This is a fairly conservative (i.e. low) choice for the ribonucleotide concentrations. For other special cases of substrates (such as

dUMP, dI, or IMP) concentrations data are not readily available so we again assumed low concentration values for these substrates. The complete list of assumed concentrations is provided in Table 13 in the Appendix.

Inhibitions: In the case that we could not find K_i values of for enzyme inhibitors, we assumed competitive inhibition so that the K_i for the inhibitor was set to be equal to the K_m for that chemical as a substrate. Inhibition kinetics data [6, 8, 81, 85, 88, 90, 97] are provided in Table 14 in the Appendix.

Computational simulations: Our group has previously published a computational model of mitochondrial deoxyribonucleotide metabolism [93]. Parameter values for the model were based, whenever available, on published experimental values [6, 8, 9, 76, 81-86, 88-93, 97-102]. As part of the present work, we updated the model to reflect the findings since the original model was defined. We refer the readers to the previous publication for a complete explanation of the basic framework of the model [93]. Briefly, enzymatic reactions were modeled with Michaelis-Menten equations (except TK2, which is modeled by the Hill equation) and rates of change of metabolites were modeled using ordinary differential equations. The updates to the model include adding (e.g. CMPK2) and removing (e.g. SLC25A19 or DNC) pathway components and updated kinetics (e.g. inhibition terms and kinetic constants). The model was written in *Mathematica 7*. The model files and model constants are available as supporting information S1-S3 in the Appendix.

Deoxynucleoside transport was modeled through the ENT protein as equilibrative between the cytoplasm and mitochondria. Thus, the net rate of deoxynucleoside transport was defined using the Michaelis-Menten equation as follows:

$$V_{ENT,\,j} = \frac{V_{\max,\,j}[dN]_{cyto,\,j}}{K_{m,\,j}\left(1+\sum_i \frac{[C_i]}{K_{i,\,i}}\right)+[dN]_{cyto,\,j}} - \frac{V_{\max,\,j}[dN]_{mito,\,j}}{K_{m,\,j}\left(1+\sum_i \frac{[C_i]}{K_{i,\,i}}\right)+[dN]_{mito,\,j}} \quad \textbf{.....Eq. 3}$$

where j represents the four deoxynucleoside species (dA, dC, dG, dT) and i represents inhibitors. V_{max} and K_m were taken to be the same for both directions of transport.

The various enzymatic reactions (i.e., phosphorylations and dephosphorylations) were modeled using the Michaelis-Menten equation. Thus, the reaction velocity was

$$V = \frac{V_{\max}[S]}{K_m\left(1+\sum_i \frac{[C_i]}{K_{I,\,i}}\right)+[S]} \quad \textbf{.....Eq. 4}$$

where S stands for substrate and [C] stand for the concentration of any competitive inhibitors. For the reaction of dT with TK2, the above equation was modified by raising the K_m and [S] terms to the power 0.5 to represent the Hill coefficient.

The model of the mtDNA polymerization process was explained in the previous publication [93]. It models polymerization using fractions of the four deoxynucleotides in the mtDNA sequence, setting the prevalence of each base in the mtDNA light and heavy strands separately to match the prevalence in the rCRS reference sequence [103]. We

have modeled mtDNA replication as asynchronous [80] using the locations of the origins of replication of the light strand and the heavy strand.

Differential equations for the concentrations of the various metabolites were defined by adding and subtracting the relevant reaction velocity equations. For example, for dNMPs (deoxyribonucleoside monophosphates), the following differential equation models the rate of change of a particular dNMP:

$$\frac{d[dNMP_j]}{dt} = NK_j - NT_j + NMPK_{rev,\,j} - NMPK_{fwd,\,j} \quad \textbf{.....Eq. 5}$$

where NK represents the nucleoside kinase reaction, NT represents the nucleotidase reaction, NMPK represents the forward and reverse monophosphate kinase reactions. The kinetic constants and inhibition parameter values are available in Tables 12-14 in the Appendix.

We used this updated model to test the hypothesis that a source of deoxyribonucleotides in addition to intra-mitochondrial salvage is essential for completing mtDNA replication in cycling cells in the experimentally observed time of 1-2 hours [80]. To be conservative, we set the 'target' replication time to be 2 hours (requiring an average replication rate = 33136 (nucleotides) / 120 (minutes) = ~276 nucleotides / minute). We ran simulations with a replication time of 120 minutes (2 hours), with all dynamics including mtDNA replication starting immediately at the beginning of the simulation. We also tested a target replication time of 10 hours (requiring an average replication rate = 33136 (nucleotides) / 600 (minutes) = ~55 nucleotides / minute), reasoning that in

quiescent cells the time constraints for completing mtDNA replication may be more relaxed.

Transport of deoxynucleotides from the cytoplasm to the mitochondrial matrix was modeled in a simple manner, by setting a constant production term of either deoxynucleosides, dNMPs, dNDPs (deoxyribonucleoside diphosphates), or dNTPs. Transport was modeled as occurring at only one phosphorylation level at a time, in order to assess the effectiveness of transport at each level. The essence of our simulation experiments was to test whether mtDNA replication was completed in the target time under varying levels of added molecules, including no addition, of various (A, C, G, T) deoxynucleosides and deoxynucleotides. We note that in principle the additional source of deoxynucleotides in this model does not necessarily have to be import from the cytoplasm but could also be from other unknown intra-mitochondrial sources. However, considering the evidence that nucleotide transport does occur between the cytoplasm and mitochondria [17, 18], we assume that the additional source we have modeled corresponds to import from the cytoplasm. We tested multiple 'transport profiles'. A transport profile is composed of simply the rate of the transported deoxynucleosides and deoxynucleotides. For each transport profile, we ran 100 simulations each beginning with a different, randomly selected (with uniform probability) set of initial mitochondrial concentrations of each deoxynucleoside and deoxynucleotide. As an initial test of the level of exogenous precursor transport needed, we set equal rates of import for all four (A, C, G, T) nucleosides (or nucleotides) at a particular phosphorylation level and then let the rate of import vary from 0 to 1200 molecules per minute, in increments of 100. Thus,

for example, for testing whether transport of deoxynucleosides alone suffices, we ran 13 sets of 100 simulations. In each of those 13 sets, deoxynucleosides alone were imported at equal rates for each of the four nucleosides, in increments of 100 starting from 0 and up to 1200. Such simulation sets of 13 different import levels were conducted similarly for each phosphorylation level of the four deoxynucleoside species.

The initial conditions of the simulations were set randomly with a uniform distribution over a set range. The allowed range (minimum and maximum) of initial deoxynucleoside concentrations was 0.05 µM to 5 µM and the range of initial deoxynucleotide concentrations was 0.1 µM to 10 µM. We set the concentrations of ribonucleosides, ribonucleotides, and non-canonical deoxynucleosides and deoxynucleotides to be proportional to the randomly selected dN and dNXP concentrations (see Table 13 in the Appendix for details) and held these concentrations (which only acted as inhibitors) constant throughout the time course of the simulation. The simulations were repeated 100 times with varying initial conditions.

We extended the transport analysis further by obtaining the minimum number of molecules of each transported dNTP required for mtDNA replication to be completed in 2 hours (representing cycling cells) or 10 hours (representing quiescent cells). For the simulations to determine the minimum transport profiles, we tested whether the replication rate exceeded 55 (‘quiescent cells’, fixed initial concentrations: dNs = 0.5 micromolar and dNXPs = 1 micromolar) or 276 (‘cycling cells’, fixed initial concentrations: dNs = 0.5 micromolar and dNXPs = 10 micromolar) nucleotides per

minute. We started at equal import of all four dNTPs at a rate such that replication would be completed in slightly less than the target time (2 hours or 10 hours). Next, we decreased the import of one dNTP at a time to check whether the target replication rate was observed. We continued this relaxation process until we obtained the minimum transport for each individual deoxyribonucleotide species necessary to support the target replication rate.

IV.4. Results

The k_{cat} / K_m ratio: In Michaelis-Menten kinetics, k_{cat} and K_m are the basic parameters of an enzyme-substrate reaction pair. The parameter k_{cat} is the number of substrate molecules catalyzed per enzyme molecule per unit time, and K_m is the substrate concentration at which the reaction proceeds at half-maximal velocity. High k_{cat} and low K_m values imply a fast and efficient reaction, and thus, a high k_{cat} / K_m ratio indicate that this substrate is catalytically preferred by the enzyme. We searched the literature [6, 8, 81-90] and databases [91] and gathered the available data on the reaction kinetics of enzymes of mitochondrial nucleotide salvage. Figure 11A shows a plot of k_{cat} / K_m values. Each group of bars is for one enzyme, and within each group the bars are arranged from lowest to highest so that the best substrates lie to the right on each plot. For clarity, the substrates that are DNA precursors (presumed to be the 'proper' substrates of these enzymes) are in green, and non-DNA precursor substrates are in red. The k_{cat} / K_m values cover a very wide range and so are plotted on a logarithmic scale.

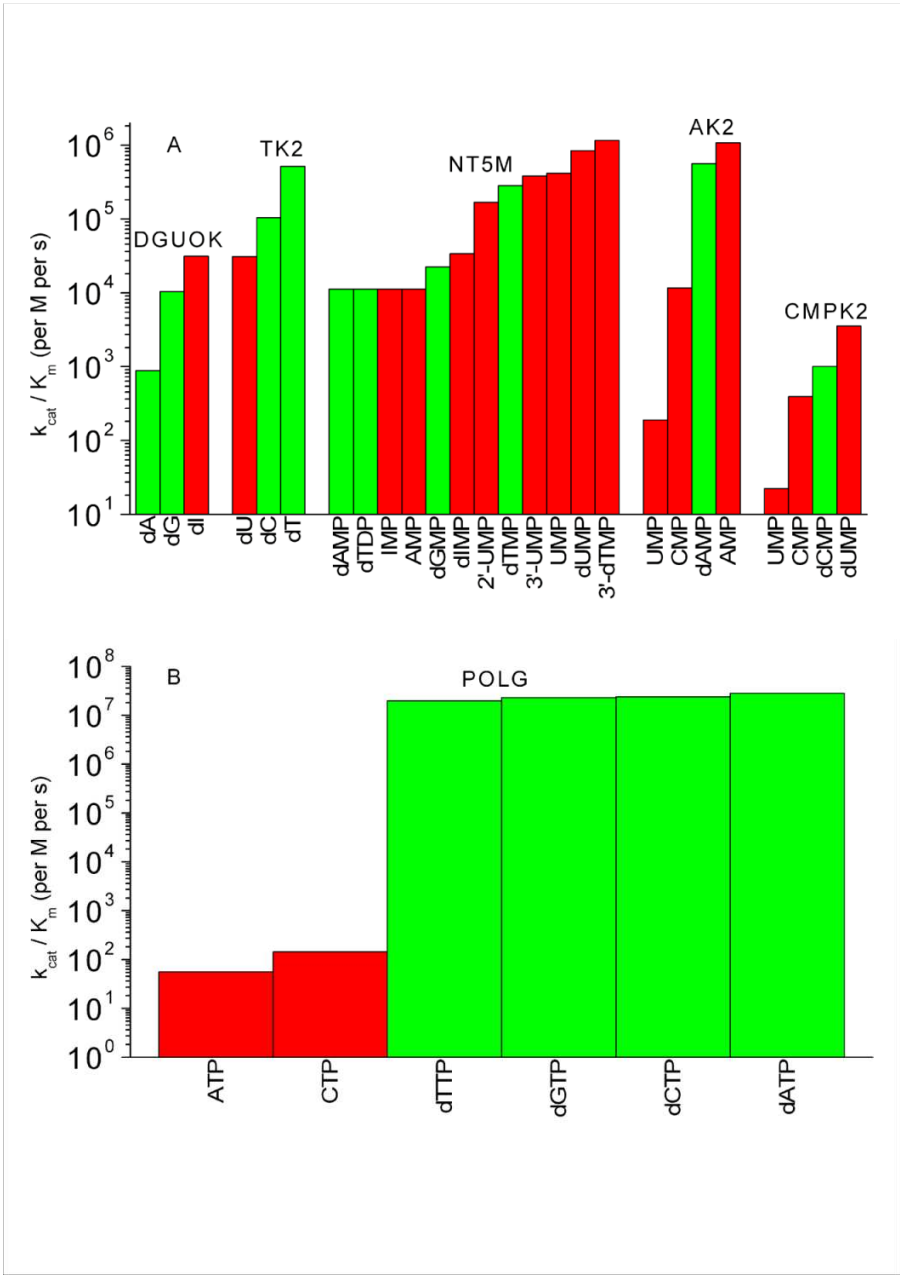

Figure 11: k_{cat} / K_m values of mitochondrial enzymes. (A) k_{cat} / K_m values of mitochondrial salvage enzymes. Each group of bars is for one enzyme, and within each such group the bars are arranged from lowest to highest so that the best substrates lie to the right on each plot. Substrates that are DNA precursors are in green, and non-DNA precursor substrates are in red. 2'-UMP and 3'-UMP refer to uridine 2' monophosphate and uridine 3' monophosphate. (B) k_{cat} / K_m values of the mitochondrial DNA polymerase POLG, justifying the use of k_{cat}/ K_m as a measure of substrate preference. Reproduced from Gandhi and Samuels (2011) [7].

Figure 11A shows that each of these enzymes has significant reactions with non-DNA precursors. More importantly, except for TK2, none of the mitochondrial enzymes have DNA precursors as their preferred substrates, as seen from the fact that the substrates which lie to the right in each group of bars are non-DNA precursors. Prior work [104] has estimated the theoretical maximum of k_{cat} / K_m for an enzyme-substrate pair. This maximum is constrained by the diffusion limit, and was estimated to be ~10^8 per M per second [104]. Compared to the diffusion limit, the k_{cat} / K_m values for reactions of the mitochondrial salvage pathway with DNA precursors are orders of magnitude lower (range = 888 to 5.63 x 10^5 per M per second). In summary, in both absolute and relative terms these enzymes of the mitochondrial salvage pathway (with the possible exception of TK2) do not appear to be optimized for discriminating mtDNA precursor substrates from chemically related non-precursor substrates.

To put the k_{cat} / K_m results in Figure 11A in perspective, Figure 11B is a plot of k_{cat} / K_m for the various substrates of the mitochondrial DNA polymerase gamma (POLG). In contrast to the enzymes of mitochondrial nucleotide metabolism, Figure 11B shows that, as expected, DNA precursors are preferably discriminated by POLG. This is true both absolutely and relatively. The k_{cat} / K_m values for the dNTP substrates approach the diffusion limit of ~10^8 per M per s, and the values for dNTP substrates are many orders of magnitude larger than the k_{cat} / K_m values of the ribonucleotide substrates. GTP and UTP kinetics data are not shown because the POLG kinetics with these potential substrates have not been measured.

The effects of substrate concentration: While the ratio k_{cat} / K_m captures the efficiency of a reaction between an enzyme and a substrate, it does not take into account the expected physiological concentration of the substrate, which may vary by several orders of magnitude between ribonucleotide and deoxyribonucleotide substrates. The ratio of '(substrate) Concentration / (substrate) K_m' provides information that is complementary to that revealed in the previous section by the ratio k_{cat} / K_m. When the substrate concentration is much smaller compared to the K_m, the enzyme is sensitive to substrate concentration and can thus operate at a range of velocities. However, the velocities in this range would be smaller than the maximum possible velocity. Depending on the relation between maximum possible velocity and the required rate of enzymatic output, substrate concentrations smaller than K_m can be a detriment. This is the case for the mitochondrial salvage enzymes because mtDNA replication has to satisfy certain time constraints. We searched the literature [6, 8, 81-90] and databases [91] for K_m values of the mitochondrial salvage enzymes for various substrates and their expected *in situ* concentrations. Figures 12A and 13A show plots of Concentration / K_m values for all of the enzyme-substrate pairs for which we could find data. As before, each group of bars is for one enzyme, and within each such group the bars are arranged from lowest to highest value of the ratio. Preferred substrates would be expected to have higher concentrations relative to the reaction K_m and thus would fall to the right in each enzyme. Substrates that are DNA precursors are plotted in green, and non-DNA precursor substrates are in red.

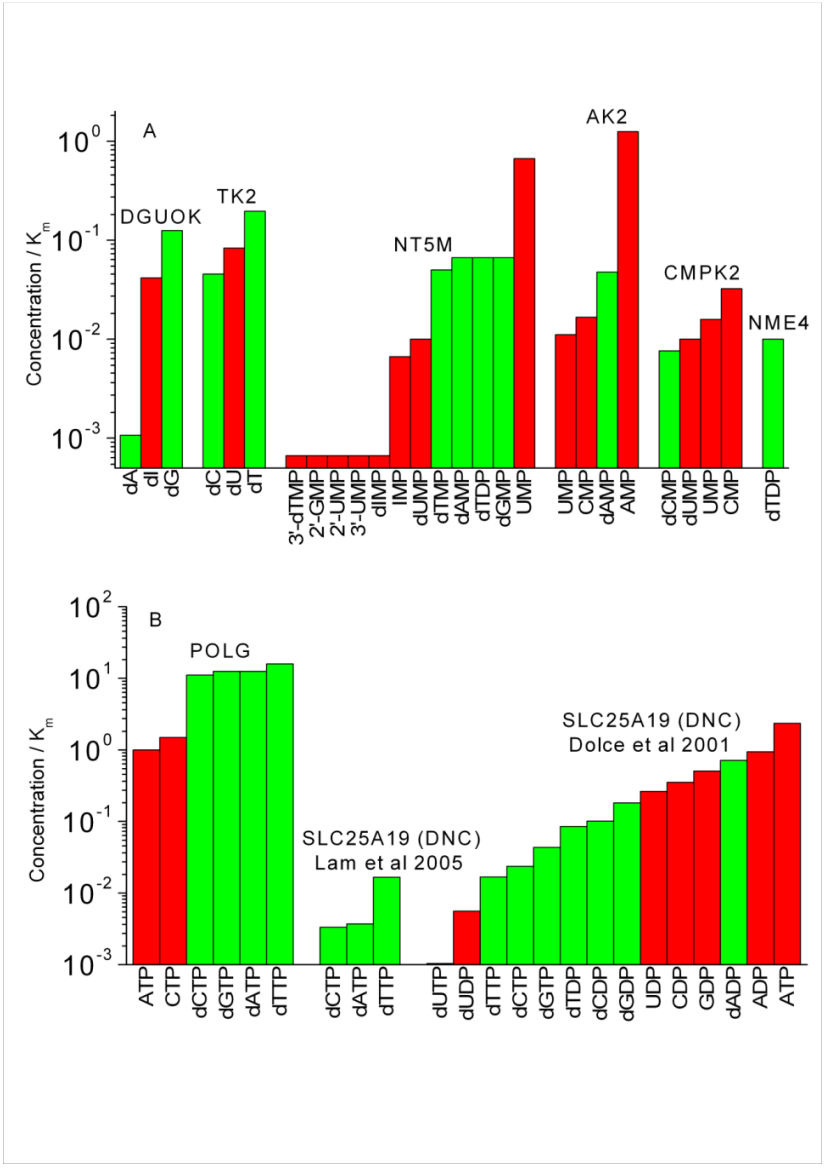

Figure 12: Concentration / K_m values in 'cycling cells' for mitochondrial enzymes. Concentration / K_m values at higher mitochondrial concentrations ('cycling cells') of the deoxyribonucleotide substrates (10 µM). (A) Values for mitochondrial salvage enzymes. All reactions involving DNA precursor substrates have Concentration / K_m values less than 1, suggesting that none of these reactions would be expected to be running at even half-maximal velocity. (B) Values for POLG and SLC25A19, justifying the principle of using the ratio Concentration / K_m as a measure of substrate preference. The Concentration / K_m ratio for dNTP substrates for POLG is about an order of magnitude larger than the ratios for reactions with rNTPs. The Concentration / K_m ratios of DNA precursor substrates of SLC25A19 are low. Reproduced from Gandhi and Samuels (2011) [7].

Figure 12A shows Concentration / K_m values at higher mitochondrial concentrations ('cycling cells') of the deoxyribonucleotide substrates (10 µM). The Concentration / K_m values for DNA precursor substrates range from 0.001 to 0.19. Thus, none of the reactions involving DNA precursor metabolism in the mitochondria would be running at maximal reaction velocity. In fact, since all reactions involving DNA precursor substrates have Concentration / K_m values less than 1, none of these reactions would be expected to be running at even half-maximal velocity. It is apparent that these enzymes of mitochondrial nucleotide metabolism have significant affinities for non-DNA precursors. In many cases, the enzymes have higher affinities for non-DNA precursors than for the DNA precursors. In the case of the nucleoside kinases TK2 and DGUOK, although they have higher affinities for DNA-precursors, there is a less than 10-fold difference from their preference of non-DNA precursors. For some reactions, the expected substrate concentrations are orders of magnitude lower than the reaction K_m values (range: 0.001 to 0.19). The same trends exist in the values of Concentration / K_m assuming lower mitochondrial concentrations of substrates (Figure 13A). Moreover, comparing Figure 13A (low deoxyribonucleotide concentrations) to Figure 12A (high deoxyribonucleotide concentrations), the disparity between DNA precursors and other substrates is more striking with an order of magnitude decrease in the Concentration / K_m ratio of the DNA precursor substrates (range: 0.0007 to 0.19). This was expected as we assumed mitochondrial ribonucleotide concentrations to be constant and independent of high or low mitochondrial deoxyribonucleotide concentrations.

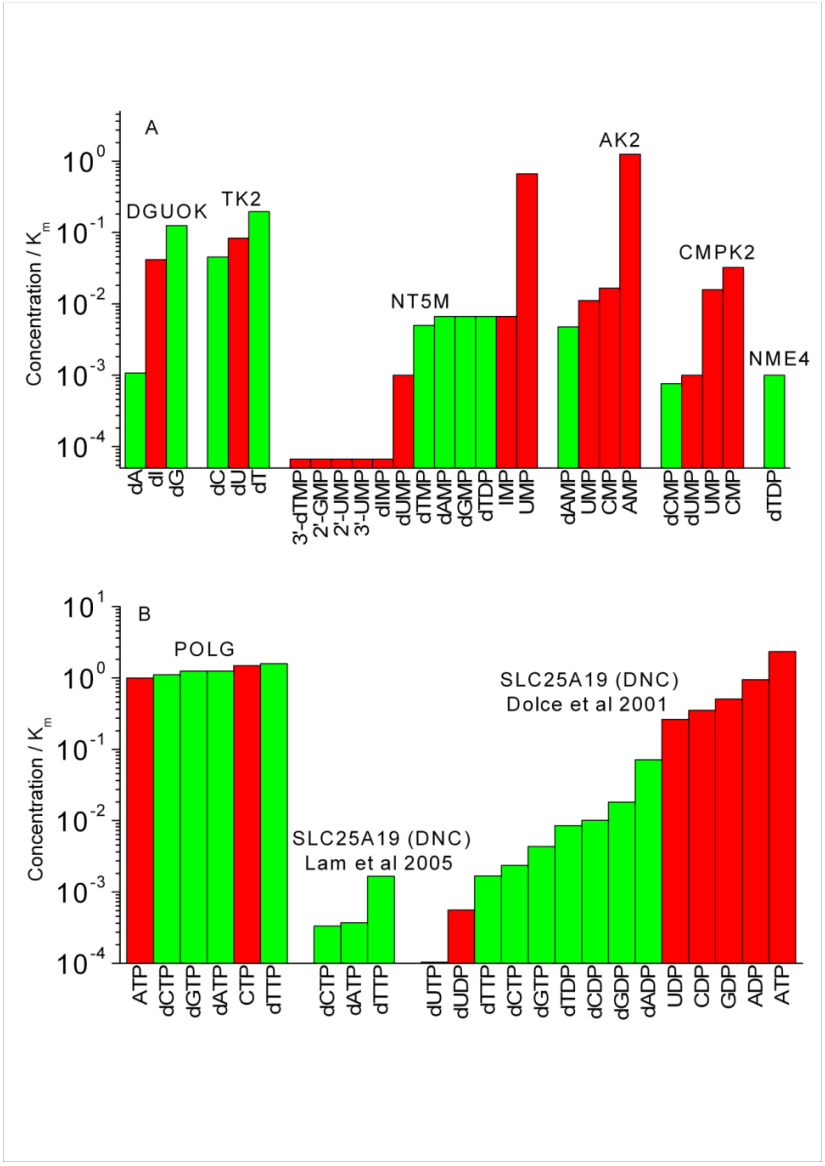

Figure 13: Concentration / K_m values in 'quiescent cells' for mitochondrial enzymes. Concentration / K_m values at lower mitochondrial concentrations ('quiescent cells') of the deoxyribonucleotide substrates (1 µM) for (A) mitochondrial salvage enzymes and (B) POLG and SLC25A19. Reproduced from Gandhi and Samuels (2011) [7].

To place these enzyme kinetics values in context Figures 12B and 13B show positive and negative examples justifying the principle of using the ratio Concentration / K_m as a measure of substrate preference. The Concentration / K_m ratio for dNTP substrates for POLG is about an order of magnitude larger than the ratios for reactions with ribonucleoside triphosphates (rNTPs) (Figure 12B). It is noteworthy that POLG is the only enzyme of the mitochondrial 'salvage' (DNA replication) pathway whose DNA precursor substrates have expected concentrations that are larger than the enzyme K_m values. For our negative example, we considered SLC25A19 (formerly named the deoxynucleotide carrier (DNC), now identified as the thiamine pyrophosphate carrier) [65] to be a suitable choice. In contrast to POLG, the Concentration / K_m ratios of DNA precursor substrates of SLC25A19 are low both in the absolute and the relative sense. Dolce et al [82] published data on the K_m and K_i values of substrates (we used K_i as a proxy for K_m if K_m was not reported) that were tested for transport by the SLC25A19 protein, and it is seen in Figures 12B and 13B that DNA precursor substrates (green bars) are not the preferred substrates of this enzyme. Eventually, it was discovered that the function of SLC25A19 had been misinterpreted [65, 105]. When we compare the concentration / K_m plots of the mitochondrial nucleotide metabolism (Figures 12A and 13A) to those of POLG and SLC25A19 (Figures 12B and 13B) we observe that the Concentration / K_m values of DNA precursors with the enzymes of mitochondrial nucleotide metabolism are at the same level as the Concentration / K_m values of the DNA precursors with SLC25A19, even though these DNA precursors are not the physiological substrates of SLC25A19. We note that SLC25A19 was not used a negative example in

Figure 11B because the enzyme kinetics values (k_{cat}) were not available for the relevant deoxyribonucleotide or ribonucleotide substrates.

As a side observation, we are intrigued by the fact that at lower dNTP concentrations the Concentration / K_m values for rNTPs are essentially equal to those for dNTPs for polymerization by POLG (Figure 13B). This observation reveals that discrimination by POLG in this case is perhaps almost completely dependent on the corresponding reaction V_{max}. As the V_{max} (or k_{cat}) of rNTPs with POLG are much lower than those for dNTPs, it is possible that in quiescent cells POLG faces more interference by ribonucleotides, thus obstructing the polymerization of deoxyribonucleotides into the DNA molecule being synthesized and at the same time promoting the incorporation of ribonucleoside triphosphates in the DNA strand. This is consistent with the reported incorporation of ribonucleotides in replicating mtDNA [106].

Substrate flow through the salvage pathway: As an initial analysis of the function of the salvage pathway, we used the Michaelis-Menten equation to calculate reaction rates under assumed substrate concentrations. We ignored the effect of inhibitions. This implies that the reaction rates we calculated (number of substrate molecules catalyzed per enzyme molecule per minute) were the upper-bound of the rates at the estimated concentrations, because inhibitions would act to lower these rates. We call such reaction rates ‘effective velocities’. As we assumed deoxyribonucleoside concentrations to be constant at 0.5 µM and deoxyribonucleotide concentrations to be either 10 µM (high, ‘cycling cells’) or 1 µM (low, ‘quiescent cells’), we obtained two sets of effective

velocities for the enzymes of mitochondrial nucleotide metabolism – one approximating the behavior in cycling cells, and one approximating the behavior in quiescent cells.

Figure 14A is a plot of the effective velocities of nucleoside kinases versus NT5M. Remember from Figure 1A that NT5M is the nucleotidase that reverses the action of the nucleoside kinases, so the amount of material fed into the salvage pathway depends in part on the balance between these two groups of enzymes. The substrate dCMP is absent for Figure 14A because no reaction was observed between NT5M and dCMP [88]. Note that the nucleoside concentrations were assumed to be constant, so the high and low concentration rates are only given for NT5M. Because of inhibitions and competing reactions, the deoxyribonucleoside output from NT5M would be much lower than represented here, but it is still instructive to compare objectively the disparity between the forward and reverse reactions at the first phosphorylation level. It is clear that the theoretical maximum velocities (at the assumed concentrations) of NT5M reverse reactions are many-fold higher than the maximum velocities from nucleoside kinases. While the situation is poor for the dG and dT substrates, it is extremely poor for the dA substrate where the reverse reaction has well over an order of magnitude advantage over the forward reaction. Furthermore, NT5M may not be the only nucleotidase in the mitochondria, thus exacerbating this issue [88].

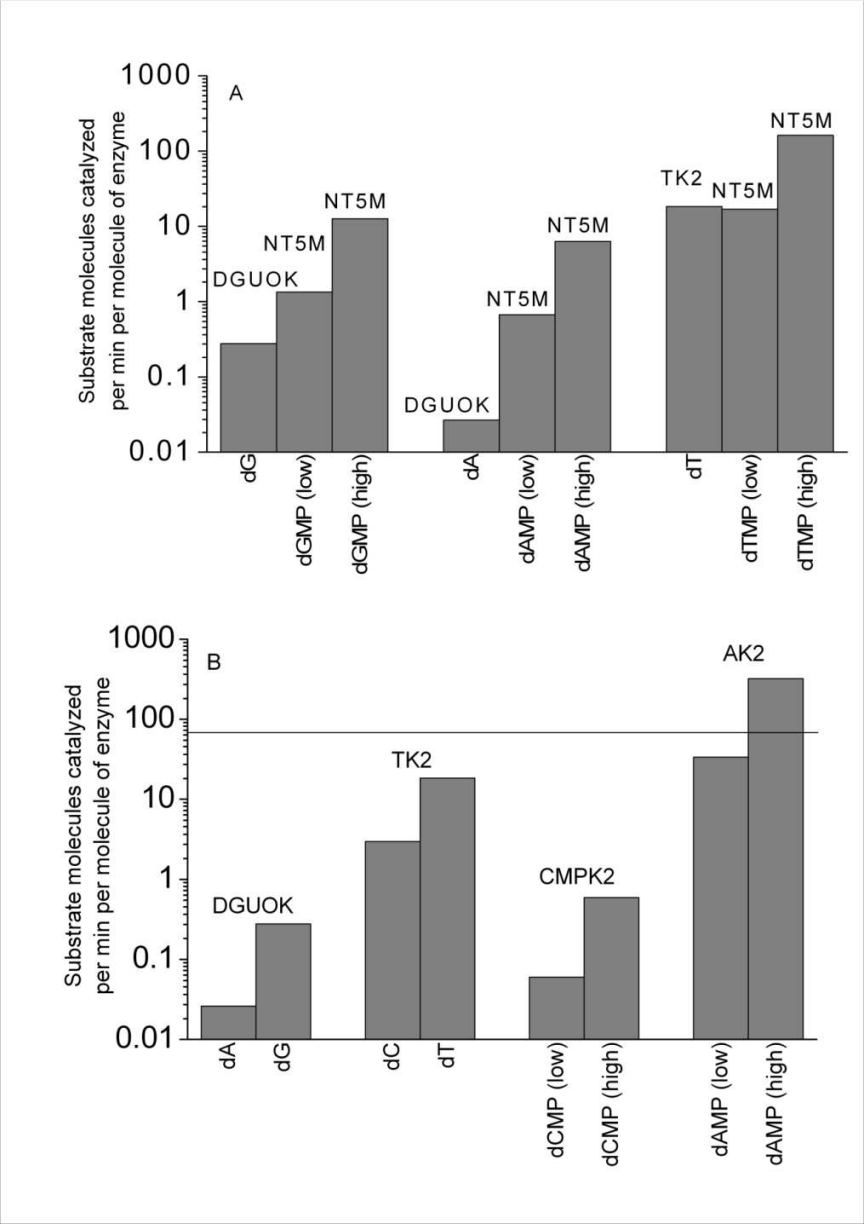

Figure 14: Effective velocities of some of the reactions of mitochondrial nucleotide metabolism. (A) Effective velocities (number of substrate molecules catalyzed per minute per enzyme molecule) of nucleoside kinase reactions versus NT5M reactions. Theoretical maximum velocities of NT5M reverse reactions are many-fold higher than the maximum velocities from nucleoside kinases. (B) A comparison of the effective velocities for deoxynucleotide substrates for enzymes of the mitochondrial salvage pathway. The horizontal reference line shows the number of nucleotides (approximately 69) of each triphosphate needed per minute on average to complete mtDNA replication in two hours. Reproduced from Gandhi and Samuels (2011) [7].

In addition to these qualitative comparisons of substrate preferences of mitochondrial nucleotide metabolism enzymes, we analyzed the reaction kinetics further to approximately quantify the flow of substrates through this enzymatic pathway. For simplicity, we ignored the inhibition terms in the Michaelis-Menten equations (inhibitions would further reduce reaction velocities). We could then investigate the effect of k_{cat}, K_m, and substrate concentrations on the upper-bound of velocity of the reactions at assumed substrate concentrations and compare the estimated velocities to the expected requirements for completing one round of mtDNA replication in a specified amount of time. It has been reported that one round of mtDNA replication in cell culture takes ~1-2 hours to complete [80]. To be conservative, we assumed that mtDNA replication takes 2 hours to complete. To replicate 16,568 bases pairs on two mtDNA strands in 2 hours, ~276 nucleotides are required per minute on average (with the log scale on Figure 14B it is unnecessary to precisely divide this quantity into the specific numbers of dATP, dCTP, dGTP, and dTTP molecules needed for the human mtDNA sequence). Figure 14B shows the effective velocities of some of the enzymes of mitochondrial nucleotide metabolism (DGUOK, TK2, CMPK2 and AK2). These are all the enzymes for which we found data that would enable us to calculate effective velocities. To facilitate comparison across these enzymes, some data for DGUOK and TK2 are repeated in Figure 14B from Figure 14A. As before, nucleoside kinase velocities in Figure 14B are the same for high or low concentration conditions because nucleoside concentrations are assumed to be constant. There exists a many-fold difference in the output of the four dNMPs, with dA nucleosides being fed into the salvage pathway by DGUOK at a rate many orders of magnitude lower than that required to support mtDNA

synthesis. Assuming a 2 hour replication duration and an approximately 276 / 4 nucleotides per minute substrate requirement, the number of molecules of the DGUOK enzyme per mitochondrion required to catalyze the requisite output of dAMP is close to 3000. The poor kinetics of DGUOK with dA is not the only problem with the dA pathway. Although there could be multiple AK isoforms in the mitochondria, some of them are reported to be lacking kinase activity and none of them appear to catalyze dAMP phosphorylation with comparable efficiency to that of AMP phosphorylation [107]. This is verified for AK2 as seen in Figures 11A, 12A, and 13A.

A calculation of dCDP production by CMPK2 at low assumed dCMP concentrations shows that more than 1000 CMPK2 enzymes per mitochondrion would be required to produce the necessary dCMP output per minute (assuming an approximate requirement of 276 / 4 nucleotides per minute). This result is important considering that CMPK2 expression was undetectable in many tissues [8], thus implying that CMPK2 function may not be essential for the production of mtDNA precursors as has been noted previously [8].

The data on the kinetic parameters of the human mitochondrial nucleoside diphosphate kinase (NME4 in Figure 1) is scarce (K_m for dTDP of approximately 1 mM, which is 100 to 1000 times the physiological concentration of dTDP) [86], which is why it is not included in Figure 14B. An NDPK isolated from the pigeon mitochondrial matrix preferred ribonucleoside diphosphates over deoxyribonucleoside diphosphates by several fold [99]. Surprisingly, it appears that both AK2 [10] and NME4 [11] are localized in the

mitochondrial intermembrane space, thus suggesting that if their reaction products participate in the mtDNA precursor synthesis, they would then have to be imported into the mitochondrial matrix. Although dAMP is not the preferred substrate for AK2 (Figures 11A, 12A, and 13A), AK2 still has a very fast reaction with dAMP (Figure 14B). Good efficiency with dAMP and the localization of AK2 in the intermembrane space instead of in the mitochondrial matrix seem to contradict each other regarding the role of AK2 in mtDNA precursor synthesis.

Computational simulations: To test our conclusions and to build upon them, we used an updated computational model to perform simulations of deoxyribonucleotide dynamics and mtDNA replication within the mitochondrion.

Figure 15 shows our simulation results. The X-axis represents the number of molecules of each nucleotide supplied to the mitochondrion in the form of a 'source' term in the differential equations in addition to the output from salvage within the mitochondrion. Each value on the X-axis is the sum of molecules supplied of all four species. For example, the X-axis value of 400 means that 100 molecules per minute of each of the four (A, C, G, T) species were supplied. The Y-axis represents the average (over 120 minutes of simulation time) mtDNA replication rate that we observed, calculated as number of nucleotides replicated divided by the time taken to replicate them. Initial values for the substrate concentration in the mitochondrion were randomly varied over a set range as described in the Methods section. Each Y value corresponds to the mean of 100 replication rates from 100 simulations with differing initial substrate conditions. The

standard deviations were far smaller than the mean values (and are therefore not shown in Figure 15) indicating that the simulation was not sensitive to the initial substrate conditions. We compared the observed replication rates to those required to complete mtDNA replication in 2 hours (‘cycling cells’) or 10 hours (‘quiescent cells’). For the mtDNA length of 33,136 nucleotides (replicating both strands), these would be 33136 (nucleotides) / 120 (minutes) and 33136 (nucleotides) / 600 (minutes) respectively or approximately 276 nucleotides per minute and 55 nucleotides per minute respectively. Since the mean observed replication rates with no additional nucleotides supplied (0 on the X-axis) fall below the 2 hour line, it is clear that the output from mitochondrial salvage cannot account for an mtDNA replication duration of 2 hours. In fact, even when a 10 hour replication target was set, mitochondrial salvage alone is an inadequate source of dNTPs, though only a slight amount of additional substrate supplied by transport is needed in this case. Next, we note that both deoxynucleoside as well as deoxynucleoside monophosphate import are insufficient to support a 2 hour replication target. Transport of either dNDPs or dNTPs is sufficient to achieve the target replication rate. The profiles of dNDP and dNTP transport are indistinguishable from one another on Figure 15 because of the extremely fast kinetics of NME4.

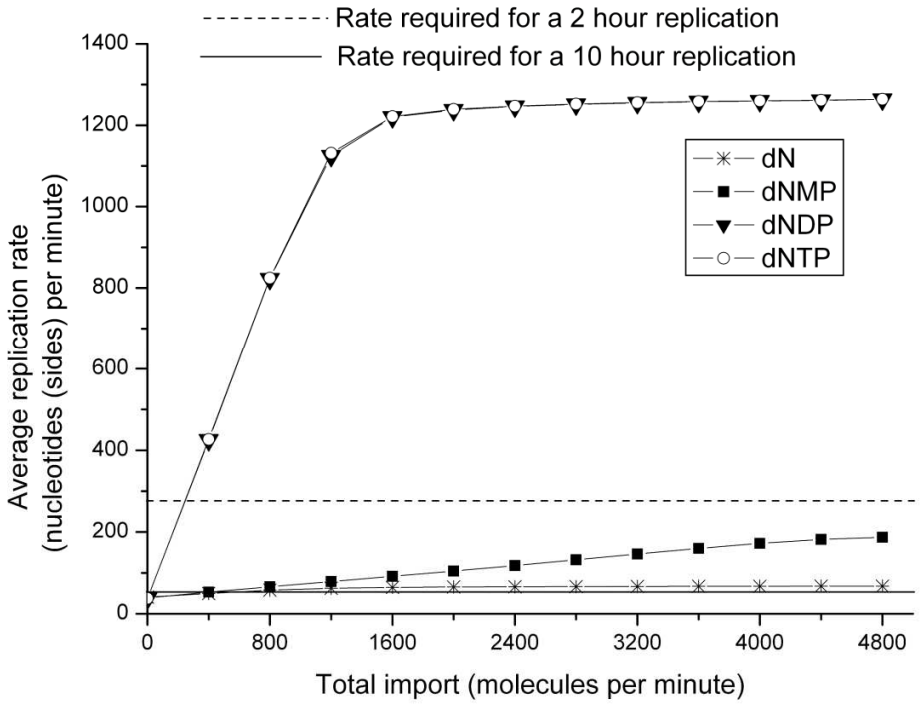

Figure 15: The effects of nucleotide import into the mitochondrion on the mtDNA replication rate. Each point is the mean mtDNA replication rate from 100 simulations with different randomly chosen initial concentrations of deoxynucleosides and deoxynucleotides. The X-axis represents the total amount of additional deoxynucleosides or deoxynucleotides supplied (sum total of equal amounts for each of the four species). Additional supply of dN, dNMP, dNDP or dNTP were simulated separately. The dNTP output from mitochondrial salvage alone is insufficient to support a replication rate of as long as 10 hours. Additional supply of dNs and dNMPs was insufficient to support a replication duration of 2 hours indicating that additional dNDPs or dNTPs are essential. The results were essentially identical for supply of either dNDPs or dNTPs. Reproduced from Gandhi and Samuels (2011) [7].

Transport of approximately 48 molecules per minute for each of the four nucleotide species was required to complete mtDNA replication in 2 hours. The longer replication time of 10 hours required a transport of 15 dNTP molecules per minute for each of the four nucleotide species. These rates were determined from the simulation by transporting all four nucleotide species at equal rates and with fixed initial concentrations (as described in Methods).We next addressed the question of the minimum transport of each dNTP species necessary to support the target replication. As described in the Methods section, the assumption of equal transport of the four dNTP species was relaxed to find the minimal amount of transport separately for each dNTP species required to meet the mtDNA replication rate goal. To achieve a replication rate of at least 276 nucleotides per minute ('cycling cells'), 47, 31, 48, and 48 molecules per minute of dTTP, dCTP, dATP, and dGTP were required. Thus, for this condition of relatively fast replication, transport of all four nucleotide species at similar rates is necessary. The total dNTP transport rate sums to 174 nucleotides per minute, a large fraction of the 276 dNTPs per minute consumed by the mtDNA replication. For the slower mtDNA replication with a target of 10 hours, Figure 15 shows that a relatively small amount of transport of dNTP molecules per minute suffices. To achieve the replication rate target of at least 55 nucleotides per minute (representing slow mtDNA replication in 'quiescent cells'), individual dNTP transport rates of 0, 3, 8, and 15 molecules per minute of dTTP, dCTP, dATP, and dGTP were required. Due to the complexity of the system (a nonlinear one because of feedbacks and inhibitions), slightly different but often practically similar transport profiles were observed to result in similar replication rates. For example, for cycling cells the transport profile of 41, 34, 48, and 41 molecules per minute also achieved the

replication rate target. For quiescent cells, the profiles of 2, 2, 8, and 15 and 0, 2, 8, and 15 molecules per minute (practically identical to the transport profile given above) also achieved the replication rate target.

In summary, rapid replication of mtDNA requires a substantial additional source of all four dNTPs (or dNDPs) to supplement the limited kinetics of the mitochondrial salvage pathway. Under the conditions of quiescent cells, the primary requirement is for the transport of dATP and dGTP molecules, and the vast majority of the dNTPs consumed by the mtDNA replication can be provided by the salvage pathway.

IV.5. Discussion

Kinetic characteristics of the mitochondrial salvage enzymes and their contribution in producing dNTP substrates for mtDNA replication: Based on this analysis of the enzyme kinetics three properties of the mitochondrial nucleoside salvage pathway are thus apparent:

i) The majority of the enzymes of this pathway are not restricted or specific for metabolism of mtDNA precursors.

ii) The majority of the characterized enzymes prefer non-DNA precursor substrates.

iii) For the majority of substrate-enzyme pairs, the kinetic constants are physiologically unreasonable for achieving efficient catalysis with the expected substrate concentrations *in situ*.

From the kinetics perspective mitochondrial nucleotide metabolism as defined by this set of enzymes (Figure 1A) cannot be expected to be the primary source of dNTP substrates for the rapid replication of mtDNA molecules. Since ribonucleotides exist at higher concentrations than deoxyribonucleotides, enzymes that take both ribonucleotide and deoxyribonucleotide substrates will, *in situ*, not favor the catalysis of deoxyribonucleotides. This is certainly true for enzymes that possess higher affinities for ribonucleotides, but also for those enzymes that have only slightly better kinetics for deoxyribonucleotides. In these cases ribonucleotide substrates will simply out-compete the deoxyribonucleotides substrates owing to the relative abundance of ribonucleotides.

The contribution of cytoplasmic nucleotide metabolism in producing dNTP substrates for mtDNA replication: One plausible interpretation of this analysis is that import of cytoplasmic deoxyribonucleotides is the primary source that supplies the direct precursors for the replication of mitochondrial genome while the mitochondrial salvage pathway acts as a back-up metabolism with a minimal role to play in cycling cells. The occurrence of deoxyribonucleotide transport between the mitochondria and cytoplasm and the substantial contribution of cytoplasm deoxynucleotides toward intra-mitochondrial dNTP pools have been demonstrated [17, 18]. Our results make it possible to comment on why this must be so, due to the kinetic properties of the enzymes of mitochondrial salvage. Our results also enable us to conclude that import of deoxyribonucleotides is in fact essential to support an mtDNA replication time of ~2 hours. Furthermore, simulations based on these enzyme kinetics indicate that this import occurs either at the dNDP or dNTP level. In cells where cytoplasmic deoxynucleotide

concentrations are low, mitochondrial salvage would assume a greater role and, in combination with some other supply such as RRM2B mediated reduction of ribonucleotides in the cytoplasm followed by deoxyribonucleotide transport into the mitochondrion, would produce the dNTPs for both the replication of mitochondrial DNA and perhaps repair of nuclear DNA. Possibly, the dNDPs produced by RRM2B activity might first undergo the terminal phosphorylation by NME4 in the intermembrane space (Figure 1B) and may then be imported into the mitochondrion matrix at the dNTP level to combine with the dNTP pool from intra-mitochondrial salvage. Indeed, this is consistent with defects in the mitochondrial salvage pathway having their most severe phenotype in postmitotic tissues. That mitochondrial salvage has only a back-up role in supporting mtDNA replication is one explanation why DGUOK and TK2 deficiency phenotypes are tissue-restricted and not systemic.

Similarities and differences between nucleotide metabolism in the cytoplasm and mitochondria: The kinetic characteristics of the cytoplasmic counterparts of mitochondrial salvage enzymes expose informative parallels and distinctions between the cytoplasmic and mitochondrial pathways of nucleotide metabolism. The good activity of the mitochondrial enzymes (except the nucleoside kinases TK2 and DGUOK) with ribonucleotide substrates implies that these enzymes might play as important a role in ribonucleotide production to support RNA synthesis as they do in supporting DNA synthesis. Based on our analysis, we would argue that future studies of the kinetics of the mitochondrial salvage enzymes would benefit from a broader characterization of the kinetics, particularly the activity of the enzymes with ribonucleotide substrates relative to

the activity with deoxyribonucleotide substrates. The majority of the cytoplasmic counterparts also show a preference for non-DNA precursors (such as dUMP) and ribonucleotide substrates [81, 100, 108]. However, the role of nucleoside salvage as a source of dNTPs for nuclear DNA replication is generally assumed to be minimal. In the S-phase of the cell cycle, ribonucleotide reductase irreversibly converts ribonucleoside diphosphates to deoxyribonucleoside diphosphates, and subsequently, deoxyribonucleotides originating from *de novo* sources proceed to become the predominant precursors to nDNA replication. Thus, ribonucleotide affinities of these cytoplasmic enzymes not only provide the ribonucleoside diphosphates for ribonucleotide reduction but also ensure an adequate supply of RNA substrates. The terminal kinase (NDPK) of the cytoplasmic salvage pathway accepts both ribonucleoside and deoxyribonucleoside diphosphates, and the products can then be appropriately diverted for either RNA or DNA synthesis. Salvage enzymes of deoxythymidine metabolism fit nicely into such a model - examples being the excellent kinetics of TK1 and TK2 with dT, and those of cytoplasmic deoxythymidylate kinase (essential for both salvage and de novo pathways of dTTP synthesis) with dTMP – since deoxythymidine is not an RNA substrate and because of the crucial allosteric control exerted by deoxythymidine nucleotides on ribonucleotide reductase [109] as well as feedback control on mitochondrial TK2 [90]. Such similarities in the enzyme kinetics of the parallel mitochondrial and cytoplasmic metabolisms lead to the question of a ribonucleotide reductase connection to mitochondrial nucleotide metabolism. Such a connection is hinted at by the data supporting a connection between the mitochondrial dNTP pool and the ribonucleotide reductase RRM2B [18, 25]. There has been at least one report of

ribonucleotide reductase activity within the mitochondrion [5], though this has never been confirmed as far as we are aware of.

The identity of the imported substrate and the contribution of import in quiescent cells: Our simulations show that mitochondrial salvage is inadequate to account for the observed replication time of ~1-2 hours in cycling cells. It is likely that the deficit is supplied by import from the cytoplasm. We propose that deoxyribonucleotide import into the mitochondria not only does occur, but is in fact essential to replicate and maintain mtDNA in cycling cells. Furthermore, in our simulations, import at the monophosphate level was not able to support mtDNA replication under the constraint of a replication duration of 2 hours or less. Our observation that either dNDP or dNTP transport are able to nearly identically support mtDNA replication is due to the extremely fast kinetics of NME4, the nucleoside diphosphate kinase. The fact that the NME4 kinetics for the conversion of dNDP to dNTP are fast lends weight to the hypothesis that transport occurs mainly at the dNDP level, and not at the dNTP level which would bypass the NME4 activity.

Our results are not necessarily in disagreement with previous reports that observed that supplementation with external dA and dG or dAMP and dGMP rescued mtDNA depletion [27, 30]. In those cases, it was undetermined whether these externally supplied substrates changed their phosphorylation level prior to or after entering the mitochondria, or even the cell. In the study conducted by Saada [27], in patient fibroblasts harboring DGUOK defects while dGTP pools were reduced compared to controls, dATP pools

were only moderately affected. In this study when these patient fibroblasts were given external supplementation of both deoxyguanosine and deoxyadenosine, mitochondrial dGTP notably increased, while the increase in mitochondrial dATP was less pronounced. Our observation on the inefficient kinetics of DGUOK with dA is consistent with these findings. We are not aware of any studies on the effects of pyrimidine supplementation in TK2 deficiency.

We have chosen a somewhat arbitrary target replication time of 10 hours for the mtDNA in quiescent cells. It has been reported that even in quiescent cells (rat hepatocytes), mitochondrial DNA is subject to rapid turnover [73]. Moreover, it is plausible to suspect that long replication durations might compromise the integrity of either or both the template and the synthesis strand by increasing the probability of damage to the exposed DNA or unfaithful replication (deletions, frameshifting, etc). Therefore, it is possible that the mtDNA replication time may be practically constrained to a shorter duration than 10 hours. In that case deoxynucleotide import could be essential even in quiescent cells. There is a lack of data on mtDNA replication times in quiescent cells, a critically important gap in our knowledge since quiescent cells are the most severely affected cells in most forms of Mitochondrial DNA Depletion Syndromes.

Could there be more than one deoxynucleotide transporter?: The fact that clinical conditions arising from altered intra-mitochondrial dNTP pools mostly manifest in postmitotic tissues is consistent with our results. The possibility of there being more than one deoxynucleotide transporter, say one for purine deoxynucleotides and one for

pyrimidine deoxynucleotides, might explain why mutations in TK2 and DGUOK which are both nucleoside kinases produce different phenotypes. It is plausible that there exists more than one mitochondrial deoxynucleotide transporter whose expression levels, possibly in conjunction with other factors, contribute to tissue specificity of mtDNA depletion syndromes. There have been reports [16, 52] asserting a role of PNC1 (pyrimidine nucleotide carrier encoded by solute carrier family 25, member 33 or *SLC25A33*) in nucleotide import into mitochondria as well as mitochondrial maintenance. PNC1 was able to transport a variety of metabolites, including purine and pyrimidine ribonucleotides and deoxyribonucleotides, with a preference for UTP. Intra-mitochondrial UTP accumulation decreased in response to siRNA-transfection against PNC1. Mitochondrial ADP, ATP, and GTP levels were not significantly altered but the effect on dNTPs was not investigated. Suppression of PNC1 was associated with reduced mtDNA while overexpressed PNC1 was associated with increased mtDNA relative to controls. Since UTP is a cofactor of the mitochondrial helicase (PEO1 or twinkle), mtDNA levels might have been altered through increased or decreased UTP [52]. It is also possible that these consequences resulted from a lack of RNA primers or lack of mtDNA precursors that might be substrates of PNC1. However, PNC1 mRNA was undetectable in skeletal muscle [16], a tissue that is a target of TK2 defects. Interestingly, ribonucleotide reductase overexpression caused mtDNA depletion in skeletal muscle of mice [110]. Also, per mg protein, PNC1 appeared to transport roughly 1.5 times more UTP compared to dTTP, the next most transported substrate. At this time, the role of PNC1 in transporting deoxyribonucleotides for mtDNA synthesis is inconclusive. Import of radioactively labeled dTMP into mitochondria has been observed [15]. However, it

was also observed that a fraction of the labeled dTMP was degraded as well as phosphorylated in the growth medium, leading to the possibility that the transport of phosphorylated states other than the monophosphate may have occurred. A transport activity with preference for dCTP has also been observed [14].

Tissue specificity of mtDNA depletion syndromes: It has been proposed that low basal TK2 expression in muscle renders the tissue vulnerable to TK2 defects, while overlapping substrate specificity of cytosolic dCK prevents mtDNA depletion from mutant DGUOK in tissues where dCK expression is high [111]. While mtDNA defects that have a basis in mutated salvage enzymes might conceivably be rescued by other factors such as overlapping substrate specificity of cytoplasmic enzymes, this hypothesis cannot account for phenotypes relating to POLG defects. Importantly, the fact that phenotypes from mutations in POLG are also tissue-specific and not systemic indicate that other factors, such as rates of mtDNA turnover or energetic demand of tissues might also be a factor in the basis of tissue selectivity. In a recent review, Liya Wang discussed deoxynucleoside salvage enzymes and their association with tissue specific phenotypes of mtDNA depletion [20]. It was hypothesized that since mtDNA turnover rates are different in different tissues and also because dNTP pools show organ-specific differences, it would be expected that the regulation of dNTP pools would also be different for different tissues. Because both muscle and liver have high amounts of mtDNA and also of mtDNA turnover, and since the dTTP pool is lowest in muscle and the dGTP pool is smallest in liver, it was proposed that these tissues would be especially vulnerable to mutations in TK2 and DGUOK respectively. Other contributing factors

could include limiting RRM2B, thymidylate synthase, or nucleotide transporter activity. In our opinion, it is probable that there is more than one underlying principle that explains tissue specificity – vulnerability of tissues to mutations might be from a combination of various factors such as transcriptional compensation, turnover rates, energetic demand, etc, and that different forms of mtDNA depletion syndromes may trace their etiology to different factors.

The applicability of our results to different tissues and species: Based on their experiments with perfused rat heart, Morris et al concluded that in isolated perfused heart, there is no de novo synthesis of dNTPs [112], stressing the importance of TK2 in rat heart. This could indicate that our observations on the inadequacy of mitochondrial salvage enzymes may not hold across all tissue types. It is also possible that the deoxyribonucleotide pools in rat heart arose in part through salvage mediated by residual TK1 activity. In a recent report of a $TK2^{-/-}$ H126N knockin mouse [113], the authors observed TK1 to be the main thymidine kinase component in heart, compared to TK2 in the brain. In this mouse, phenotypic manifestation of TK2 deficiency was related to TK1 down-regulation and transcriptional compensation. Although by postnatal day 13 both brain and heart had suffered substantial mtDNA depletion, in contrast to brain, heart was spared as respiratory chain proteins were still at normal levels in this organ when assayed at postnatal day 13. This could indicate a difference in the importance of TK2 in the heart tissue of rats compared to mice. A recent report claimed that a cytosolic localization of TK2 is present in many rat tissues [12]. For the knockin mouse [113], a compensatory mechanism involving increased mtDNA transcription through suppression of MTERF3

(mitochondrial transcription termination factor 3) expression was implicated in alleviating some of the effects of mtDNA depletion. It was unclear why dTTP but not dCTP levels were affected and whether cytosolic ribonucleotide reduction had any influence in this observation. In humans, even in quiescent patient fibroblasts with only 5-40% of residual TK2 activity, mitochondrial and cytosolic dTTP pools were unaltered [58]. This finding would be consistent with the possibility that the activities of mitochondrial salvage enzymes may not be strictly necessary even for quiescent cells. Alternatively, it is also possible for there to be practical important differences between species with regard to this metabolism. In their study of the rat heart, Morris et al [112] noted that although known as a substrate of TK2, dU was not converted to dUMP possibly due to ENT1 nucleoside transporter not being localized to mitochondria in rodents, unlike humans, suggesting that dU may not be transported into the mitochondria in rodents. It has been noted that genes involved in mtDNA depletion syndromes etiology are essential for life in mouse models [20]. However, the severe phenotype of knock-out mice is not identical to the phenotype in humans [114], although multi-organ phenotypes have come to light in humans also [115]. This divergence could perhaps be due to species differences or because of the complete absence of enzyme activity in knock-out models [114].

Limitations of our analysis: One limitation of modeling biochemical pathways is that kinetic parameters as reported in the literature and obtained from recombinant enzymes may not reflect the *in situ* reality, for instance, if the enzyme conformation is unknowingly affected in the *in vitro* analysis, or if the assay conditions do not represent

the cellular environment adequately. Similarly, we have relied on the literature and our judgment for selecting appropriate concentrations and enzyme copies within the mitochondrion. In our analysis we have assumed a nucleoside concentration of 0.5 μM [94]. There have been reports of nucleoside concentrations of approximately 50-fold lower [96]. Such lower concentrations would have two effects on this analysis. First, the problems that we point out concerning the function of the nucleoside kinases TK2 and DGUOK would be even worse with significantly lower nucleoside concentrations. Second, there is a more subtle problem that the enzyme kinetics for TK2 were measured at much higher substrate concentrations (1 μM to more than 100 μM) [90]. If the true substrate concentrations were on the order of 10 nM, then the kinetics would have to be extrapolated to much lower concentrations, which could introduce additional uncertainty in the kinetic constants. Finally, our estimate of time taken to replicate mtDNA (2 hours) comes from a study of mouse cells [80]. It is worth mentioning that POLG kinetics suggest that polymerization itself is capable of proceeding at a rate much faster than 2 hours [83]. A more comprehensive investigation into mtDNA replication durations in a variety of human cells and particularly in the cell types affected by mtDNA depletion syndromes would thus be very beneficial.

For simplicity, we assumed that only one mtDNA molecule is replicating at any given time in a particular mitochondrion. If two or more mtDNA molecules were replicating simultaneously, then the deficit in the required dNTPs would be even larger than our analysis indicates. It should also be noted that mitochondria are very dynamic and undergo continuous fusion and fission. However, the effects of fusion and fission on the

mitochondrial dNTP content would most likely average out. While fusion of two mitochondria would result in a larger dNTP pool (measured as number of molecules per organelle), fission would result in a smaller dNTP pool.

Summary: Since the known elements of the mitochondrial salvage pathway do not have sufficient enzyme kinetics to support mtDNA replication in the observed duration of ~1-2 hours, an alternative source of mtDNA precursors must be essential. Despite the intensive focus of research on this pathway associated with mitochondrial depletion syndromes, it seems likely that our knowledge of mitochondrial nucleotide metabolism is still incomplete and that this pathway might need to be considerably expanded in the future to include new enzymes, mechanisms, nucleotide transporters and modes of regulation.

CHAPTER V

CONCLUSION

V.1. Summary and future directions

Mitochondrial DNA depletion syndromes are a consequence of defective maintenance of mitochondrial DNA. Defective maintenance of mtDNA results from problems in the homeostasis of mitochondrial dNTP pools or with problems in the replication apparatus that maintains mitochondrial DNA. As noted in Chapter I, mitochondrial dNTP pools and mtDNA integrity are significant also in numerous other human pathologies. Thus, also from a clinical perspective, it is imperative that we increase our knowledge of the biology of mitochondrial dNTP pools. This dissertation has presented the results obtained from an extensive investigation into mitochondrial deoxyribonucleotide metabolism, the pathway that generates dNTPs within the mitochondria. Together with dNTPs generated in the cytoplasm, mitochondrial dNTPs become the substrates for mitochondrial DNA replication and repair.

Through the research described in Chapter II, I discovered that cytoplasmic and mitochondrial dNTPs are strongly and highly statistically significantly correlated in normal cells but not in transformed cells. This discovery is significant due to several reasons. The mitochondrial matrix space is generally not considered to be in equilibrium with the cytoplasmic space, particularly to charged molecules such as deoxyribonucleoside phosphates owing to the double membrane that bounds the

mitochondrial matrix. The extent of the contribution of cytoplasmic deoxyribonucleotides to mitochondrial deoxyribonucleotides was also unclear. The cytoplasmic pathway that generates dNTPs is also much more complex than the pathway carrying out the same function in the mitochondria. Moreover, dNTP generation in the cytoplasm is tightly controlled, and coordinated with cell cycle progression, to ensure the integrity of genomic DNA. At the time I commenced my research, the prevailing notion was that mitochondrial dNTP levels are not stringently controlled. Although this notion is consistent with the fact that mitochondrial DNA replication is not strictly synchronized with nDNA replication, the results I described in Chapter II clearly show that mitochondrial dNTP levels are not independent of cytoplasmic dNTP levels (which are under stringent control) in normal cells. However, this correlation is broken in transformed cells. There are practical implications of this observation. Transformed cells are commonly used for experiments in this field. The advantage of transformed cell lines is that they are more readily available and more maneuverable compared to normal cell lines. Through my research, I alerted other researchers in this field of the disadvantages of transformed cell lines. My research served to caution that if something about mitochondrial dNTPs is fundamentally different in transformed cells compared to normal cells, then conclusions meant to apply to the normal functioning of intra-mitochondrial deoxyribonucleotide metabolism from studies on transformed cells may not be reliable. Another practical benefit of my work presented in Chapter II was the resource comprising estimated dNTP concentrations that I created by converting previously published data to a more meaningful form. This resource enables comparisons between

existing data as well as of future data to existing data, something which was not strictly possible prior to my work.

The results described in Chapter II gave rise to several important hypotheses, one of which was tested in Chapter III. An alternative to that hypothesis is that the correlation in mitochondrial and cytoplasmic dNTP concentrations results from a strong cytoplasmic control on mitochondrial dNTP concentrations.

One plausible mechanism for enforcing such control would be through the regulation of deoxyribonucleotide transport between the cytoplasm and mitochondria. In that case, the hypothetical transport protein could be a candidate gene for mitochondrial DNA depletion syndromes. Particularly, its tissue-expression patterns might reveal critical insights regarding the tissue-specificity of mtDNA depletion syndromes. Similarly, many of the genes coding for enzymes acting in cytoplasmic dNTP production would also be candidates for mtDNA depletion syndromes.

Regarding the disruption of the correlation in transformed cells, we might hypothesize that the disruption is connected to the Warburg effect. Otto Warburg observed that cancerous cells derive most of their energy from cytoplasmic glycolysis even in the availability of oxygen [69]. One way to shut down oxidative phosphorylation in the mitochondria would be reduced transcription or translation of the mitochondrial genome thereby limiting the availability of mtDNA-encoded components of the oxidative

phosphorylation machinery. The results in chapter II suggest that unlike cytoplasmic dNTP concentrations, mitochondrial dNTP concentrations are not unusually elevated in transformed cells compared to normal cells.

Might diminished import of cytoplasmic deoxyribonucleotides into the mitochondria be a mechanism through which transformed cells suppress oxidative phosphorylation?

Although the correlations in dNTP concentrations described in Chapter II were highly statistically significant, the underlying data came from a small set of cell lines and only a handful of labs. It would be very beneficial for a research group to test my conclusions in a controlled environment with a variety of cycling, non-cycling, and transformed cell lines; and particularly the cell types affected in mtDNA depletion syndromes. It is also important to verify whether all four of the canonical deoxyribonucleotides have similar behavior with respect to the observed correlations, or whether there are differences between the four dNTPs. Are there qualitative or quantitative differences in the origins of the four dNTPs?

To further understand the results obtained from the research presented in Chapter II, namely the strong association between cytoplasmic and mitochondrial dNTPs in normal cells and the disappearance of that association in transformed cells, I hypothesized that correlation patterns in the expression of genes of the cytoplasmic and mitochondrial deoxyribonucleotide metabolisms would be consistent with the correlation patterns in the

corresponding dNTP concentrations. I obtained tissue expression data for a selected set of nDNA-encoded genes that code for enzymes that participate in the cytoplasmic and mitochondrial metabolisms. The pattern of correlations in expression profiles suggested that in normal tissues, the cytoplasmic and mitochondrial deoxyribonucleotide metabolisms coordinately generate dNTPs. However, consistent with the disruption in dNTP concentrations seen in Chapter II, the correlation structure in gene expression profiles is also disrupted in transformed tissues. Specifically, the results suggested that in transformed tissues, when dNTP levels are high in the cytoplasm, dNTP production in the mitochondria would be suppressed. Three correlations involving mitochondrial DGUOK were statistically significantly different between normal and transformed tissues suggesting that control on DGUOK expression relative to the expression of other genes might be important for transformed tissues.

Dissecting the correlation patterns in transformed tissues hinted that the distinction between the metabolism in the mitochondrial matrix space and the intermembrane space, which is generally considered to be a subtle point, may actually be crucial. This is because in transformed tissues the matrix space metabolism is negatively regulated relative to the cytoplasmic metabolism whereas the intermembrane space is in fact positively regulated relative to the cytoplasmic metabolism. This fits with the fact that the mitochondrial intermembrane space is generally considered to be in equilibrium with the cytoplasm.

I also observed that genes of cytoplasmic nucleotide metabolism have higher expression in transformed tissues. This observation adds information to the correlation in dNTP concentrations that I observed in Chapter II and supports the proposition that the correlation in dNTP concentrations is broken in transformed cells perhaps due to an increase in cytoplasmic dNTPs without a similar increase in the mitochondrial production of dNTPs. The higher expression of cytoplasmic protein genes in transformed tissues and the lack of such an increase in the expression of the mitochondrial protein genes can be interpreted in the context of the Warburg effect. The production of mt-DNA encoded components of oxidative phosphorylation is partially dependent on the mitochondrial dNTP levels that are available to maintain mtDNA.

Might suppressed expression of nuclear genes of mitochondrial deoxyribonucleotide metabolism be a mechanism through which cancer tissues suppress oxidative phosphorylation?

The research presented in Chapter III helped discover a large number of correlations. However, it is not necessary to verify each of those correlations. It would be valuable to test either the strongest, most statistically significant, or the most biologically interesting correlations. Additionally, since DGUOK expression appears to be so important for transformed tissues, the correlations it participates in deserve special attention. An important future study would involve manipulating DGUOK expression to determine the effects of the manipulation on the transformation state of the cells or tissues. A key

extension to the work presented in Chapter III would be to test corresponding normal and transformed samples from the same tissue.

The dynamics of mitochondrial dNTP pools were studied in Chapter IV. The research presented in Chapter IV involved building a computational model of mitochondrial deoxyribonucleotide metabolism and mtDNA replication. To accomplish this, I surveyed the literature for the purposes of accurately defining the set of reactions to model and obtaining the experimental data necessary for the construction of a relevant model. By computationally simulating mitochondrial deoxyribonucleotide metabolism and mitochondrial DNA replication, I discovered three properties of the mitochondrial enzymes of this pathway: i) The majority of the enzymes of this pathway are not restricted or specific for metabolism of mtDNA precursors. ii) The majority of the characterized enzymes prefer non-DNA precursor substrates. iii) For the majority of substrate-enzyme pairs, the kinetic constants are physiologically unreasonable for achieving efficient catalysis with the expected substrate concentrations *in situ*. Significantly, my results showed that the output from mitochondrial salvage is inadequate to support the experimentally observed mtDNA replication duration of 1-2 hours in cycling cells. Additional sources of either dNDPs or dNTPs are required. Importantly, an additional source of nucleotides at the dNMP level does not suffice.

Although other researchers had observed that deoxyribonucleotide import from the cytoplasm to the mitochondria occurs, my results suggest that import is in fact essential. Furthermore, despite intensive study from wet lab groups, we scarcely knew any details

about the transport mechanism. My results strongly suggest that transport at the dNMP level is not sufficient to explain previously published experimental results regarding the rate of mtDNA replication. Transport at the dNDP or dNTP level is also consistent with the results presented in Chapters II and III. The fact that the mitochondrial metabolism has minimal contribution towards mitochondrial dNTP pools in most conditions is also one explanation for the fact that the depletion of mitochondrial in cases of mtDNA depletion syndromes is observed in only a small subset of all tissues.

My results on the kinetic characteristics of the mitochondrial enzymes of deoxyribonucleotide metabolism also point towards the need for exploring the role of these enzymes in generating ribonucleoside triphosphates.

Do the enzymes of mitochondrial deoxyribonucleotide metabolism also influence mitochondrial ribonucleoside triphosphate and mitochondrial RNA levels?

My results from Chapter IV also generate numerous ideas for future studies. It would be advisable for researchers in the field to estimate the mtDNA replication duration in a variety of human cell lines, but particularly cells in the tissues that are affected by mtDNA depletion syndromes. This information could then help calibrate the model I have developed more precisely to the affected tissues. Another important area for future investigation is the identity of the transported substrate. My results indicate that dNMP is not a viable import candidate and this hypothesis should be tested. Finally, the very slow

kinetics of DGUOK with deoxyadenosine appear to be one of the major bottlenecks of this pathway. These kinetics should be verified to ensure their accuracy.

V.2. Concluding remarks

At the time I commenced my research, there were several open questions regarding the biology of mitochondrial deoxyribonucleotide metabolism. I addressed many of these open questions through the research presented here in my dissertation. The process of inquiry is of course never-ending. I have attempted to contribute to broadening the horizons of this research field, and I hope my attempts at highlighting the importance of mitochondrial deoxyribonucleotide metabolism to the fields of cancer biology and maintenance of mitochondrial ribonucleoside triphosphates receive the attention they deserve.

Appendix

Table 9: Gene expression in normal tissues.

Tissue	TK2	DGUOK	NT5M	AK2	NME4	RRM1	RRM2	RRM2B	TK1	DCK	AK1	AK5	GUK1	CMPK1	DTYMK	NME1	NME3	ADK	NT5E	NT5C2	NT5C1B	NT5C	NT5C3	UCK1	UCK2
Adipose tissue	76	0	0	152	152	76	0	76	0	76	76	76	76	76	76	0	0	0	0	76	0	0	0	0	0
Adrenal gland	30	60	0	150	120	60	30	0	60	30	0	0	90	30	0	301	60	0	0	0	0	0	0	30	0
Bladder	0	33	0	168	0	134	201	67	67	67	33	0	67	336	0	235	0	67	33	100	0	33	134	33	0
Blood	8	113	16	194	16	275	356	24	129	24	16	0	72	72	48	315	16	56	16	186	0	64	64	48	16
Bone	69	55	13	195	97	111	167	41	111	0	83	13	153	139	69	362	55	83	41	27	0	27	27	0	13
Bone marrow	0	143	0	225	20	614	286	0	40	81	0	20	20	61	0	122	0	20	40	20	0	0	0	0	0
Brain	52	26	8	88	34	219	128	38	23	43	42	46	127	65	28	125	29	31	53	261	0	20	19	54	47
Cervix	124	41	20	435	20	394	332	0	290	0	103	0	186	41	103	166	0	62	62	20	0	0	124	145	83
Connective tissue	33	80	6	120	13	388	80	20	0	0	46	100	53	80	20	234	6	683	428	147	0	0	33	26	6
Ear	61	0	0	0	0	123	0	61	0	0	0	0	61	123	0	61	0	0	0	0	0	0	0	0	0
Embryonic tissue	9	78	4	199	74	88	111	37	148	27	4	4	64	64	88	361	55	27	55	97	0	13	32	27	74
Esophagus	0	49	0	98	49	1533	2276	0	49	0	0	0	148	0	0	197	0	0	49	98	0	0	0	49	49
Eye	14	75	9	213	66	108	127	33	104	23	56	14	260	47	56	407	94	28	23	94	0	42	23	47	66
Heart	44	189	11	234	78	167	100	0	22	33	189	0	278	11	44	245	44	33	33	55	0	22	44	22	66
Intestine	8	68	0	179	63	132	243	4	179	29	89	8	200	98	76	260	42	29	51	76	0	46	29	63	76
Kidney	33	51	14	226	28	283	283	47	70	56	18	9	132	99	80	207	18	33	151	94	0	23	18	61	47
Larynx	41	0	0	0	41	621	0	0	0	0	0	0	0	0	0	165	0	0	0	82	0	0	0	0	41
Liver	4	52	14	120	48	81	240	28	43	43	19	9	62	96	24	462	4	48	43	33	0	24	33	14	33
Lung	35	74	5	183	62	121	83	14	56	20	124	2	234	106	35	302	35	29	130	62	0	26	32	35	47

Lymph	0	45	0	564	0	225	519	0	813	90	0	0	135	135	67	542	90	0	0	180	0	22	0	0	45
Lymph node	10	87	0	185	21	141	76	130	174	98	0	0	240	87	141	130	0	21	87	76	0	0	120	10	54
Mammary gland	6	91	6	182	182	228	110	32	365	32	58	13	150	45	52	411	19	228	39	91	0	26	6	39	26
Mouth	14	29	0	74	59	313	492	29	29	0	14	0	29	208	0	74	0	14	104	611	0	0	29	14	44
Muscle	37	46	27	157	27	37	278	55	18	0	445	0	120	120	111	139	46	102	18	83	0	18	139	46	9
Nerve	190	0	0	126	63	63	63	63	63	0	63	0	63	126	0	190	63	0	0	126	0	0	0	126	0
Ovary	0	107	9	225	107	48	88	0	274	19	88	0	274	68	88	284	19	9	9	48	0	97	39	29	9
Pancreas	13	107	0	167	55	41	79	9	125	37	135	0	228	93	46	274	97	23	18	41	0	41	79	0	41
Parathyroid	0	243	0	584	0	194	0	97	0	0	146	0	243	0	97	292	97	0	0	48	0	0	0	48	48
Pharynx	24	290	0	24	72	96	0	0	24	0	0	0	72	0	0	435	0	96	0	72	0	0	24	0	0
Pituitary gland	60	60	0	60	0	0	0	0	0	0	0	0	60	60	60	361	0	0	60	0	0	0	0	0	0
Placenta	35	56	0	156	24	156	188	53	99	21	21	3	106	64	46	160	10	28	121	138	0	14	14	28	99
Prostate	26	63	0	137	359	184	52	21	110	31	31	0	195	68	63	274	68	58	42	73	0	52	0	52	36
Salivary gland	0	49	0	99	99	49	99	49	198	0	347	0	893	148	99	446	0	0	0	49	0	99	49	49	0
Skin	14	61	0	280	99	175	289	23	194	33	33	0	322	113	90	579	33	37	204	80	0	47	18	85	61
Spleen	0	0	0	166	37	166	129	0	0	18	55	0	92	74	0	0	0	0	18	166	0	0	55	55	0
Stomach	10	10	0	144	62	124	538	10	155	20	20	10	113	165	72	269	51	31	41	41	0	20	31	20	20
Testis	57	42	12	114	9	311	257	6	3	57	57	15	63	18	18	96	21	9	63	517	311	12	27	60	27
Thymus	24	24	0	172	0	788	1898	0	0	98	0	0	12	24	24	12	0	0	24	850	0	12	73	123	12
Thyroid	42	21	0	252	21	63	147	84	42	0	42	0	84	105	0	84	0	0	231	358	0	0	21	84	0
Tonsil	0	176	0	0	0	58	235	0	705	0	0	0	352	0	0	117	0	58	0	0	0	117	58	235	0
Trachea	0	57	0	171	0	209	19	95	0	0	38	0	0	76	0	0	0	0	209	1774	0	0	38	38	0
Umbilical cord	0	0	0	73	73	219	146	0	0	0	146	0	0	0	0	511	0	0	0	0	0	0	0	0	219
Uterus	12	72	8	214	72	120	94	38	98	30	51	12	257	128	77	218	51	47	184	128	0	21	17	30	30
Vascular	0	38	0	135	19	347	289	38	0	19	38	0	38	173	19	173	0	0	347	173	0	38	38	19	0

Table 10: Gene expression in transformed tissues.

Tissue	TK2	DGUOK	NT5M	AK2	NME4	RRM1	RRM2	RRM2B	TK1	DCK	AK1	AK5	GUK1	CMPK1	DTYMK	NME1	NME3	ADK	NT5E	NT5C2	NT5C1B	NT5C	NT5C3	UCK1	UCK2
Adrenal tumor	78	156	0	156	78	0	78	0	156	0	0	0	0	0	0	547	0	0	0	0	0	0	0	0	0
Bladder carcinoma	0	57	0	57	0	114	57	0	0	57	0	0	171	114	0	114	0	0	0	0	0	57	57	0	57
Breast (mammary gland) tumor	0	74	0	212	233	318	159	31	584	31	31	10	180	31	63	530	31	318	31	106	0	42	0	31	21
Cervical tumor	58	58	29	436	0	436	378	0	261	0	145	0	116	58	87	145	0	87	29	29	0	0	174	174	58
Chondrosarcoma	84	60	24	169	72	156	181	36	60	0	108	12	108	169	60	169	36	24	169	36	0	12	12	12	36
Colorectal tumor	17	35	0	192	35	157	315	0	280	26	105	0	201	70	26	297	61	52	52	70	0	0	43	17	52
Esophageal tumor	0	57	0	115	57	1792	2660	0	57	0	0	0	173	0	0	231	0	0	0	115	0	0	0	57	57
Gastrointestinal tumor	8	25	8	309	83	276	695	8	217	33	83	41	192	117	75	309	58	41	16	117	0	67	16	67	100
Germ cell tumor	18	41	0	204	34	458	363	45	128	75	34	72	117	49	34	208	3	30	53	250	3	41	15	56	60
Glioma	0	65	56	112	84	140	205	0	84	18	37	18	187	46	140	93	84	37	65	9	0	74	18	74	74
Head and neck tumor	29	29	0	132	80	183	300	36	58	0	58	0	176	124	14	176	0	0	124	425	0	14	22	22	14
Kidney tumor	29	29	0	72	72	43	58	14	188	87	43	14	188	87	87	261	0	29	0	87	0	14	29	58	43
Leukemia	0	104	20	239	20	417	219	0	114	73	0	0	104	52	52	313	10	62	83	177	0	31	41	20	31
Liver tumor	10	41	0	124	62	124	415	31	83	20	10	10	51	83	20	373	10	51	72	51	0	20	51	31	31
Lung tumor	19	67	19	203	126	106	135	19	174	9	58	0	416	58	38	533	19	67	87	9	0	19	29	38	77
Lymphoma	0	27	0	404	0	181	487	0	668	83	0	0	153	167	55	445	55	0	0	125	0	13	55	55	27
Ovarian tumor	0	117	0	247	39	52	78	13	234	26	91	0	286	91	117	286	26	13	0	52	0	78	52	13	13
Pancreatic tumor	19	9	0	152	76	66	114	19	258	0	191	0	296	76	95	353	114	0	38	57	0	47	19	0	38
Primitive neuroectodermal tumor	7	7	31	198	135	310	1034	0	302	7	55	15	198	15	127	286	95	71	87	23	0	23	31	87	127
Prostate cancer	9	87	0	107	253	214	97	29	194	48	0	0	233	68	68	477	68	87	19	77	0	9	0	68	58
Retinoblastoma	43	21	21	172	107	302	496	43	302	0	21	0	517	21	86	992	107	0	0	43	0	21	0	21	172
Skin tumor	16	72	0	256	112	112	360	24	312	32	0	0	464	88	120	824	16	48	56	32	0	40	24	136	64
Soft tissue/ muscle tissue tumor	31	103	0	215	79	343	311	23	159	39	23	119	159	103	111	367	47	910	343	31	0	7	23	23	15

Uterine tumor	11	55	0	166	66	44	88	33	55	22	44	22	243	121	33	188	11	77	77	110	0	44	44	44	22

Table 11: List of correlations.

Gene 1	Gene 2	Normal tissues		Transformed tissues	
		Spearman Rho	p-value	Spearman Rho	p-value
DGUOK	TK2	-0.27	0.08	-0.07	0.73
NT5M	TK2	0.28	0.07	0.10	0.65
NT5M	DGUOK	0.22	0.16	-0.10	0.63
AK2	TK2	-0.10	0.50	-0.01	0.95
AK2	DGUOK	0.34	0.02	0.11	0.60
AK2	NT5M	0.31	0.04	0.20	0.35
NME4	TK2	0.10	0.54	0.11	0.61
NME4	DGUOK	0.11	0.48	0.04	0.84
NME4	NT5M	0.11	0.50	0.18	0.40
NME4	AK2	0.05	0.74	-0.13	0.56
RRM1	TK2	-0.13	0.42	-0.15	0.48
RRM1	DGUOK	-0.15	0.34	-0.07	0.73
RRM1	NT5M	0.02	0.91	0.27	0.20
RRM1	AK2	0.07	0.65	0.33	0.12
RRM1	NME4	-0.30	0.05	-0.07	0.76
RRM2	TK2	-0.25	0.10	-0.07	0.74
RRM2	DGUOK	-0.18	0.24	-0.45	0.03
RRM2	NT5M	0.20	0.20	0.31	0.14
RRM2	AK2	0.22	0.16	0.40	0.05
RRM2	NME4	-0.20	0.18	0.00	1.00
RRM2	RRM1	0.43	0.00	0.68	0.00
RRM2B	TK2	0.13	0.41	0.40	0.05

RRM2B	DGUOK	-0.14	0.37	-0.09	0.68
RRM2B	NT5M	0.02	0.88	-0.20	0.36
RRM2B	AK2	0.14	0.35	-0.08	0.72
RRM2B	NME4	-0.08	0.62	0.34	0.11
RRM2B	RRM1	-0.20	0.19	0.00	0.99
RRM2B	RRM2	-0.22	0.15	-0.05	0.82
TK1	TK2	-0.21	0.17	-0.01	0.95
TK1	DGUOK	0.35	0.02	-0.18	0.40
TK1	NT5M	0.16	0.29	0.08	0.73
TK1	AK2	0.38	0.01	0.58	0.00
TK1	NME4	0.31	0.04	0.27	0.20
TK1	RRM1	-0.22	0.16	0.10	0.63
TK1	RRM2	0.30	0.05	0.28	0.18
TK1	RRM2B	-0.06	0.71	-0.10	0.64
DCK	TK2	-0.08	0.62	-0.42	0.04
DCK	DGUOK	0.12	0.44	0.11	0.61
DCK	NT5M	0.09	0.56	-0.34	0.10
DCK	AK2	0.36	0.02	0.15	0.49
DCK	NME4	0.06	0.72	-0.21	0.32
DCK	RRM1	0.16	0.31	0.04	0.86
DCK	RRM2	0.22	0.16	-0.17	0.42
DCK	RRM2B	-0.01	0.94	-0.06	0.77
DCK	TK1	0.21	0.17	0.11	0.59
AK1	TK2	0.09	0.55	0.36	0.08
AK1	DGUOK	0.02	0.91	-0.32	0.13
AK1	NT5M	0.36	0.02	0.31	0.15
AK1	AK2	0.27	0.08	0.18	0.40

AK1	NME4	0.34	0.03	0.00	0.99
AK1	RRM1	-0.23	0.13	-0.12	0.57
AK1	RRM2	-0.12	0.45	-0.04	0.84
AK1	RRM2B	0.22	0.15	0.12	0.58
AK1	TK1	0.02	0.87	0.11	0.60
AK1	DCK	-0.16	0.30	-0.39	0.06
AK5	TK2	0.21	0.18	0.04	0.86
AK5	DGUOK	0.07	0.64	-0.15	0.50
AK5	NT5M	0.41	0.01	0.14	0.51
AK5	AK2	0.08	0.61	0.02	0.93
AK5	NME4	0.18	0.23	0.17	0.44
AK5	RRM1	0.09	0.55	0.14	0.52
AK5	RRM2	0.06	0.69	0.12	0.58
AK5	RRM2B	0.15	0.34	0.28	0.18
AK5	TK1	0.02	0.88	-0.19	0.37
AK5	DCK	0.34	0.02	0.26	0.23
AK5	AK1	0.13	0.41	0.18	0.40
GUK1	TK2	-0.09	0.56	-0.06	0.78
GUK1	DGUOK	0.47	0.00	-0.24	0.27
GUK1	NT5M	0.21	0.18	-0.01	0.98
GUK1	AK2	0.43	0.00	0.00	1.00
GUK1	NME4	0.37	0.01	0.51	0.01
GUK1	RRM1	-0.34	0.02	-0.29	0.18
GUK1	RRM2	-0.01	0.93	-0.08	0.70
GUK1	RRM2B	0.03	0.83	0.20	0.35
GUK1	TK1	0.65	0.00	0.39	0.06
GUK1	DCK	0.11	0.48	-0.07	0.75

GUK1	AK1	0.38	0.01	0.25	0.24
GUK1	AK5	-0.01	0.94	-0.15	0.48
CMPK1	TK2	0.00	1.00	0.08	0.72
CMPK1	DGUOK	-0.31	0.04	-0.14	0.53
CMPK1	NT5M	-0.02	0.89	-0.25	0.23
CMPK1	AK2	0.12	0.43	0.11	0.61
CMPK1	NME4	0.01	0.95	-0.25	0.23
CMPK1	RRM1	-0.22	0.16	-0.32	0.13
CMPK1	RRM2	0.20	0.19	-0.20	0.34
CMPK1	RRM2B	0.50	0.00	0.24	0.25
CMPK1	TK1	0.20	0.20	-0.17	0.43
CMPK1	DCK	0.06	0.68	0.28	0.19
CMPK1	AK1	0.14	0.38	0.24	0.26
CMPK1	AK5	0.05	0.74	0.12	0.57
CMPK1	GUK1	0.04	0.82	0.00	0.98
DTYMK	TK2	0.06	0.68	-0.01	0.95
DTYMK	DGUOK	0.27	0.08	-0.03	0.90
DTYMK	NT5M	0.38	0.01	0.41	0.05
DTYMK	AK2	0.52	0.00	0.33	0.12
DTYMK	NME4	0.24	0.12	0.39	0.06
DTYMK	RRM1	-0.21	0.18	0.01	0.97
DTYMK	RRM2	0.05	0.77	0.08	0.70
DTYMK	RRM2B	0.24	0.12	-0.02	0.91
DTYMK	TK1	0.47	0.00	0.55	0.01
DTYMK	DCK	0.21	0.16	0.07	0.76
DTYMK	AK1	0.36	0.02	0.30	0.16
DTYMK	AK5	0.16	0.30	0.26	0.21

DTYMK	GUK1	0.59	0.00	0.43	0.04
DTYMK	CMPK1	0.19	0.21	-0.02	0.92
NME1	TK2	-0.22	0.15	0.10	0.65
NME1	DGUOK	0.39	0.01	0.15	0.48
NME1	NT5M	0.17	0.27	-0.22	0.31
NME1	AK2	0.17	0.26	0.27	0.21
NME1	NME4	0.42	0.00	0.46	0.02
NME1	RRM1	-0.23	0.13	-0.10	0.64
NME1	RRM2	-0.03	0.82	0.10	0.64
NME1	RRM2B	-0.20	0.20	0.17	0.43
NME1	TK1	0.43	0.00	0.56	0.00
NME1	DCK	0.01	0.92	0.07	0.76
NME1	AK1	0.14	0.36	-0.38	0.07
NME1	AK5	0.00	1.00	-0.29	0.17
NME1	GUK1	0.32	0.03	0.28	0.19
NME1	CMPK1	0.00	0.99	-0.25	0.25
NME1	DTYMK	0.33	0.03	0.07	0.76
NME3	TK2	0.13	0.41	-0.11	0.62
NME3	DGUOK	0.31	0.04	-0.29	0.17
NME3	NT5M	0.30	0.05	0.31	0.14
NME3	AK2	0.40	0.01	0.14	0.52
NME3	NME4	0.34	0.02	0.46	0.02
NME3	RRM1	-0.26	0.09	0.04	0.84
NME3	RRM2	-0.07	0.64	0.21	0.32
NME3	RRM2B	0.08	0.62	0.07	0.75
NME3	TK1	0.35	0.02	0.51	0.01
NME3	DCK	0.22	0.16	-0.06	0.78

NME3	AK1	0.33	0.03	0.24	0.25
NME3	AK5	0.23	0.13	0.14	0.51
NME3	GUK1	0.45	0.00	0.51	0.01
NME3	CMPK1	0.11	0.48	-0.04	0.87
NME3	DTYMK	0.41	0.01	0.57	0.00
NME3	NME1	0.45	0.00	0.30	0.15
ADK	TK2	0.12	0.44	-0.03	0.88
ADK	DGUOK	0.44	0.00	0.32	0.13
ADK	NT5M	0.57	0.00	0.18	0.40
ADK	AK2	0.14	0.36	0.31	0.14
ADK	NME4	0.16	0.28	0.30	0.16
ADK	RRM1	-0.02	0.88	0.28	0.19
ADK	RRM2	0.18	0.25	0.04	0.86
ADK	RRM2B	0.01	0.93	0.07	0.74
ADK	TK1	0.40	0.01	0.19	0.38
ADK	DCK	0.11	0.48	0.23	0.28
ADK	AK1	0.14	0.37	0.11	0.61
ADK	AK5	0.34	0.02	0.38	0.07
ADK	GUK1	0.31	0.04	0.05	0.83
ADK	CMPK1	0.08	0.61	-0.09	0.67
ADK	DTYMK	0.27	0.07	0.30	0.15
ADK	NME1	0.26	0.09	0.10	0.64
ADK	NME3	0.23	0.13	0.15	0.47
NT5E	TK2	0.12	0.45	0.23	0.28
NT5E	DGUOK	0.05	0.74	0.07	0.74
NT5E	NT5M	0.21	0.18	0.29	0.17
NT5E	AK2	0.22	0.14	0.10	0.65

NT5E	NME4	-0.14	0.37	0.25	0.23
NT5E	RRM1	0.28	0.06	0.14	0.51
NT5E	RRM2	0.27	0.08	0.11	0.62
NT5E	RRM2B	0.23	0.14	0.33	0.12
NT5E	TK1	-0.02	0.92	-0.25	0.25
NT5E	DCK	0.10	0.53	-0.16	0.47
NT5E	AK1	-0.02	0.89	0.29	0.17
NT5E	AK5	0.30	0.05	0.39	0.06
NT5E	GUK1	-0.06	0.70	-0.09	0.69
NT5E	CMPK1	0.28	0.07	0.19	0.36
NT5E	DTYMK	0.12	0.43	0.12	0.59
NT5E	NME1	-0.18	0.25	-0.14	0.51
NT5E	NME3	-0.08	0.59	0.14	0.52
NT5E	ADK	0.23	0.13	0.49	0.02
NT5C2	TK2	-0.03	0.83	-0.24	0.26
NT5C2	DGUOK	-0.25	0.11	-0.27	0.20
NT5C2	NT5M	0.04	0.78	-0.34	0.10
NT5C2	AK2	0.11	0.49	0.15	0.49
NT5C2	NME4	-0.25	0.10	-0.21	0.33
NT5C2	RRM1	0.41	0.01	0.34	0.10
NT5C2	RRM2	0.30	0.05	0.24	0.27
NT5C2	RRM2B	0.28	0.06	0.29	0.17
NT5C2	TK1	-0.17	0.26	-0.02	0.92
NT5C2	DCK	0.17	0.27	0.33	0.12
NT5C2	AK1	-0.07	0.63	-0.02	0.92
NT5C2	AK5	0.08	0.61	0.08	0.71
NT5C2	GUK1	-0.27	0.08	-0.06	0.78

NT5C2	CMPK1	0.20	0.19	0.22	0.29
NT5C2	DTYMK	-0.16	0.31	-0.24	0.25
NT5C2	NME1	-0.37	0.01	-0.05	0.80
NT5C2	NME3	-0.05	0.74	-0.10	0.65
NT5C2	ADK	-0.09	0.54	-0.08	0.70
NT5C2	NT5E	0.41	0.01	-0.04	0.86
NT5C1B	TK2	0.19	0.22	0.08	0.72
NT5C1B	DGUOK	-0.09	0.56	-0.09	0.67
NT5C1B	NT5M	0.22	0.16	-0.14	0.50
NT5C1B	AK2	-0.14	0.37	0.11	0.62
NT5C1B	NME4	-0.16	0.29	-0.23	0.29
NT5C1B	RRM1	0.16	0.29	0.32	0.13
NT5C1B	RRM2	0.11	0.46	0.14	0.53
NT5C1B	RRM2B	-0.08	0.61	0.36	0.09
NT5C1B	TK1	-0.13	0.41	-0.11	0.62
NT5C1B	DCK	0.19	0.21	0.29	0.17
NT5C1B	AK1	0.09	0.56	-0.02	0.94
NT5C1B	AK5	0.24	0.11	0.35	0.09
NT5C1B	GUK1	-0.12	0.44	-0.20	0.36
NT5C1B	CMPK1	-0.17	0.26	-0.17	0.44
NT5C1B	DTYMK	-0.09	0.55	-0.14	0.53
NT5C1B	NME1	-0.17	0.26	-0.17	0.44
NT5C1B	NME3	0.06	0.72	-0.17	0.44
NT5C1B	ADK	-0.06	0.69	-0.05	0.83
NT5C1B	NT5E	0.13	0.41	0.05	0.83
NT5C1B	NT5C2	0.22	0.15	0.32	0.13
NT5C	TK2	-0.28	0.07	-0.49	0.01

NT5C	DGUOK	0.34	0.02	-0.10	0.64
NT5C	NT5M	0.29	0.06	0.08	0.70
NT5C	AK2	0.20	0.19	0.04	0.85
NT5C	NME4	0.25	0.10	0.11	0.62
NT5C	RRM1	-0.23	0.14	-0.23	0.27
NT5C	RRM2	0.27	0.08	-0.21	0.32
NT5C	RRM2B	0.00	0.98	0.14	0.53
NT5C	TK1	0.61	0.00	-0.02	0.91
NT5C	DCK	0.27	0.07	0.23	0.28
NT5C	AK1	0.24	0.11	0.12	0.56
NT5C	AK5	0.07	0.63	0.27	0.20
NT5C	GUK1	0.57	0.00	0.36	0.08
NT5C	CMPK1	0.27	0.07	0.14	0.50
NT5C	DTYMK	0.37	0.01	0.33	0.11
NT5C	NME1	0.43	0.00	-0.15	0.49
NT5C	NME3	0.37	0.01	0.25	0.24
NT5C	ADK	0.43	0.00	-0.08	0.73
NT5C	NT5E	0.00	0.99	-0.02	0.92
NT5C	NT5C2	-0.05	0.73	0.05	0.82
NT5C	NT5C1B	-0.04	0.81	0.14	0.53
NT5C3	TK2	-0.18	0.25	-0.21	0.33
NT5C3	DGUOK	0.16	0.29	-0.10	0.64
NT5C3	NT5M	0.32	0.03	-0.01	0.96
NT5C3	AK2	0.14	0.35	0.25	0.24
NT5C3	NME4	-0.20	0.18	-0.60	0.00
NT5C3	RRM1	-0.12	0.46	-0.21	0.31
NT5C3	RRM2	0.28	0.06	-0.08	0.73

NT5C3	RRM2B	0.04	0.79	-0.37	0.08
NT5C3	TK1	0.20	0.19	0.01	0.95
NT5C3	DCK	0.06	0.71	0.27	0.21
NT5C3	AK1	0.24	0.11	0.17	0.43
NT5C3	AK5	-0.18	0.24	-0.13	0.55
NT5C3	GUK1	0.18	0.24	-0.08	0.72
NT5C3	CMPK1	0.21	0.17	0.42	0.04
NT5C3	DTYMK	0.20	0.20	0.02	0.91
NT5C3	NME1	-0.14	0.36	-0.30	0.15
NT5C3	NME3	-0.15	0.33	-0.21	0.33
NT5C3	ADK	0.37	0.01	0.13	0.54
NT5C3	NT5E	0.17	0.26	0.05	0.80
NT5C3	NT5C2	0.15	0.34	-0.11	0.59
NT5C3	NT5C1B	0.00	1.00	-0.17	0.44
NT5C3	NT5C	0.35	0.02	0.12	0.57
UCK1	TK2	0.01	0.93	-0.16	0.44
UCK1	DGUOK	-0.04	0.78	-0.14	0.52
UCK1	NT5M	0.16	0.30	0.28	0.19
UCK1	AK2	0.21	0.17	0.20	0.35
UCK1	NME4	-0.07	0.65	0.27	0.21
UCK1	RRM1	0.10	0.53	0.32	0.12
UCK1	RRM2	0.31	0.04	0.45	0.03
UCK1	RRM2B	0.07	0.66	-0.09	0.69
UCK1	TK1	0.24	0.11	0.26	0.23
UCK1	DCK	-0.03	0.87	0.18	0.41
UCK1	AK1	0.20	0.20	-0.07	0.75
UCK1	AK5	-0.09	0.57	0.30	0.16

UCK1	GUK1	0.33	0.03	0.15	0.47
UCK1	CMPK1	-0.09	0.57	-0.16	0.45
UCK1	DTYMK	0.10	0.53	0.42	0.04
UCK1	NME1	-0.20	0.20	-0.08	0.70
UCK1	NME3	0.09	0.58	0.03	0.89
UCK1	ADK	0.11	0.47	0.43	0.03
UCK1	NT5E	0.18	0.24	0.05	0.83
UCK1	NT5C2	0.32	0.03	0.08	0.72
UCK1	NT5C1B	0.16	0.29	0.11	0.62
UCK1	NT5C	0.24	0.11	-0.03	0.87
UCK1	NT5C3	0.23	0.13	0.02	0.93
UCK2	TK2	0.03	0.85	-0.03	0.88
UCK2	DGUOK	0.15	0.32	-0.40	0.05
UCK2	NT5M	0.26	0.08	0.56	0.00
UCK2	AK2	0.32	0.03	0.01	0.97
UCK2	NME4	0.19	0.21	0.30	0.16
UCK2	RRM1	0.31	0.04	0.27	0.21
UCK2	RRM2	0.25	0.10	0.44	0.03
UCK2	RRM2B	-0.10	0.52	-0.06	0.79
UCK2	TK1	0.28	0.06	0.22	0.30
UCK2	DCK	0.19	0.22	-0.03	0.88
UCK2	AK1	0.19	0.21	0.06	0.78
UCK2	AK5	0.14	0.37	0.09	0.69
UCK2	GUK1	0.32	0.03	0.42	0.04
UCK2	CMPK1	-0.23	0.14	-0.32	0.13
UCK2	DTYMK	0.40	0.01	0.32	0.13
UCK2	NME1	0.29	0.05	0.00	0.99

UCK2	NME3	0.35	0.02	0.35	0.09
UCK2	ADK	0.18	0.24	0.09	0.68
UCK2	NT5E	0.23	0.13	-0.03	0.87
UCK2	NT5C2	0.00	0.98	-0.22	0.31
UCK2	NT5C1B	0.01	0.97	0.17	0.44
UCK2	NT5C	0.13	0.42	0.15	0.48
UCK2	NT5C3	-0.05	0.77	-0.13	0.53
UCK2	UCK1	0.08	0.61	0.54	0.01

Table 12: k_{cat}/K_m. Molecular weights taken for multimer forms of the proteins.

	Molecular weight (kd)	References (for molecular weight)	Vmax (µmol per min per mg)	References (for V_{max})	K_m (µM)	V_{max}/K_m (µmol per min per mg per µM)	k_{cat}/K_m (per M per s)	Notes
DGUOK	58	[91]						
dG			0.04	[89]	4.00	0.01	10391.67	
dA			0.43	[89]	467.00	0.00	888.01	
dI			0.39	[89]	12.00	0.03	31416.67	
TK2	87	[91]						TK2 exists both as dimer and tetramer: mean molecular weight assumed
dT			1.29	[90]	3.61	0.36	517979.04	Hill kinetics: 'K_m' = 13^0.5
dC			0.79	[90]	11.00	0.07	104004.55	
dU				[6]			31078.74	dU activity is about 6% of dT activity
NT5M	46	[92]						
dUMP			110.00	[85]	100.00	1.10	843333.33	
dTMP			74.00	[85]	200.00	0.37	283666.67	
dCMP			0.00	[88]	150.00	0.00	0.00	
dGMP			4.40	[88]	150.00	0.03	22488.89	
dAMP			2.20	[88]	150.00	0.01	11244.44	
dIMP			6.60	[88]	150.00	0.04	33733.33	
UMP			81.40	[88]	150.00	0.54	416044.44	
CMP			0.00	[88]	150.00	0.00	0.00	
GMP			0.00	[88]	150.00	0.00	0.00	
AMP			2.20	[88]	150.00	0.01	11244.44	

IMP			2.20	[88]	150.00	0.01	11244.44	
3’-dTMP			226.60	[88]	150.00	1.51	1158177.78	
3’-UMP			74.80	[88]	150.00	0.50	382311.11	
3’-CMP			0.00	[88]	150.00	0.00	0.00	
2’-UMP			33.00	[88]	150.00	0.22	168666.67	
2’-GMP			0.00	[88]	150.00	0.00	0.00	
dTDP			2.20	[88]	150.00	0.01	11244.44	
dTTP			0.00	[88]	150.00	0.00	0.00	
AK2	26	[91]						
AMP			198.40	[81]	80.00	2.48	1074666.67	
dAMP			272.80	[81]	210.00	1.30	562920.63	
CMP			161.20	[81]	6000.00	0.03	11642.22	
UMP			3.96	[81]	9000.00	0.00	190.67	
CMPK2	44.5	[8]						
dUMP			0.48	[8]	100.00	0.00	3560.00	
dCMP			1.77	[8]	1310.00	0.00	1002.10	
CMP			1.64	[8]	3090.00	0.00	393.64	
UMP			0.19	[8]	6300.00	0.00	22.37	
POLG								POLG V_{max}s are $_{K}$cat (per s), and reduced by 1/2
dTTP			12.50	[83]	0.63		19841269.84	
dCTP			21.50	[83]	0.90		23888888.89	
dATP			22.50	[83]	0.80		28125000.00	
dGTP			18.50	[83]	0.80		23125000.00	

CTP			0.01	[87]	67.00		143.28	
ATP			0.01	[87]	100.00		56.00	
DNC (Lam et al 2005)	32	[84]						Presence of cholesterol and iADP assumed
dCTP			0.04	[84]	3000.00	0.00	7.89	
dATP			0.01	[84]	2700.00	0.00	2.39	
dTTP			0.00	[84]	600.00	0.00	4.00	

Table 13: Concentration/K_m values. Concentration assumptions can be thought of as approximating the substrate concentrations in mitochondria of 'quiescent' (Low) or 'cycling' (High) cells. dNXP = dNMP or dNDP or dNTP.

			High concentrations		Low concentrations		
	K_m (μM)	**References (for K_m)**	**Concentration (μM)**	**Concentration / K_m**	**Concentration (μM)**	**Concentration / K_m**	**Notes**
DGUOK							
dG	4.0	[89]	0.5	0.13	0.50	0.13	
dA	467.0	[89]	0.5	0.00	0.50	0.00	
dI	12.0	[89]	0.5	0.04	0.50	0.04	
TK2							
dT	3.6	[90]	0.71	0.20	0.71	0.20	Hill kinetics: 'K_m' = 13^0.5, 'Concentration' = 0.5^0.5
dC	11.0	[90]	0.5	0.05	0.50	0.05	
dU	6.0	[6]	0.5	0.08	0.50	0.08	
NT5M							
dUMP	100.0	[85]	1	0.01	0.10	0.00	dUMP and dTMP K_ms were available, rest assumed to be 150 μM
dTMP	200.0	[85]	10	0.05	1.00	0.01	
dCMP	150.0	[88]	10	0.07	1.00	0.01	No reaction (V_{max} = 0)
dGMP	150.0	[88]	10	0.07	1.00	0.01	
dAMP	150.0	[88]	10	0.07	1.00	0.01	
dIMP	150.0	[88]	0.1	0.00	0.01	0.00	
UMP	150.0	[88]	100	0.67	100.00	0.67	
CMP	150.0	[88]	100	0.67	100.00	0.67	No reaction (V_{max} = 0)
GMP	150.0	[88]	100	0.67	100.00	0.67	No reaction (V_{max} = 0)
AMP	150.0	[88]	100	0.67	100.00	0.67	

IMP	150.0	[88]	1	0.01	1.00	0.01	
3’-dTMP	150.0	[88]	0.1	0.00	0.01	0.00	
3’-UMP	150.0	[88]	0.1	0.00	0.01	0.00	
3’-CMP	150.0	[88]	0.1	0.00	0.01	0.00	No reaction (V_{max} = 0)
2’-UMP	150.0	[88]	0.1	0.00	0.01	0.00	
2’-GMP	150.0	[88]	0.1	0.00	0.01	0.00	
dTDP	150.0	[88]	10	0.07	1.00	0.01	
dTTP	150.0	[88]	10	0.07	1.00	0.01	No reaction (V_{max} = 0)
AK2							
AMP	80.0	[81]	100	1.25	100.00	1.25	
dAMP	210.0	[81]	10	0.05	1.00	0.00	
CMP	6000.0	[81]	100	0.02	100.00	0.02	
UMP	9000.0	[81]	100	0.01	100.00	0.01	
CMPK2							
dUMP	100.0	[8]	1	0.01	0.10	0.00	
dCMP	1310.0	[8]	10	0.01	1.00	0.00	
CMP	3090.0	[8]	100	0.03	100.00	0.03	
UMP	6300.0	[8]	100	0.02	100.00	0.02	
POLG							
dTTP	0.6	[83]	10	15.87	1.00	1.59	
dCTP	0.9	[83]	10	11.11	1.00	1.11	
dATP	0.8	[83]	10	12.50	1.00	1.25	
dGTP	0.8	[83]	10	12.50	1.00	1.25	
CTP	67.0	[87]	100	1.49	100.00	1.49	
ATP	100.0	[87]	100	1.00	100.00	1.00	
NME4							

dTDP	1000.0	[86]	10	0.01	1.00	0.00	
DNC (Dolce et al 2001)							
ATP	42.6	[82]	100	2.35	100.00	2.35	ATP and ADP K_ms available, rest assumed to be same as K_i
ADP	106.0	[82]	100	0.94	100.00	0.94	
GDP	197.0	[82]	100	0.51	100.00	0.51	
CDP	284.0	[82]	100	0.35	100.00	0.35	
UDP	380.0	[82]	100	0.26	100.00	0.26	
dADP	14.0	[82]	10	0.71	1.00	0.07	
dGDP	55.0	[82]	10	0.18	1.00	0.02	
dCDP	99.0	[82]	10	0.10	1.00	0.01	
dTDP	117.0	[82]	10	0.09	1.00	0.01	
dUDP	179.0	[82]	1	0.01	0.10	0.00	
dGTP	230.0	[82]	10	0.04	1.00	0.00	
dCTP	423.0	[82]	10	0.02	1.00	0.00	
dTTP	595.0	[82]	10	0.02	1.00	0.00	
dUTP	963.0	[82]	1	0.00	0.10	0.00	
DNC (Lam et al 2005)							Presence of cholesterol and iADP assumed
dCTP	3000.0	[84]	10	0.00	1.00	0.00	
dATP	2700.0	[84]	10	0.00	1.00	0.00	
dTTP	600.0	[84]	10	0.02	1.00	0.00	

Table 14: Enzyme inhibitions. K_i taken to be K_m when K_i not available. 'high' = High concentrations, 'low' = Low concentrations.

	Concentration (μM) ('high')	K_i (μM)	References (for K_i)	$[i]/K_i$ ('high')	Sum($[i]/K_i$) ('high')	Concentration (μM) ('low')	$[i]/K_i$ ('low')	Sum($[i]/K_i$) ('low')	Notes
DGUOK					28.27			2.98	
dG	0.50	4.00	[89]	0.13		0.50	0.13		
dA	0.50	467.00	[89]	0.00		0.50	0.00		
dI	0.50	12.00	[89]	0.04		0.50	0.04		
dGMP	10.00	4.00	[97]	2.50		1.00	0.25		
dAMP	10.00	28.00	[97]	0.36		1.00	0.04		
dIMP	0.10	78.00	[97]	0.00		0.01	0.00		
dGTP	10.00	0.40	[97]	25.00		1.00	2.50		
dATP	10.00	41.00	[97]	0.24		1.00	0.02		
dITP	0.10	41.00	[97]	0.00		0.01	0.00		K_i of dITP set equal to dATP K_i
TK2					17.24			1.83	
dT	0.50	4.90	[90]	0.10		0.50	0.10		
dC	0.50	40.00	[90]	0.01		0.50	0.01		
dU	0.50	227.00	[6]	0.00		0.50	0.00		K_i of dU set as geometric mean
dTTP	10.00	2.30	[90]	4.35		1.00	0.43		
dCTP	10.00	0.83	[90]	12.05		1.00	1.20		
dUTP	1.00	1.38	[90]	0.72		0.10	0.07		K_i of dUTP on TK2 geometric mean of dCTP and dTTP values
NT5M					3.07			2.71	
dUMP	1.00	100.00	[85]	0.01		0.10	0.00		
dTMP	10.00	200.00	[85]	0.05		1.00	0.01		

dCMP	10.00	150.00	[88]	0.07		1.00	0.01		
dGMP	10.00	150.00	[88]	0.07		1.00	0.01		
dAMP	10.00	150.00	[88]	0.07		1.00	0.01		
dIMP	0.10	150.00	[88]	0.00		0.01	0.00		
UMP	100.00	150.00	[88]	0.67		100.00	0.67		
CMP	100.00	150.00	[88]	0.67		100.00	0.67		
GMP	100.00	150.00	[88]	0.67		100.00	0.67		
AMP	100.00	150.00	[88]	0.67		100.00	0.67		
IMP	1.00	150.00	[88]	0.01		1.00	0.01		
3’-dTMP	0.10	150.00	[88]	0.00		0.01	0.00		
3’-UMP	0.10	150.00	[88]	0.00		0.01	0.00		
3’-CMP	0.10	150.00	[88]	0.00		0.01	0.00		
2’-UMP	0.10	150.00	[88]	0.00		0.01	0.00		
2’-GMP	0.10	150.00	[88]	0.00		0.01	0.00		
dTDP	10.00	150.00	[88]	0.07		1.00	0.01		
dTTP	10.00	150.00	[88]	0.07		1.00	0.01		
AK2					1.33			1.28	
AMP	100.00	80.00	[81]	1.25		100.00	1.25		
dAMP	10.00	210.00	[81]	0.05		1.00	0.00		
CMP	100.00	6000.00	[81]	0.02		100.00	0.02		
UMP	100.00	9000.00	[81]	0.01		100.00	0.01		
CMPK2					0.07			0.05	
dUMP	1.00	100.00	[8]	0.01		0.10	0.00		
dCMP	10.00	1310.00	[8]	0.01		1.00	0.00		
CMP	100.00	3090.00	[8]	0.03		100.00	0.03		
UMP	100.00	6300.00	[8]	0.02		100.00	0.02		

S1: Simulation parameters (not *Mathematica*-readable).

Start of L strand replication
Lstrandstart=10969;

The fractions of A, C, G, T on the heavy and light strands of mtDNA
fdTH=0.309;
fdTL=0.247;
fdCH=0.131;
fdCL=0.313;
fdAH=0.247;
fdAL=0.309;
fdGH=0.313;
fdGL=0.131;

Hill coefficient of TK2-deoxythymidine reaction
Reference [6]
tk2hill=0.5;

The length of both strands of mtDNA
DNAlength=33136;
The length of one strand of mtDNA
strandDNA=DNAlength / 2;

Volume of a mitochondrion
Reference [93]
volmito=2 x 10^{-16};

Conversion factor used to convert Kms and concentrations from micromolar to molecules per mitochondrion
(conversion = 120.4;)
conversion=1 x 10^{-6} x 6.022 x 10^{23} x volmito;
secondsperminute=60;

Factor used to decrease the Vmax of the polymerase on double stranded templates with lower primer density
Reference [93]
dsfact=1 / 2;

Polymerase kinetic constants
Reference [83]
VmaxPoldT=25.0 x dsfact x secondsperminute;
VmaxPoldC=43.0 x dsfact x secondsperminute;
VmaxPoldA=45.0 x dsfact x secondsperminute;

VmaxPoldG=37.0 x dsfact x secondsperminute;
KmPoldT=0.63 x conversion;
KmPoldC=0.9 x conversion;
KmPoldA=0.8 x conversion;
KmPoldG=0.8 x conversion;

Ki of dTTP on TK2
Reference [90]
kidttptk2=2.3 x conversion;

Ki of dUTP on TK2: geometric mean of dCTP and dTTP values
kidutptk2=1.38 x conversion;

Ki of dCTP on TK2
Reference [90]
kidctptk2=0.83 x conversion;

Ki of dU on TK2: geometric mean
Reference [6]
kidutk2=227 x conversion;

Ki of dC on TK2
Reference [90]
kidctk2=40 x conversion;

Ki of dT on TK2
Reference [90]
kidttk2=4.9 x conversion;

(Substrate Kis on DGUOK set equal to substrate Kms)

Ki of dI on DGUOK set equal to Km
Reference [89]
kididgk=12 x conversion;

Ki of dIMP on DGUOK
Reference [97]
kidimpdgk=78 x conversion;

Ki of dITP on DGUOK set equal to dATP Ki
kiditpdgk=kidatpdgk;

Ki of dGMP on DGUOK
Reference [97]
kidgmpdgk=4 x conversion;

Ki of dAMP on DGUOK
Reference [97]
kidampdgk=28 x conversion;

Ki of dATP on DGUOK
Reference [97]
kidatpdgk=41 x conversion;

Ki of dGTP on DGUOK
Reference [97]
kidgtpdgk=0.4 x conversion;

Estimated nucleoside transporter (ENT) molecular weight in kilodalton
Reference [93]
transporterMW=50;

TK2 and DGUOK molecular weights in kilodalton
(DGUOK is a dimer, TK2 exists both as dimer and tetramer (mean taken))
Reference [76, 101]
dgkMW=58;
tk2MW=87;

Molecular weight of NT5M in kilodalton (dimer)
Reference [88, 92]
dnt2MW=46;

Ectonucleotidase molecular weight in kilodalton (tetramer)
Reference [91]
enMW=210;

TMPK2 molecular weight in kilodalton
Reference [9]
tmpk2MW=44;

GMPK2 assumed molecular weight in kilodalton
Reference [91]
gmpk2MW=22;

CMPK2 molecular weight in kilodalton
Reference [8]
cmpk2MW=44.5;

AK2 molecular weight in kilodalton
Reference [UniProt accession P54819]
akMW=26;

NME4 molecular weight in kilodalton (homohexamer)
Reference [86]
ndpkMW=120;

Nucleoside kinase molecules in each mitochondrion
Reference [93]
tk2moleculespermito=100;
dgkmoleculespermito=200;

NT5M molecules in each mitochondrion
Reference [93]
dnt2moleculespermito=50;

Ectonucleotidase molecules in each mitochondrion
enmoleculespermito=50;

TMPK2 molecules in each mitochondrion
Reference [93]
tmpk2moleculespermito=50;

GMPK2 molecules in each mitochondrion
Reference [93]
gmpk2moleculespermito=50;

CMPK2 molecules in each mitochondrion
Reference [93]
cmpk2moleculespermito=50;

NME4 molecules in each mitochondrion
Reference [93]
ndpkmoleculespermito=300;

The factor that the reverse reaction is faster than the forward reaction for NMPK
factorMD=0.1; (AMP/ADP)

The factor that the reverse reaction is faster than the forward reaction for NDPK
factorDT=0.1; (ADP/ATP)

ENT molecules per mitochondrion
Reference [93]
transportermoleculespermito=38;

Adenylate kinase molecules per mitochondrion
Reference [93]
akmoleculespermito=450;

ENT Vmax converting from micromoles substrate/mg enzyme/minute to molecules substrate/mitochondrion/minute
Reference [98, 102]
transportervmax=0.000086/0.0000021 x transportermoleculespermito;

Vmax of the first phosphorylation of dT in the forward direction converting from micromoles substrate/mg enzyme/minute to molecules substrate/mitochondrion/minute
Reference [90]
Vmax1PfdT=1.288 x tk2MW x tk2moleculespermito;

Vmax of the first phosphorylation of dC in the forward direction converting from micromoles substrate/mg enzyme/minute to molecules substrate/mitochondrion/minute
Reference [90]
Vmax1PfdC=0.789 x tk2MW x tk2moleculespermito;

Vmax of dC with DGUOK converting from micromoles substrate/mg enzyme/minute to molecules substrate/mitochondrion/minute
Reference [89]
Vmax1PfdCdgk=0.059 x dgkMW x dgkmoleculespermito;

Vmax of the first phosphorylation of dA in the forward direction converting from micromoles substrate/mg enzyme/minute to molecules substrate/mitochondrion/minute
Reference [89]
Vmax1PfdA=0.429 x dgkMW x dgkmoleculespermito;

Vmax of the first phosphorylation of dG in the forward direction converting from micromoles substrate/mg enzyme/minute to molecules substrate/mitochondrion/minute
Reference [89]
Vmax1PfdG=0.043 x dgkMW x dgkmoleculespermito;

Vmax of the first phosphorylation of dT in the reverse direction converting from micromoles substrate/mg enzyme/minute to molecules substrate/mitochondrion/minute
Reference [85]
Vmax1PrdT=74 x dnt2MW x dnt2moleculespermito;

Ectonucleotidase Vmax of the first phosphorylation of dT in the reverse direction converting from micromoles substrate/mg enzyme/minute to molecules substrate/mitochondrion/minute
Vmax1PrdTen=4.5 x enMW x enmoleculespermito;

Vmax of the first phosphorylation of dC in the reverse direction converting from micromoles substrate/mg enzyme/minute to molecules substrate/mitochondrion/minute
Vmax1PrdC=4.5 x enMW x enmoleculespermito;

Vmax of the first phosphorylation of dA in the reverse direction converting from micromoles substrate/mg enzyme/minute to molecules substrate/mitochondrion/minute
Vmax1PrdA=4.5 x enMW x enmoleculespermito;

Vmax of the first phosphorylation of dG in the reverse direction converting from micromoles substrate/mg enzyme/minute to molecules substrate/mitochondrion/minute
Vmax1PrdG=4.5 x enMW x enmoleculespermito;

Vmax of the second phosphorylation of dT in the forward direction converting from micromoles substrate/mg enzyme/minute to molecules substrate/mitochondrion/minute
Reference [91]
Vmax2PfdT=0.821 x tmpk2MW x tmpk2moleculespermito;

Vmax of the second phosphorylation of dC in the forward direction converting from micromoles substrate/mg enzyme/minute to molecules substrate/mitochondrion/minute
Reference [8]

Vmax2PfdC=1.77 x cmpk2MW x cmpk2moleculespermito;

Vmax of the second phosphorylation of dA in the forward direction converting from micromoles substrate/mg enzyme/minute to molecules substrate/mitochondrion/minute
Reference [81]
Vmax2PfdA=272.8 x akMW x akmoleculespermito;

Vmax of the second phosphorylation of dG in the forward direction converting from micromoles substrate/mg enzyme/minute to molecules substrate/mitochondrion/minute
Reference [81]
Vmax2PfdG=1.54 x gmpk2MW x gmpk2moleculespermito;

Vmax of the second phosphorylation of dT in the reverse direction
Vmax2PrdT=Vmax2PfdT x factorMD;

Vmax of the second phosphorylation of dC in the reverse direction
Vmax2PrdC=Vmax2PfdC x factorMD;

Vmax of the second phosphorylation of dA in the reverse direction
Vmax2PrdA=Vmax2PfdA x factorMD;

Vmax of the second phosphorylation of dG in the reverse direction
Vmax2PrdG=Vmax2PfdG x factorMD;

Vmax of the third phosphorylation of dT in the forward direction converting from micromoles substrate/mg enzyme/minute to molecules substrate/mitochondrion/minute
Reference [99]
Vmax3PfdT=140 x ndpkMW x ndpkmoleculespermito;

Vmax of the third phosphorylation of dC in the forward direction converting from micromoles substrate/mg enzyme/minute to molecules substrate/mitochondrion/minute
Reference [99]
Vmax3PfdC=50 x ndpkMW x ndpkmoleculespermito;

Vmax of the third phosphorylation of dA in the forward direction converting from micromoles substrate/mg enzyme/minute to molecules substrate/mitochondrion/minute
Reference [86]
Vmax3PfdA=225 x ndpkMW x ndpkmoleculespermito; (set equal to dGDP Vmax)

Vmax of the third phosphorylation of dG in the forward direction converting from micromoles substrate/mg enzyme/minute to molecules substrate/mitochondrion/minute
Reference [99]
Vmax3PfdG=225 x ndpkMW x ndpkmoleculespermito;

Vmax of the third phosphorylation of dT in the reverse direction
Vmax3PrdT=Vmax3PfdT x factorDT;

Vmax of the third phosphorylation of dC in the reverse direction
Vmax3PrdC=Vmax3PfdC x factorDT;

Vmax of the third phosphorylation of dA in the reverse direction
Vmax3PrdA=Vmax3PfdA x factorDT;

Vmax of the third phosphorylation of dG in the reverse direction
Vmax3PrdG=Vmax3PfdG x factorDT;

ENT Km
Reference [98]
transporterkm=2 x conversion;

Km of the first phosphorylation of dT in the forward direction
Reference [90]
km1PfdT=13 x conversion;

Km of the first phosphorylation of dC in the forward direction
Reference [90]
km1PfdC=11 x conversion;

Km of dC with DGUOK
Reference [89]
km1PfdCdgk=336 x conversion;

Km of the first phosphorylation of dA in the forward direction
Reference [89]
km1PfdA=467 x conversion;

Km of the first phosphorylation of dG in the forward direction
Reference [89]
km1PfdG=4 x conversion;

Km of the first phosphorylation of dT, dU in the reverse direction
Reference [88]
km1PrdT=200 x conversion;
km1PrdU=100 x conversion;
km1PrrU=1.5 x km1PrdT;

Ectonucleotidase data: geometric means for substrate Kms, higher Kms plugged for inhibitions to be conservative
Reference [91, 92]
Ectonucleotidase Km of the first phosphorylation of dT, dU, rU in the reverse direction
km1PrdTen=22.5 x conversion;
km1PrdUen=110 x conversion; (set equal to UMP Km)
km1PrrUen=110 x conversion; (set equal to Km)

Ectonucleotidase Km of the first phosphorylation of dC, rC in the reverse direction
km1PrdC=290 x conversion;
km1PrrC=360 x conversion;

Ectonucleotidase Km of the first phosphorylation of da, rA in the reverse direction

km1PrdA=62 x conversion;
km1PrrA=19 x conversion; (set equal to Km)

kiadpen=17 x conversion;
kiatpen=15 x conversion;

Ectonucleotidase Km of the first phosphorylation of dG, rG in the reverse direction
km1PrdG=48 x conversion;
km1PrrG=59 x conversion; (set equal to Km)

Ectonucleotidase Km of the first phosphorylation of dI, rI in the reverse direction
km1PrdI=100 x conversion; (set equal to Km of IMP)
km1PrrI=100 x conversion; (set equal to Km)

Km of the second phosphorylation of dT in the forward direction
Reference [81]
km2PfdT=20 x conversion;
km2PfdUtmpk2=2600 x conversion; (Km is 170, but Ki is 2600)

Miscellaneous inhibitions
Reference [91]
kidttptmpk2=700 x conversion;
kidttmpk2=180 x conversion;

Km of the second phosphorylation of dC in the forward direction
Reference [8]
km2PfdC=1310 x conversion;
km2PfrC=3090 x conversion;
km2PfrU=6300 x conversion;
km2PfdUcmpk2=100 x conversion;

CMPK1 can phosphorylate AMP and dAMP
Reference [100]
km2PfrAcmpk2=km2PrrAcmpk2=km2PfdAcmpk2=km2PrdAcmpk2=100 x 500 x conversion; (Km of CMP is 500 micromolar)

Km of the second phosphorylation of dA in the forward direction
Reference [81]
km2PfdA=210 x conversion;
km2PfrA=80 x conversion;

CMP and UMP have some reactivity with AK2 - included as inhibitions
Reference [81]
km2PfrCak2=6000 x conversion;
km2PfrUak2=9000 x conversion;

Km of the second phosphorylation of dG in the forward direction

Reference [91]
km2PfdG=112 x conversion;
km2PfrG=18 x conversion;

Km of the second phosphorylation of dT in the reverse direction
km2PrdT=km2PfdT;
km2PrdUtmpk2=km2PfdUtmpk2;

Km of the second phosphorylation of dC in the reverse direction
km2PrdC=km2PfdC;
km2PrrC=km2PfrC;
km2PrrU=km2PfrU;
km2PrdUcmpk2=km2PfdUcmpk2;

Km of the second phosphorylation of dA in the reverse direction
km2PrdA=km2PfdA;
km2PrrA=km2PfrA;

km2PrrCak2=km2PfrCak2;
km2PrrUak2=km2PfrUak2;

Km of the second phosphorylation of dG in the reverse direction
km2PrdG=km2PfdG;
km2PrrG=km2PfrG;

(Reaction is linear for dTDP and UDP until at least 1000 uM)
Km of the third phosphorylation of dT in the forward direction
Reference [99]
km3PfdT=1000 x conversion;
km3PfdU=km3PfdT;
km3PfrU=km3PfdT;

Km of the third phosphorylation of dC in the forward direction
Reference [99]
km3PfdC=1000 x conversion; (dNDPs are weaker substrates than rNDPs: author statement but data n/a so same value used)
km3PfrC=1000 x conversion; (Reaction linear until at least 1000 uM)

Km of the third phosphorylation of dA in the forward direction
Reference [99]
km3PfdA=70 x conversion; (Km of ADP is about 70 micromolar, Km of dADP set equal to that of dGDP)
km3PfrA=300 x conversion; (substrate inhibition, Ki)

Km of the third phosphorylation of dG in the forward direction
Reference [99]
km3PfdG=75 x conversion;

km3PfrG=100 x conversion; (substrate inhibition, Ki)

Inosine inhibitions
km3PfrI=km3PrrI=km3PfdI=km3PrdI=1000 x conversion;

Km of the third phosphorylation of dT in the reverse direction
km3PrdT=km3PfdT;
km3PrdU=km3PrdT;
km3PrrU=km3PrdT;

Km of the third phosphorylation of dC in the reverse direction
km3PrdC=km3PfdC;
km3PrrC=km3PrdC;

Km of the third phosphorylation of dA in the reverse direction
km3PrdA=km3PfdA;
km3PrrA=km3PrdA;

Km of the third phosphorylation of dG in the reverse direction
km3PrdG=km3PfdG;
km3PrrG=km3PrdG;

(Initial concentrations selected randomly)

Initial dN concentrations
dTcyto=RandomReal[{0.05 x conversion, 5 x conversion}];
dCcyto=RandomReal[{0.05 x conversion, 5 x conversion}];
dAcyto=RandomReal[{0.05 x conversion, 5 x conversion}];
dGcyto=RandomReal[{0.05 x conversion, 5 x conversion}];

dT0=dTcyto;
dC0=dCcyto;
dA0=dAcyto;
dG0=dGcyto;

Initial dNXP and rNXP levels
If[celltype==1,dTTPcyto=RandomReal[{0.1 x conversion, 10 x conversion}]];
If[celltype==1,dCTPcyto=RandomReal[{0.1 x conversion, 10 x conversion}]];
If[celltype==1,dATPcyto=RandomReal[{0.1 x conversion, 10 x conversion}]];
If[celltype==1,dGTPcyto=RandomReal[{0.1 x conversion, 10 x conversion}]];

dTMP0=RandomReal[{0.01 x conversion, 10 x conversion}];
dTDP0=RandomReal[{0.01 x conversion, 10 x conversion}];
dTTP0=dTTPcyto;

dCMP0=RandomReal[{0.01 x conversion, 10 x conversion}];

```
dCDP0=RandomReal[{0.01 x conversion, 10 x conversion}];
dCTP0=dCTPcyto;

dAMP0=RandomReal[{0.01 x conversion, 10 x conversion}];
dADP0=RandomReal[{0.01 x conversion, 10 x conversion}];
dATP0=dATPcyto;

dGMP0=RandomReal[{0.01 x conversion, 10 x conversion}];
dGDP0=RandomReal[{0.01 x conversion, 10 x conversion}];
dGTP0=dGTPcyto;

dU=dUcyto=dTcyto;
rU=rUcyto=dTcyto;
dI=dIcyto=0.1 x dAcyto;
rI=rIcyto=0.1 x dAcyto;
rC=rCcyto=dCcyto;
rA=rAcyto=dAcyto;
rG=rGcyto=dGcyto;

dUMP=1 x conversion; (0.1 x dTMP0;)
rUMP=10 x conversion; (10 x dTMP0;)
dIMP=1 x conversion; (0.1 x dAMP0;)
rIMP=1 x conversion; (0.1 x dAMP0;)
rCMP=10 x conversion; (10 x dCMP0;)
rAMP=10 x conversion; (10 x dAMP0;)
rGMP=10 x conversion; (10 x dGMP0;)

dUDP=1 x conversion; (0.1 x dTDP0;)
rUDP=10 x conversion; (10 x dTDP0;)
dIDP=1 x conversion; (0.1 x dADP0;)
rIDP=1 x conversion; (0.1 x dADP0;)
rCDP=10 x conversion; (10 x dCDP0;)
rADP=10 x conversion; (10 x dADP0;)
rGDP=10 x conversion; (10 x dGDP0;)

dUTP=1 x conversion; (0.1 x dTTP0;)
rUTP=10 x conversion; (10 x dTTP0;)
dITP=1 x conversion; (0.1 x dATP0;)
rITP=1 x conversion; (0.1 x dATP0;)
rCTP=10 x conversion; (10 x dCTP0;)
rATP=10 x conversion; (10 x dATP0;)
rGTP=10 x conversion; (10 x dGTP0;)

DNA0=0;
LDNA0=0;
HDNA0=0;
```

S2: *Mathematica* simulation code.

```
(*Mitochondrial deoxynucleotide metabolism and DNA replication*)
(*Vishal V Gandhi and David C Samuels*)
(*The model simulates transport of deoxynucleosides and dexoynucleotides into and out of a mitochondrion,*)(*their subsequent phosphorylation and
dephosphorylation and uptake into mtDNA*)

ClearAll["Global`*"]; (*clear any previous variables in memory*)
Off[General::spell1]; (*Turn off spelling checker*)
        Off[General::spell];

(* directory where this file and constants file is located *)
SetDirectory["C:\\Documents and Settings\\gandhiv\\My Documents\\pro\\data\\mathematicaexpbase\\transport_experiments"];

 celltype=1;

(*Choose the number of separate mitochondrial DNA replication events*)
(*Partially overlapping mtDNA replication events are not supported in this version of the code*)
numDNAmols=1;
replication=1; (*0 = Off, 1 = On, starts immediately with the simulation*)

(*Set the length of the total simulation in minutes*)
(*Replication time is determined by initial and spot dNTP levels*)

simtime=120;(*Total simulation time (min)*)

replengths = {};
repdurations = {};
parameters = {};

Do[
<<modelconstants.txt;(*Load constants file*)

parameters = Append[parameters,{dT0,dC0,dA0,dG0,dTMP0,dTDP0,dTTP0,dCMP0,dCDP0,dCTP0,dAMP0,dADP0,dATP0,dGMP0,dGDP0,dGTP0}];
```

```
count = 0;
Do[
count++;

(*Michaelis Menten equations of deoxythymidine metabolism*)

dTnucleosidetransport=
mm10[transportervmax,transporterkm,dTcyto,dCcyto,transporterkm,dAcyto,transporterkm,dGcyto,transporterkm,dUcyto,transporterkm,rUcyto,transporterkm,rC
cyto,transporterkm,rAcyto,transporterkm,rGcyto,transporterkm,dIcyto,transporterkm,rIcyto,transporterkm]-
mm10[transportervmax,transporterkm,dT[t],dC[t],transporterkm,dA[t],transporterkm,dG[t],transporterkm,dU,transporterkm,rU,transporterkm,rC,transporterkm,r
A,transporterkm,rG,transporterkm,dI,transporterkm,rI,transporterkm];
(*nucleoside transport in and out*)
dTnucleosidekinase= hill5[Vmax1PfdT,km1PfdT,dT[t],dTTP[t],kidttptk2,dC[t],kidctk2,dCTP[t],kidctptk2,dU,kidutk2,dUTP,kidutptk2,tk2hill];(*nucleoside
kinase*)
dTnucleotidase=mm2[Vmax1PrdT,km1PrdT,dTMP[t],dUMP,km1PrdU,rUMP,km1PrrU]+mm12[Vmax1PrdTen,km1PrdTen,dTMP[t],dCMP[t],km1PrdC,dAMP
[t],km1PrdA,dGMP[t],km1PrdG,dUMP,km1PrdUen,rUMP,km1PrrUen,rCMP,km1PrrC,rAMP,km1PrrA,rGMP,km1PrrG,dIMP,km1PrdI,rIMP,km1PrrI,rADP,ki
adpen,rATP,kiatpen];(*nucleotidase modeled through both dnt2 and ectonucleotidase*)
dTmpkforward= mm5[Vmax2PfdT,km2PfdT,dTMP[t],dTDP[t],km2PrdT,dUMP,km2PfdUtmpk2,dUDP,km2PrdUtmpk2,dTTP[t],kidttptmpk2,dT[t],kidttmpk2];
(*nucleoside monophosphate kinase forward*)
dTmpkreverse=mm5[Vmax2PrdT,km2PrdT,dTDP[t], dTMP[t], km2PfdT, dUMP,
km2PfdUtmpk2,dUDP,km2PrdUtmpk2,dTTP[t],kidttptmpk2,dT[t],kidttmpk2];(*nucleoside monophosphate kinase reverse*)
dTdpkforward= mm21[Vmax3PfdT,km3PfdT,dTDP[t],dCDP[t],km3PfdC,dADP[t],km3PfdA,dGDP[t],km3PfdG,dTTP[t], km3PrdT, dCTP[t],km3PrdC,
dATP[t],km3PrdA,dGTP[t],km3PrdG,dUDP,km3PfdU,dUTP,km3PrdU,rUDP,km3PfrU,rUTP,km3PrrU,rCDP,km3PfrC,rCTP,km3PrrC,rADP,km3PfrA,rATP,k
m3PrrA,rGDP,km3PfrG,rGTP,km3PrrG,rIDP,km3PfrI,rITP,km3PrrI,dIDP,km3PfdI,dITP,km3PrdI];(*nucleoside diphosphate kinase forward*)
dTdpkreverse=mm21[Vmax3PrdT,km3PrdT,dTTP[t],dTDP[t],km3PfdT,dCDP[t],km3PfdC,dADP[t],km3PfdA,dGDP[t],km3PfdG,dCTP[t],km3PrdC,
dATP[t],km3PrdA,dGTP[t],km3PrdG,dUDP,km3PfdU,dUTP,km3PrdU,rUDP,km3PfrU,rUTP,km3PrrU,rCDP,km3PfrC,rCTP,km3PrrC,rADP,km3PfrA,rATP,k
m3PrrA,rGDP,km3PfrG,rGTP,km3PrrG,rIDP,km3PfrI,rITP,km3PrrI,dIDP,km3PfdI,dITP,km3PrdI];(*nucleoside diphosphate kinase reverse*)

 (*Michaelis Menten equations of deoxycytidine metabolism*)

dCnucleosidetransport
=mm10[transportervmax,transporterkm,dCcyto,dTcyto,transporterkm,dAcyto,transporterkm,dGcyto,transporterkm,dUcyto,transporterkm,rUcyto,transporterkm,r
Ccyto,transporterkm,rAcyto,transporterkm,rGcyto,transporterkm,dIcyto,transporterkm,rIcyto,transporterkm]-
mm10[transportervmax,transporterkm,dC[t],dT[t],transporterkm,dA[t],transporterkm,dG[t],transporterkm,dU,transporterkm,rU,transporterkm,rC,transporterkm,r
A,transporterkm,rG,transporterkm,dI,transporterkm,rI,transporterkm];
(*nucleoside transport in and out*)
```

```
dCnucleosidekinase =
mm5[Vmax1PfdC,km1PfdC,dC[t],dTTP[t],kidttptk2,dT[t],kidttk2,dCTP[t],kidctptk2,dU,kidutk2,dUTP,kidutptk2]+mm9[Vmax1PfdCdgk,km1PfdCdgk,dC[t],d
ATP[t],kidatpdgk,dGTP[t],kidgtpdgk,dGMP[t],kidgmpdgk,dAMP[t],kidampdgk,dG[t],km1PfdG,dA[t],km1PfdA,dI,kididgk,dIMP,kidimpdgk,dITP,kiditpdgk];
(*nucleoside kinase, dC transformation modeled through both tk2 and dgk routes*)
dCnucleotidase=mm12[Vmax1PrdC,km1PrdC,dCMP[t],dTMP[t],km1PrdTen,dAMP[t],km1PrdA,dGMP[t],km1PrdG,dUMP,km1PrdUen,rUMP,km1PrrUen,rC
MP,km1PrrC,rAMP,km1PrrA,rGMP,km1PrrG,dIMP,km1PrdI,rIMP,km1PrrI,rADP,kiadpen,rATP,kiatpen];
dCmpkforward
=mm11[Vmax2PfdC,km2PfdC,dCMP[t],dCDP[t],km2PrdC,rCMP,km2PfrC,rCDP,km2PrrC,dUMP,km2PfdUcmpk2,dUDP,km2PrdUcmpk2,rUMP,km2PfrU,rU
DP,km2PrrU,rAMP,km2PfrAcmpk2,rADP,km2PrrAcmpk2,dAMP[t],km2PfdAcmpk2,dADP[t],km2PrdAcmpk2];(*nucleoside monophosphate kinase forward*)
dCmpkreverse
=mm11[Vmax2PrdC,km2PrdC,dCDP[t],dCMP[t],km2PfdC,rCMP,km2PfrC,rCDP,km2PrrC,dUMP,km2PfdUcmpk2,dUDP,km2PrdUcmpk2,rUMP,km2PfrU,rU
DP,km2PrrU ,rAMP,km2PfrAcmpk2,rADP,km2PrrAcmpk2,dAMP[t],km2PfdAcmpk2,dADP[t],km2PrdAcmpk2]; (*nucleoside monophosphate kinase
reverse*)
dCdpkforward = mm21[Vmax3PfdC,km3PfdC,dCDP[t],dTDP[t],km3PfdT,dADP[t],km3PfdA,dGDP[t],km3PfdG,dTTP[t], km3PrdT, dCTP[t],km3PrdC,
dATP[t],km3PrdA,dGTP[t],km3PrdG,dUDP,km3PfdU,dUTP,km3PrdU,rUDP,km3PfrU,rUTP,km3PrrU,rCDP,km3PfrC,rCTP,km3PrrC,rADP,km3PfrA,rATP,k
m3PrrA,rGDP,km3PfrG,rGTP,km3PrrG,rIDP,km3PfrI,rITP,km3PrrI,dIDP,km3PfdI,dITP,km3PrdI];(*nucleoside diphosphate kinase forward*)
dCdpkreverse = mm21[Vmax3PrdC,km3PrdC,dCTP[t],dCDP[t],km3PfdC,dTDP[t],km3PfdT,dADP[t],km3PfdA,dGDP[t],km3PfdG,dTTP[t],
km3PrdT,dATP[t],km3PrdA,dGTP[t],km3PrdG,dUDP,km3PfdU,dUTP,km3PrdU,rUDP,km3PfrU,rUTP,km3PrrU,rCDP,km3PfrC,rCTP,km3PrrC,rADP,km3Pfr
A,rATP,km3PrrA,rGDP,km3PfrG,rGTP,km3PrrG,rIDP,km3PfrI,rITP,km3PrrI,dIDP,km3PfdI,dITP,km3PrdI];(*nucleoside diphosphate kinase reverse*)

(*Michaelis Menten equations of deoxyadenosine metabolism*)

dAnucleosidetransport=mm10[transportervmax,transporterkm,dAcyto,dCcyto,transporterkm,dTcyto,transporterkm,dGcyto,transporterkm,dUcyto,transporterkm,r
Ucyto,transporterkm,rCcyto,transporterkm,rAcyto,transporterkm,rGcyto,transporterkm,dIcyto,transporterkm,rIcyto,transporterkm]-
mm10[transportervmax,transporterkm,dA[t],dC[t],transporterkm,dT[t],transporterkm,dG[t],transporterkm,dU,transporterkm,rU,transporterkm,rC,transporterkm,r
A,transporterkm,rG,transporterkm,dI,transporterkm,rI,transporterkm];
(*nucleoside transport in and out*)
dAnucleosidekinase=
mm8[Vmax1PfdA,km1PfdA,dA[t],dG[t],km1PfdG,dATP[t],kidatpdgk,dGTP[t],kidgtpdgk,dGMP[t],kidgmpdgk,dAMP[t],kidampdgk,dI,kididgk,dIMP,kidimpdg
k,dITP,kiditpdgk];
(*nucleoside kinase*)
dAnucleotidase=mm12[Vmax1PrdA,km1PrdA,dAMP[t],dTMP[t],km1PrdTen,dCMP[t],km1PrdC,dGMP[t],km1PrdG,dUMP,km1PrdUen,rUMP,km1PrrUen,rC
MP,km1PrrC,rAMP,km1PrrA,rGMP,km1PrrG,dIMP,km1PrdI,rIMP,km1PrrI,rADP,kiadpen,rATP,kiatpen];
dAmpkforward=
mm7[Vmax2PfdA,km2PfdA,dAMP[t],dADP[t],km2PrdA,rAMP,km2PfrA,rADP,km2PrrA,rCMP,km2PfrCak2,rUMP,km2PfrUak2,rCDP,km2PrrCak2,rUDP,km
2PrrUak2];(*nucleoside monophosphate kinase forward*)
```

```
dAmpkreverse
=mm7[Vmax2PrdA,km2PrdA,dADP[t],dAMP[t],km2PfdA,rADP,km2PrrA,rAMP,km2PfrA,rCMP,km2PfrCak2,rUMP,km2PfrUak2,rCDP,km2PrrCak2,rUDP,k
m2PrrUak2];(*nucleoside monophosphate kinase reverse*)
dAdpkforward= mm21[Vmax3PfdA,km3PfdA,dADP[t],dCDP[t],km3PfdC,dTDP[t],km3PfdT,dATP[t],km3PrdA,dGDP[t],km3PfdG,dTTP[t], km3PrdT,
dCTP[t],km3PrdC,dGTP[t],km3PrdG,dUDP,km3PfdU,dUTP,km3PrdU,rUDP,km3PfrU,rUTP,km3PrrU,rCDP,km3PfrC,rCTP,km3PrrC,rADP,km3PfrA,rATP,k
m3PrrA,rGDP,km3PfrG,rGTP,km3PrrG,rIDP,km3PfrI,rITP,km3PrrI,dIDP,km3PfdI,dITP,km3PrdI ];(*nucleoside diphosphate kinase forward*)
dAdpkreverse =mm21[Vmax3PrdA,km3PrdA,dATP[t],dCDP[t],km3PfdC,dTDP[t],km3PfdT,dADP[t],km3PfdA,dGDP[t],km3PfdG,dTTP[t], km3PrdT,
dCTP[t],km3PrdC,dGTP[t],km3PrdG,dUDP,km3PfdU,dUTP,km3PrdU,rUDP,km3PfrU,rUTP,km3PrrU,rCDP,km3PfrC,rCTP,km3PrrC,rADP,km3PfrA,rATP,k
m3PrrA,rGDP,km3PfrG,rGTP,km3PrrG,rIDP,km3PfrI,rITP,km3PrrI,dIDP,km3PfdI,dITP,km3PrdI ];(*nucleoside diphosphate kinase reverse*)

(*Michaelis Menten equations of deoxyguanosine metabolism*)

dGnucleosidetransport=
mm10[transportervmax,transporterkm,dGcyto,dCcyto,transporterkm,dTcyto,transporterkm,dAcyto,transporterkm,dUcyto,transporterkm,rUcyto,transporterkm,rC
cyto,transporterkm,rAcyto,transporterkm,rGcyto,transporterkm,dIcyto,transporterkm,rIcyto,transporterkm]-
mm10[transportervmax,transporterkm,dG[t],dC[t],transporterkm,dT[t],transporterkm,dA[t],transporterkm,dU,transporterkm,rU,transporterkm,rC,transporterkm,r
A,transporterkm,rG,transporterkm,dI,transporterkm,rI,transporterkm];
(*nucleoside transport in and out*)
dGnucleosidekinase=
mm8[Vmax1PfdG,km1PfdG,dG[t],dA[t],km1PfdA,dATP[t],kidatpdgk,dGTP[t],kidgtpdgk,dGMP[t],kidgmpdgk,dAMP[t],kidampdgk,dI,kididgk,dIMP,kidimpdg
k,dITP,kiditpdgk];
(*nucleoside kinase*)
dGnucleotidase=mm12[Vmax1PrdG,km1PrdG,dGMP[t],dTMP[t],km1PrdTen,dAMP[t],km1PrdA,dCMP[t],km1PrdC,dUMP,km1PrdUen,rUMP,km1PrrUen,rC
MP,km1PrrC,rAMP,km1PrrA,rGMP,km1PrrG,dIMP,km1PrdI,rIMP,km1PrrI,rADP,kiadpen,rATP,kiatpen];
dGmpkforward=mm3[Vmax2PfdG,km2PfdG,dGMP[t],dGDP[t],km2PrdG,rGMP,km2PfrG,rGDP,km2PrrG];(*nucleoside monophosphare kinase forward*)
dGmpkreverse=mm3[Vmax2PrdG,km2PrdG,dGDP[t],dGMP[t],km2PfdG,rGMP,km2PfrG,rGDP,km2PrrG];(*nucleoside monophosphate kinase reverse*)
dGdpkforward=mm21[Vmax3PfdG,km3PfdG,dGDP[t],dCDP[t],km3PfdC,dTDP[t],km3PfdT,dADP[t],km3PfdA,dATP[t],km3PrdA,dTTP[t], km3PrdT,
dCTP[t],km3PrdC,dGTP[t],km3PrdG,dUDP,km3PfdU,dUTP,km3PrdU,rUDP,km3PfrU,rUTP,km3PrrU,rCDP,km3PfrC,rCTP,km3PrrC,rADP,km3PfrA,rATP,k
m3PrrA,rGDP,km3PfrG,rGTP,km3PrrG ,rIDP,km3PfrI,rITP,km3PrrI,dIDP,km3PfdI,dITP,km3PrdI];(*nucleoside diphosphate kinase forward*)
dGdpkreverse =mm21[Vmax3PrdG,km3PrdG,dGTP[t],dCDP[t],km3PfdC,dTDP[t],km3PfdT,dADP[t],km3PfdA,dATP[t],km3PrdA,dTTP[t],
km3PrdT,dCTP[t],km3PrdC,dGDP[t],km3PfdG,dUDP,km3PfdU,dUTP,km3PrdU,rUDP,km3PfrU,rUTP,km3PrrU,rCDP,km3PfrC,rCTP,km3PrrC,rADP,km3Pfr
A,rATP,km3PrrA,rGDP,km3PfrG,rGTP,km3PrrG,rIDP,km3PfrI,rITP,km3PrrI,dIDP,km3PfdI,dITP,km3PrdI ];(*nucleoside diphosphate kinase reverse*)

(*Rates of polymerization for individual dNTP species alone*)
rdT:=If[replication>0,1,0]*mm[VmaxPoldT,KmPoldT,dTTP[t]];
rdC:=If[replication>0,1,0]*mm[VmaxPoldC,KmPoldC,dCTP[t]];
rdA:=If[replication>0,1,0]*mm[VmaxPoldA,KmPoldA,dATP[t]];
```

```
rdG:=If[replication>0,1,0]*mm[VmaxPoldG,KmPoldG,dGTP[t]];

(*Heavy Strand Polymerization Start and Stop Directions*)
 PolrateH:=If[ (startPol> t)  || ((HDNA[t])>strandDNA)  ,0,1]*HPolrate[t];
(*Light Strand Polymerization Start and Stop Directions*)
 PolrateL:= If[ ((startPol> t)  || ((LDNA[t])>strandDNA)|| ((HDNA[t])< Lstrandstart)),0,1]*LPolrate[t];

(*                                                                    *)
(*Definition of michaelis menten and hill functions*)

(*Michaelis Menten function with no inhibitors*)
mm[vmax_,km_,s_]:= If[s>0,1,0]*vmax*s/(km+s);

(*Michaelis Menten function with 1 inhibitor*)
mm1[vmax_,km_,s_,i_,ki_]:=If[s>0,1,0]*vmax*s/(s+km+km*(If[i>0,1,0]*(i/ki)));

   (*Michaelis Menten function with 2 inhibitors*)
mm2[vmax_,km_,s_,i1_,ki1_,i2_,ki2_]:=If[s>0,1,0]*vmax*s/(s+km+km*(If[i1>0,1,0]*(i1/ki1)+If[i2>0,1,0]*(i2/ki2)));

(*Michaelis Menten function with 3 inhibitors*)
mm3[vmax_,km_,s_,i1_,ki1_,i2_,ki2_,i3_,ki3_]:=If[s>0,1,0]*vmax*s/(s+km+km*(If[i1>0,1,0]*(i1/ki1)+If[i2>0,1,0]*(i2/ki2)+If[i3>0,1,0]*(i3/ki3)));

(*Michaelis Menten function with 4 inhibitors*)
mm4[vmax_,km_,s_,i1_,ki1_,i2_,ki2_,i3_,ki3_,i4_,ki4_]:=If[s>0,1,0]*vmax*s/(s+km+km*(If[i1>0,1,0]*(i1/ki1)+If[i2>0,1,0]*(i2/ki2)+If[i3>0,1,0]*(i3/ki3)+If[i
4>0,1,0]*(i4/ki4)));

(*Michaelis Menten function with 5 inhibitors*)
mm5[vmax_,km_,s_,i1_,ki1_,i2_,ki2_,i3_,ki3_,i4_,ki4_,i5_,ki5_]:=If[s>0,1,0]*vmax*s/(s+km+km*(If[i1>0,1,0]*(i1/ki1)+If[i2>0,1,0]*(i2/ki2)+If[i3>0,1,0]*(i3/
ki3)+If[i4>0,1,0]*(i4/ki4)+If[i5>0,1,0]*(i5/ki5)));

(*Michaelis Menten function with 6 inhibitors*)
mm6[vmax_,km_,s_,i1_,ki1_,i2_,ki2_,i3_,ki3_,i4_,ki4_,i5_,ki5_,i6_,ki6_]:=If[s>0,1,0]*
  vmax*s/(s+km+km*(If[i1>0,1,0]*(i1/ki1)+If[i2>0,1,0]*(i2/ki2)+If[i3>0,1,0]*(i3/ki3)+If[i4>0,1,0]*(i4/ki4)+If[i5>0,1,0]*(i5/ki5)+If[i6>0,1,0]*(i6/ki6)));

(*Michaelis Menten function with 7 inhibitors*)
mm7[vmax_,km_,s_,i1_,ki1_,i2_,ki2_,i3_,ki3_,i4_,ki4_,i5_,ki5_,i6_,ki6_,i7_,ki7_]:=If[s>0,1,0]*
```

```
vmax*s/(s+km+km*(If[i1>0,1,0]*(i1/ki1)+If[i2>0,1,0]*(i2/ki2)+If[i3>0,1,0]*(i3/ki3)+If[i4>0,1,0]*(i4/ki4)+If[i5>0,1,0]*(i5/ki5)+If[i6>0,1,0]*(i6/ki6)+If[i7>0,1
,0]*(i7/ki7)));

(*Michaelis menten function with 8 inhibitors*)
mm8[vmax_,km_,s_,i1_,ki1_,i2_,ki2_,i3_,ki3_,i4_,ki4_,i5_,ki5_,i6_,ki6_,i7_,ki7_,i8_,ki8_]:=If[s>0,1,0]*vmax*s/(s+km+km*(If[i1>0,1,0]*(i1/ki1)+If[i2>0,1,0]
*(i2/ki2)+If[i3>0,1,0]*(i3/ki3)+If[i4>0,1,0]*(i4/ki4)+If[i5>0,1,0]*(i5/ki5)+If[i6>0,1,0]*(i6/ki6)+If[i7>0,1,0]*(i7/ki7)+If[i8>0,1,0]*(i8/ki8)));

(*Michaelis menten function with 9 inhibitors*)
mm9[vmax_,km_,s_,i1_,ki1_,i2_,ki2_,i3_,ki3_,i4_,ki4_,i5_,ki5_,i6_,ki6_,i7_,ki7_,i8_,ki8_,i9_,ki9_]:=If[s>0,1,0]*vmax*s/(s+km+km*(If[i1>0,1,0]*(i1/ki1)+If[
i2>0,1,0]*(i2/ki2)+If[i3>0,1,0]*(i3/ki3)+If[i4>0,1,0]*(i4/ki4)+If[i5>0,1,0]*(i5/ki5)+If[i6>0,1,0]*(i6/ki6)+If[i7>0,1,0]*(i7/ki7)+If[i8>0,1,0]*(i8/ki8)+If[i9>0,1,0
]*(i9/ki9)));

(*Michaelis menten function with 10 inhibitors*)
mm10[vmax_,km_,s_,i1_,ki1_,i2_,ki2_,i3_,ki3_,i4_,ki4_,i5_,ki5_,i6_,ki6_,i7_,ki7_,i8_,ki8_,i9_,ki9_,i10_,ki10_]:=If[s>0,1,0]*vmax*s/(s+km+km*(If[i1>0,1,0]
*(i1/ki1)+If[i2>0,1,0]*(i2/ki2)+If[i3>0,1,0]*(i3/ki3)+If[i4>0,1,0]*(i4/ki4)+If[i5>0,1,0]*(i5/ki5)+If[i6>0,1,0]*(i6/ki6)+If[i7>0,1,0]*(i7/ki7)+If[i8>0,1,0]*(i8/ki8)
+If[i9>0,1,0]*(i9/ki9)+If[i10>0,1,0]*(i10/ki10)));

(*Michaelis menten function with 11 inhibitors*)
mm11[vmax_,km_,s_,i1_,ki1_,i2_,ki2_,i3_,ki3_,i4_,ki4_,i5_,ki5_,i6_,ki6_,i7_,ki7_,i8_,ki8_,i9_,ki9_,i10_,ki10_,i11_,ki11_]:=If[s>0,1,0]*vmax*s/(s+km+km*(
If[i1>0,1,0]*(i1/ki1)+If[i2>0,1,0]*(i2/ki2)+If[i3>0,1,0]*(i3/ki3)+If[i4>0,1,0]*(i4/ki4)+If[i5>0,1,0]*(i5/ki5)+If[i6>0,1,0]*(i6/ki6)+If[i7>0,1,0]*(i7/ki7)+If[i8>0,1
,0]*(i8/ki8)+If[i9>0,1,0]*(i9/ki9)+If[i10>0,1,0]*(i10/ki10)+If[i11>0,1,0]*(i11/ki11)));

(*Michaelis menten function with 12 inhibitors*)
mm12[vmax_,km_,s_,i1_,ki1_,i2_,ki2_,i3_,ki3_,i4_,ki4_,i5_,ki5_,i6_,ki6_,i7_,ki7_,i8_,ki8_,i9_,ki9_,i10_,ki10_,i11_,ki11_,i12_,ki12_]:=If[s>0,1,0]*vmax*s/(s
+km+km*(If[i1>0,1,0]*(i1/ki1)+If[i2>0,1,0]*(i2/ki2)+If[i3>0,1,0]*(i3/ki3)+If[i4>0,1,0]*(i4/ki4)+If[i5>0,1,0]*(i5/ki5)+If[i6>0,1,0]*(i6/ki6)+If[i7>0,1,0]*(i7/ki7
)+If[i8>0,1,0]*(i8/ki8)+If[i9>0,1,0]*(i9/ki9)+If[i10>0,1,0]*(i10/ki10)+If[i11>0,1,0]*(i11/ki11)+If[i12>0,1,0]*(i12/ki12)));

(*Michaelis Menten function with 17 inhibitors*)
mm21[vmax_,km_,s_,i1_,ki1_,i2_,ki2_,i3_,ki3_,i4_,ki4_,i5_,ki5_,i6_,ki6_,i7_,ki7_,i8_,ki8_,i9_,ki9_,i10_,ki10_,i11_,ki11_,i12_,ki12_,i13_,ki13_,i14_,ki14_,i1
5_,ki15_,i16_,ki16_,i17_,ki17_,i18_,ki18_,i19_,ki19_,i20_,ki20_,i21_,ki21_]:=If[s>0,1,0]*vmax*s/(s+km+km*(If[i1>0,1,0]*(i1/ki1)+If[i2>0,1,0]*(i2/ki2)+If[i3
>0,1,0]*(i3/ki3)+If[i4>0,1,0]*(i4/ki4)+If[i5>0,1,0]*(i5/ki5)+If[i6>0,1,0]*(i6/ki6)+If[i7>0,1,0]*(i7/ki7)+If[i8>0,1,0]*(i8/ki8)+
+If[i9>0,1,0]*(i9/ki9)+If[i10>0,1,0]*(i10/ki10)+If[i11>0,1,0]*(i11/ki11)+If[i12>0,1,0]*(i12/ki12)+If[i13>0,1,0]*(i13/ki13)+If[i14>0,1,0]*(i14/ki14)+If[i15>0,1
,0]*(i15/ki15)+If[i16>0,1,0]*(i16/ki16)+If[i17>0,1,0]*(i17/ki17)+If[i18>0,1,0]*(i18/ki18)+If[i19>0,1,0]*(i19/ki19)+If[i20>0,1,0]*(i20/ki20)+If[i21>0,1,0]*(i21
/ki21)));

(*Hill equation function with 5 inhibitors*)
```

```
hill5[vmax_,km_,s_,i1_,ki1_,i2_,ki2_,i3_,ki3_,i4_,ki4_,i5_,ki5_,hc_]:=If[s>0,1,0]*vmax*(s^hc)/((s^hc)+(km^hc+km^hc*(If[i1>0,1,0]*(i1/ki1)+If[i2>0,1,0]*(i2/
ki2)+If[i3>0,1,0]*(i3/ki3)+If[i4>0,1,0]*(i4/ki4)+If[i5>0,1,0]*(i5/ki5))));

(*                                                                    *)

(*The total simulation time is broken up so that one mtDNA molecule is copied each time through a loop*)
(*the amount of time of each separate differential equation*)

DNAmolreptime=simtime/numDNAmols;

(*A Do loop that replicates one molecule of mtDNA each time through, the loop counter i counts from 1 to numDNAmols*)

Timing[Do[
(*Hold all simulation results in an array called solution, first mtDNA molecule synthesized in solution[1],
second mtDNA molecule replicated in solution[2], so on*)
If[i!=1, Table[solution[i-1]]];

(*Variable k holds a data Table of time (min) and dNTP molecules/mitochondrion*)
If[i!=1,k=Flatten[Table[{t,dTTP[t],dCTP[t],dATP[t],dGTP[t]} /.solution[i-1],{t,start,end,1}],1]];

(*Get rid of blank lines in between each data line*)
 If[i!=1,data=ToString[TableForm[k],OutputForm]];
If[i!=1,data2=StringReplace[data,{"\n\n"-> "\n"}]];
If[i!=1,data3=ToExpression["data2"]];
(*output 5 columns, the time (min), dTTP, dCTP, dATP, dGTP (molecules) to a file called dNTPs.txt*)
If[i!=1, OutputForm[data3] >>>"dNTPs.txt"];


(*loop counter used outside of loop for last iteration*)
lin=i;
(*Start polymerization at beginning*)
startPol=DNAmolreptime*(i)-DNAmolreptime;(*start time of each differential equation loop where polymerase starts*)
start=If[i==1,0,end];(*beginning time of each differential equation loop*)
end=If[i==1,DNAmolreptime,start+DNAmolreptime];(*ending time of each differential equation loop*)

(*Set the nucleotide levels initially or this time through loop to the concentrations at the end of the last loop*)
dT0=If[i==1,dT0,First[dT[start]/.solution[i-1]]];
```

```
dTMP0=If[i==1,dTMP0,First[dTMP[start]/.solution[i-1]]];
dTDP0=If[i==1,dTDP0,First[dTDP[start]/.solution[i-1]]];
dTTP0=If[i==1,dTTP0,First[dTTP[start]/.solution[i-1]]];
dC0=If[i==1,dC0,First[dC[start]/.solution[i-1]]];
dCMP0=If[i==1,dCMP0,First[dCMP[start]/.solution[i-1]]];
dCDP0=If[i==1,dCDP0,First[dCDP[start]/.solution[i-1]]];
dCTP0=If[i==1,dCTP0,First[dCTP[start]/.solution[i-1]]];
dA0=If[i==1,dA0,First[dA[start]/.solution[i-1]]];
dAMP0=If[i==1,dAMP0,First[dAMP[start]/.solution[i-1]]];
dADP0=If[i==1,dADP0,First[dADP[start]/.solution[i-1]]];
dATP0=If[i==1,dATP0,First[dATP[start]/.solution[i-1]]];
dG0=If[i==1,dG0,First[dG[start]/.solution[i-1]]];
dGMP0=If[i==1,dGMP0,First[dGMP[start]/.solution[i-1]]];
dGDP0=If[i==1,dGDP0,First[dGDP[start]/.solution[i-1]]];
dGTP0=If[i==1,dGTP0,First[dGTP[start]/.solution[i-1]]];

(*                                                                    *)
(*differential equations*)
(*Determine individual pool levels over time by adding and subtracting kinetic equations*)

(*transport*)
ri = Range[0,1200,100];
(*OutputForm[ri] >>>"ri.txt";*)

solution[i]=NDSolve [{
dT'[t]==dTnucleosidetransport-dTnucleosidekinase+dTnucleotidase,
dTMP'[t]==dTnucleosidekinase-dTnucleotidase-dTmpkforward+dTmpkreverse,
dTDP'[t]==dTmpkforward-dTmpkreverse-dTdpkforward+dTdpkreverse,
dTTP'[t]==dTdpkforward-dTdpkreverse- PolrateL*fdTL- PolrateH*fdTH+ri[[count]],
dC'[t]==dCnucleosidetransport-dCnucleosidekinase+dCnucleotidase,
dCMP'[t]==dCnucleosidekinase-dCmpkforward+dCmpkreverse-dCnucleotidase,
dCDP'[t]==dCmpkforward-dCmpkreverse-dCdpkforward+dCdpkreverse,
dCTP'[t]==dCdpkforward-dCdpkreverse- PolrateL*fdCL-PolrateH*fdCH+ri[[count]],
dA'[t]==dAnucleosidetransport-dAnucleosidekinase+dAnucleotidase,
dAMP'[t]==dAnucleosidekinase-dAmpkforward+dAmpkreverse-dAnucleotidase,
dADP'[t]==dAmpkforward-dAmpkreverse-dAdpkforward+dAdpkreverse,
dATP'[t]==dAdpkforward-dAdpkreverse- PolrateL*fdAL-PolrateH*fdAH+ri[[count]],
```

```
dG'[t]==dGnucleosidetransport-dGnucleosidekinase+dGnucleotidase,
dGMP'[t]==dGnucleosidekinase-dGmpkforward+dGmpkreverse-dGnucleotidase,
dGDP'[t]==dGmpkforward-dGmpkreverse-dGdpkforward+dGdpkreverse,
dGTP'[t]==dGdpkforward-dGdpkreverse-  PolrateL*fdGL-  PolrateH*fdGH+ri[[count]],
LDNA'[t]==PolrateL ,
HDNA'[t]==PolrateH ,
LPolrate[t]==rdT*rdC*rdA *rdG/((fdTL*rdC*rdA*rdG)+(fdCL*rdT*rdA*rdG)+(fdAL*rdT*rdC*rdG)+ (fdGL*rdT*rdC*rdA)+0.1),
HPolrate[t]==rdT*rdC*rdA *rdG/((fdTH*rdC*rdA*rdG)+(fdCH*rdT*rdA*rdG)+(fdAH*rdT*rdC*rdG)+(fdGH*rdT*rdC*rdA)+0.1),
dT[start]==dT0,
dTMP[start]==dTMP0,
dTDP[start]==dTDP0,
dTTP[start]==dTTP0,
dC[start]==dC0,
dCMP[start]==dCMP0,
dCDP[start]==dCDP0,
dCTP[start]==dCTP0,
dA[start]==dA0,
dAMP[start]==dAMP0,
dADP[start]==dADP0,
dATP[start]==dATP0,
dG[start]==dG0,
dGMP[start]==dGMP0,
dGDP[start]==dGDP0,
dGTP[start]==dGTP0,
LDNA[start]==LDNA0,
HDNA[start]==HDNA0,
LPolrate'[start]==0,
HPolrate'[start]==0},
{dT,dTMP,dTDP,dTTP,dC,dCMP,dCDP,dCTP,dA,dAMP,dADP,dATP,dG,dGMP,dGDP,dGTP,LDNA,HDNA,LPolrate,HPolrate},
{t,start,end},MaxSteps->10000000,PrecisionGoal->4,Method->Automatic ],{i,1,numDNAmols}]];
     (*end loop*)

(*Analysis*)

k=Flatten[Table[{PolrateL+PolrateH} /.solution[lin],{t,start,end,0.1}],2];
        reptime=(10*end-Count[k,0])*0.1;(*calculate the replication time of the last mtDNA molecule replicated*)
```

```
hd=HDNA[end]/.solution[1];
ld=LDNA[end]/.solution[1];
replengths = Append[replengths,hd[[1]]+ld[[1]]];
repdurations = Append[repdurations,reptime];
reprates = replengths/repdurations;

(*OutputForm[reprates] >>>"reprates.txt"; *)

,{13}];

,{100}];
(*Analysis*)

replengths
repdurations
reprates
Max[replengths]
Min[repdurations]
TableForm[Partition[reprates,13]]
TableForm[parameters]

(*Data & Plots*)

(*write last iteration to end of file*)
(*Variable k* holds a data Table of time (min) and dN and dNXP molecules per mitochondrion*)
kn=Flatten[Table[{t, dT[t],dC[t],dA[t],dG[t]} /.solution[lin],{t,start,end,1}],1];
(*Get rid of blank lines in between each data line*)
datan=ToString[TableForm[kn],OutputForm];
data2n=StringReplace[datan,{"\n\n"-> "\n"}];
data3n=ToExpression["data2n"];
(*output 5 columns, the time (min), dT, dC, dA, dG (molecules) to a file called dNs.txt*)
OutputForm[data3n] >>>"dNs.txt";

kmono=Flatten[Table[{t, dTMP[t],dCMP[t],dAMP[t],dGMP[t]} /.solution[lin],{t,start,end,1}],1];
(*Get rid of blank lines in between each data line*)
datamono=ToString[TableForm[kmono],OutputForm];
data2mono=StringReplace[datamono,{"\n\n"-> "\n"}];
```

```
data3mono=ToExpression["data2mono"];
(*output 5 columns, the time (min), dTMP, dCMP, dAMP, dGMP (molecules) to a file called dNMPs.txt*)
OutputForm[data3mono] >>>"dNMPs.txt";

kdi=Flatten[Table[{t, dTDP[t],dCDP[t],dADP[t],dGDP[t]} /.solution[lin],{t,start,end,1}],1];
(*Get rid of blank lines in between each data line*)
datadi=ToString[TableForm[kdi],OutputForm];
data2di=StringReplace[datadi,{"\n\n"-> "\n"}];
data3di=ToExpression["data2di"];
(*output 5 columns, the time (min), dTDP, dCDP, dADP, dGdP (molecules) to a file called dNDPs.txt*)
OutputForm[data3di] >>>"dNDPs.txt";

ktri=Flatten[Table[{t, dTTP[t],dCTP[t],dATP[t],dGTP[t]} /.solution[lin],{t,start,end,1}],1];
(*Get rid of blank lines in between each data line*)
datatri=ToString[TableForm[ktri],OutputForm];
data2tri=StringReplace[datatri,{"\n\n"-> "\n"}];
data3tri=ToExpression["data2tri"];
(*output 5 columns, the time (min), dTTP, dCTP, dATP, dGTP (molecules) to a file called dNTPs.txt*)
OutputForm[data3tri] >>>"dNTPs.txt";

kT=Flatten[Table[{t, dT[t],dTMP[t],dTDP[t],dTTP[t]} /.solution[lin],{t,start,end,1}],1];
(*Get rid of blank lines in between each data line*)
dataT=ToString[TableForm[kT],OutputForm];
data2T=StringReplace[dataT,{"\n\n"-> "\n"}];
data3T=ToExpression["data2T"];
(*output 5 columns, the time (min), dT, dTMP, dTDP, dTTP (molecules) to a file called t.txt*)
OutputForm[data3T] >>>"T.txt";

kC=Flatten[Table[{t, dC[t],dCMP[t],dCDP[t],dCTP[t]} /.solution[lin],{t,start,end,1}],1];
(*Get rid of blank lines in between each data line*)
dataC=ToString[TableForm[kC],OutputForm];
data2C=StringReplace[dataC,{"\n\n"-> "\n"}];
data3C=ToExpression["data2C"];
(*output 5 columns, the time (min), dC, dCMP, dCDP, dCTP (molecules) to a file called C.txt*)
OutputForm[data3C] >>>"C.txt";

kA=Flatten[Table[{t, dA[t],dAMP[t],dADP[t],dATP[t]} /.solution[lin],{t,start,end,1}],1];
```

```
(*Get rid of blank lines in between each data line*)
dataA=ToString[TableForm[kA],OutputForm];
data2A=StringReplace[dataA,{"\n\n"-> "\n"}];
data3A=ToExpression["data2A"];
(*output 5 columns, the time (min), dA, dAMP, dADP, dATP (molecules) to a file called A.txt*)
OutputForm[data3A] >>>"A.txt";

kG=Flatten[Table[{t, dG[t],dGMP[t],dGDP[t],dGTP[t]} /.solution[lin],{t,start,end,1}],1];
(*Get rid of blank lines in between each data line*)
dataG=ToString[TableForm[kG],OutputForm];
data2G=StringReplace[dataG,{"\n\n"-> "\n"}];
data3G=ToExpression["data2G"];
(*output 5 columns, the time (min), dG, dGMP, dGDP, dGTP (molecules) to a file called G.txt*)
OutputForm[data3G] >>>"G.txt";
(*                                                                    *)
(*Plots of simulation results*)
(*Change simulation array solution[lin] to observe other mtDNA molecules besides the last*)
(*                                                                    *)

(*In the graphs of different dNTPs, T=Red, C=Green, A=Blue, G=Black*)
(*In the graphs of different phosphorylated states, dN=Red, dNMP=Green, dNDP=Blue, dNTP=Black*)

(*Plot the levels of dNTPs for all mtDNA replications separately*)
For[i=1,i<(lin+1),i++,dNTP[i]=Plot[Evaluate[{dTTP[t]/conversion,dCTP[t]/conversion,dATP[t]/conversion,dGTP[t]/conversion} /. solution[i]],
{t,DNAmolreptime*(i-1),DNAmolreptime*i}, AxesLabel -> {"Time (min)", "concentration dNTPs (micromoles/L)"}, PlotRange-> {0,dTTPcyto},
PlotStyle->{Red,Green,Blue,Black}]

If[i==lin && i>1,Show[dNTP[i],dNTP[i-1]]]]; (*Plot dNTP levels for last two mtDNA replications together*)

(*dTXP concentration plots for the last mtDNA replication*)
Plot[Evaluate[{dT[t]/conversion,dTMP[t]/conversion,dTDP[t]/conversion,dTTP[t]/conversion} /. solution[lin]],
{t,start,end}, AxesLabel -> {"Time (min)", "Concentration T (uM)"}, PlotRange-> {0,dTTPcyto/conversion},
PlotStyle->{Red,Green,Blue,Black}]

(*dCXP concentration plots for the last mtDNA replication*)
Plot[Evaluate[{dC[t]/conversion,dCMP[t]/conversion,dCDP[t]/conversion,dCTP[t]/conversion} /. solution[lin]],
{t,start,end}, AxesLabel -> {"Time (min)", "Concentration C (uM)"}, PlotRange-> {0,dTTPcyto/conversion},
```

```
PlotStyle->{Red,Green,Blue,Black}]

(*dAXP concentration plots for the last mtDNA replication*)
Plot[Evaluate[{dA[t]/conversion,dAMP[t]/conversion,dADP[t]/conversion,dATP[t]/conversion} /. solution[lin]],
{t,start,end}, AxesLabel -> {"Time (min)", "Concentration A (uM)"}, PlotRange-> {0,dTTPcyto/conversion},
PlotStyle->{Red,Green,Blue,Black}]

(*dGXP concentration plots for the last mtDNA replication*)
Plot[Evaluate[{dG[t]/conversion,dGMP[t]/conversion,dGDP[t]/conversion,dGTP[t]/conversion} /. solution[lin]],
{t,start,end}, AxesLabel -> {"Time (min)", "Concentration G (uM)"}, PlotRange-> {0,dTTPcyto/conversion},
PlotStyle->{Red,Green,Blue,Black}]

(*Plot dNs*)
Plot[Evaluate[{dT[t],dC[t],dA[t],dG[t]} /. solution[1]],
{t,start,end}, AxesLabel -> {"Time (min)", "dNs (molecules/mitochondrion)"}, PlotRange-> {0,100},
PlotStyle->{Red,Green,Blue,Black}]

(*Plot dNMPs*)
Plot[Evaluate[{dTMP[t],dCMP[t],dAMP[t],dGMP[t]} /. solution[1]],
{t,start,end}, AxesLabel -> {"Time (min)", "dNMPs (molecules/mitochondrion)"}, PlotRange-> {0,dTTPcyto},
PlotStyle->{Red,Green,Blue,Black}]

(*Plot dNDPs*)
Plot[Evaluate[{dTDP[t],dCDP[t],dADP[t],dGDP[t]} /. solution[1]],
{t,start,end}, AxesLabel -> {"Time (min)", "dNDPs (molecules/mitochondrion)"}, PlotRange-> {0,dTTPcyto},
PlotStyle->{Red,Green,Blue,Black}]

(*Plot dNTPs*)
Plot[Evaluate[{dTTP[t],dCTP[t],dATP[t],dGTP[t]} /. solution[1]],
{t,start,end}, AxesLabel -> {"Time (min)", "dNTPs (molecules/mitochondrion)"}, PlotRange-> {0,dTTPcyto},
PlotStyle->{Red,Green,Blue,Black}]

(*Plot dNs'*)
Plot[Evaluate[{dT'[t],dC'[t],dA'[t],dG'[t]} /. solution[1]],
{t,start,end}, AxesLabel -> {"Time (min)", "dNs' (molecules per minute)"}, PlotRange-> {0,100},
PlotStyle->{Red,Green,Blue,Black}]
```

```
(*Plot dNMPs'*)
Plot[Evaluate[{dTMP'[t],dCMP'[t],dAMP'[t],dGMP'[t]} /. solution[1]],
{t,start,end}, AxesLabel -> {"Time (min)", "dNMPs' (molecules per minute)"}, PlotRange-> {0,100},
PlotStyle->{Red,Green,Blue,Black}]

(*Plot dNDPs'*)
Plot[Evaluate[{dTDP'[t],dCDP'[t],dADP'[t],dGDP'[t]} /. solution[1]],
{t,start,end}, AxesLabel -> {"Time (min)", "dNDPs' (molecules per minute)"}, PlotRange-> {0,100},
PlotStyle->{Red,Green,Blue,Black}]

(*Plot dNTPs'*)
Plot[Evaluate[{dTTP'[t],dCTP'[t],dATP'[t],dGTP'[t]} /. solution[1]],
{t,start,end}, AxesLabel -> {"Time (min)", "dNTPs' (molecules per minute)"}, PlotRange-> {0,100},
PlotStyle->{Red,Green,Blue,Black}]

Plot[Evaluate[{HDNA[t], LDNA[t], (HDNA[t]+LDNA[t])}/.solution[1]],{t,DNAmolreptime/2,end}, AxesLabel ->
{"Time(min)","DNA(nucleotides)"},PlotRange -> {0,17000}, PlotStyle -> {Red,Blue, Black}]

Plot[Evaluate[{HDNA'[t], LDNA'[t], (HDNA'[t]+LDNA'[t])}/.solution[1]],{t,DNAmolreptime/2,end}, AxesLabel -> {"Time(min)","DNA'(nucleotides per
minute)"},PlotRange -> {0,500}, PlotStyle -> {Red,Blue, Black}]

Plot[Evaluate[{dTnucleosidekinase,dCnucleosidekinase,dAnucleosidekinase,dGnucleosidekinase}/.solution[1]],{t,start,end},AxesLabel->{"Time
(min)","nucleoside kinase output (molecules per minute)"},PlotRange->{0,1000},PlotStyle->{Red,Green,Blue,Black}]

Plot[Evaluate[{dTnucleotidase,dCnucleotidase,dAnucleotidase,dGnucleotidase}/.solution[1]],{t,start,end},AxesLabel->{"Time (min)","nucleotidase output
(molecules per minute)"},PlotRange->{0,1000},PlotStyle->{Red,Green,Blue,Black}]

Plot[Evaluate[{dTmpkforward,dCmpkforward,dAmpkforward,dGmpkforward}/.solution[1]],{t,start,end},AxesLabel->{"Time (min)","monophosphate kinase
forward output (molecules per minute)"},PlotRange->{0,1000},PlotStyle->{Red,Green,Blue,Black}]

Plot[Evaluate[{dTmpkreverse,dCmpkreverse,dAmpkreverse,dGmpkreverse}/.solution[1]],{t,start,end},AxesLabel->{"Time (min)","monophosphate kinase
reverse output (molecules per minute)"},PlotRange->{0,1000},PlotStyle->{Red,Green,Blue,Black}]

Plot[Evaluate[{dTdpkforward,dCdpkforward,dAdpkforward,dGdpkforward}/.solution[1]],{t,start,end},AxesLabel->{"Time (min)","diphosphate kinase forward
output (molecules per minute)"},PlotRange->{0,1000},PlotStyle->{Red,Green,Blue,Black}]
```

```
Plot[Evaluate[{dTdpkreverse,dCdpkreverse,dAdpkreverse,dGdpkreverse}/.solution[1]],{t,start,end},AxesLabel->{"Time (min)","diphosphate kinase reverse output (molecules per minute)"},PlotRange->{0,1000},PlotStyle->{Red,Green,Blue,Black}]

Plot[Evaluate[{dTnucleosidetransport,dCnucleosidetransport,dAnucleosidetransport,dGnucleosidetransport}/.solution[1]],{t,start,end},AxesLabel->{"Time (min)","nucleoside transport reaction output (molecules per minute)"},PlotRange->{-1000,1000},PlotStyle->{Red,Green,Blue,Black}]

Plot[Evaluate[{(dTnucleosidekinase-dTnucleotidase),(dCnucleosidekinase-dCnucleotidase),(dAnucleosidekinase-dAnucleotidase),(dGnucleosidekinase-dGnucleotidase)}/.solution[1]],{t,start,end},AxesLabel->{"Time (min)","net monophosphate production (molecules per minute)"},PlotRange->{-1000,1000},PlotStyle->{Red,Green,Blue,Black}]

Plot[Evaluate[{(dTmpkforward-dTmpkreverse),(dCmpkforward-dCmpkreverse),(dAmpkforward-dAmpkreverse),(dGmpkforward-dGmpkreverse)}/.solution[1]],{t,start,end},AxesLabel->{"Time (min)","net diphosphate production (molecules per minute)"},PlotRange->{0,1000},PlotStyle->{Red,Green,Blue,Black}]

Plot[Evaluate[{(dTdpkforward-dTdpkreverse),(dCdpkforward-dCdpkreverse),(dAdpkforward-dAdpkreverse),(dGdpkforward-dGdpkreverse)}/.solution[1]],{t,start,end},AxesLabel->{"Time (min)","net triphosphate production (molecules per minute)"},PlotRange->{-1000,1000},PlotStyle->{Red,Green,Blue,Black}]

t

{dT[t],dC[t],dA[t],dG[t]}/.solution[1]

{dTMP[t],dCMP[t],dAMP[t],dGMP[t]}/.solution[1]

{dTDP[t],dCDP[t],dADP[t],dGDP[t]}/.solution[1]

{dTTP[t],dCTP[t],dATP[t],dGTP[t]}/.solution[1]

{dT'[t],dC'[t],dA'[t],dG'[t]}/.solution[1]

{dTMP'[t],dCMP'[t],dAMP'[t],dGMP'[t]}/.solution[1]

{dTDP'[t],dCDP'[t],dADP'[t],dGDP'[t]}/.solution[1]

{dTTP'[t],dCTP'[t],dATP'[t],dGTP'[t]}/.solution[1]

{HDNA[t], LDNA[t], HDNA[t] + LDNA[t]}/.solution[1]
```

{HDNA'[t], LDNA'[t], HDNA'[t] + LDNA'[t]}/.solution[1]

{dTnucleosidetransport,dCnucleosidetransport,dAnucleosidetransport,dGnucleosidetransport}/.solution[1]

{dTnucleosidekinase,dCnucleosidekinase,dAnucleosidekinase,dGnucleosidekinase}/.solution[1]

{dTnucleotidase,dCnucleotidase,dAnucleotidase,dGnucleotidase}/.solution[1]

{dTmpkforward,dCmpkforward,dAmpkforward,dGmpkforward}/.solution[1]

{dTmpkreverse,dCmpkreverse,dAmpkreverse,dGmpkreverse}/.solution[1]

{dTdpkforward,dCdpkforward,dAdpkforward,dGdpkforward}/.solution[1]

{dTdpkreverse,dCdpkreverse,dAdpkreverse,dGdpkreverse}/.solution[1]

{(dTnucleosidekinase-dTnucleotidase),(dCnucleosidekinase-dCnucleotidase),(dAnucleosidekinase-dAnucleotidase),(dGnucleosidekinase-dGnucleotidase)}/.solution[1]

{(dTmpkforward-dTmpkreverse),(dCmpkforward-dCmpkreverse),(dAmpkforward-dAmpkreverse),(dGmpkforward-dGmpkreverse)}/.solution[1]

{(dTdpkforward-dTdpkreverse),(dCdpkforward-dCdpkreverse),(dAdpkforward-dAdpkreverse),(dGdpkforward-dGdpkreverse)}/.solution[1]

S3: Simulation parameters (*Mathematica*-readable).

```
(*Mitochondrial Deoxyribonucleoside Salvage Pathway*)
(*Vishal V Gandhi and David C Samuels*)

(*DeoxynucleotideModelConstants.txt*)
(*This file is the constants file for the Mathematica*)
(*mitochondrial deoxynucleotide metabolism and mtDNA*)
(*synthesis model*)

Lstrandstart=10969;

(*the fractions of A,C,T, and G on the heavy and light strands of mtDNA*)
fdTH=0.309;
fdTL=0.247;
fdCH=0.131;
fdCL=0.313;
fdAH=0.247;
fdAL=0.309;
fdGH=0.313;
fdGL=0.131;

(*the Hill coefficient of TK2 for deoxythymidine*)
tk2hill=0.5;

(*The length of both strands of mtDNA*)
DNAlength=33136;
(*the length of one strand of mtDNA*)
strandDNA=DNAlength/2;

(*volume of a mitochondrion*)
volmito=2*^-16;

(*conversion factor used to convert kms and concentrations from microMolar to molecules/mitochondrion*)
```

```
(*conversion = 120.4;*)
conversion=1*^-6*6.022*^23*volmito;
secondsperminute=60;

(*factor used to decrease the vmax of the polymerase on double stranded templates with lower primer density*)
dsfact=1/2;

(*Polymerase kinetic constants Johnson 01 JBC*)
VmaxPoldT=25.0*dsfact*secondsperminute;
VmaxPoldC=43.0*dsfact*secondsperminute;
VmaxPoldA=45.0*dsfact*secondsperminute;
VmaxPoldG=37.0*dsfact*secondsperminute;
KmPoldT=0.63*conversion;
KmPoldC=0.9*conversion;
KmPoldA=0.8*conversion;
KmPoldG=0.8*conversion;

(*Ki of dTTP on tk2 Wang 03 DOI 10.1074/jbc.M206143200*)
kidttptk2=2.3*conversion;

(*Ki of dUTP on tk2 Geometric mean of dCTP and dTTP values*)
kidutptk2=1.38*conversion;

(*Ki of dCTP on tk2 Wang 03 DOI 10.1074/jbc.M206143200*)
kidctptk2=0.83*conversion;

(*Ki of dU on tk2 Geometric mean Munch-Petersen 91 JBC*)
kidutk2=227*conversion;

(*Ki of dC on tk2 Wang 03 DOI 10.1074/jbc.M206143200*)
kidctk2=40*conversion;

(*Ki of dT on tk2 Wang 03 DOI 10.1074/jbc.M206143200*)
kidttk2=4.9*conversion;

(*Substrate Kis on dgk set equal to substrate kms*)
```

```
(*Ki of dI on dgk set equal to km Sjoberg 98 Molecular Pharmacology*)
kididgk=12*conversion;

(*Sjoberg 01 DOI: 10.1128/AAC.45.3.739–742.2001, Ki of dITP on dgk set equal to dATP Ki*)
kidimpdgk=78*conversion;
kiditpdgk=kidatpdgk;

(*Ki of dGMP on dgk Sjoberg 01 DOI: 10.1128/AAC.45.3.739–742.2001*)
kidgmpdgk=4*conversion;

(*Ki of dAMP on dgk Sjoberg 01 DOI: 10.1128/AAC.45.3.739–742.2001*)
kidampdgk=28*conversion;

(*Ki of dATP on dgk Sjoberg 01 DOI: 10.1128/AAC.45.3.739–742.2001*)
kidatpdgk=41*conversion;

(*Ki of dGTP on dgk Sjoberg 01 DOI: 10.1128/AAC.45.3.739–742.2001*)
kidgtpdgk=0.4*conversion;

(*estimated nucleoside transporter molecular weight in kD Griffiths 97 Nature Medicine assumed monomer?*)
transporterMW=50;

(*tk2 and dgk molecular weight in kD=29 Wang 99 Febs Letters, Mandel 01 doi:10.1038/ng746*)
(*dgk is a dimer, tk2 exists both as dimer and tetramer: tetramer is more active but less abundant, transition between the 2 states is possible and ATP-mediated
(mean taken)*)
dgkMW=58;
tk2MW=87;

(*molecular weight of dnt2 in kD Rampazzo 00 PNAS Hunsucker 05 dimer = 2*23*)
dnt2MW=46;

(*Ectonucleotidase molecular weight Tetramer Brenda*)
enMW=210;

(*tmpk2 molecular weight in kD Chen 08 Genes to Cells*)
tmpk2MW=44;
```

```
(*gmpk2 molecular weight in kD Brenda*)
gmpk2MW=22;

(*cmpk2 molecular weight in kD Xu08 JBC*)
cmpk2MW=44.5;

(*ak2 molecular weight in kD Uniprot/other literature*)
akMW=26;

(*human nme4 molecular weight in kD=20 Uniprot/Milon 00, homohexamer*)
ndpkMW=120;

(*nucleoside kinase molecules in each mitochondrion from Saada 01 and 03 Nature Genetics and Mol Gen Metabolism*)
(*as much as 20-fold variation may exist between tissues*)
tk2moleculespermito=100;
dgkmoleculespermito=200;

(*dnt2 molecules in each mitochondrion*)
dnt2moleculespermito=50;

(*Ectonucleotidase molecules in each mitochondrion*)
enmoleculespermito=50;

(*tmpk2 molecules in each mitochondrion*)
tmpk2moleculespermito=50;

(*gmpk2 molecules in each mitochondrion*)
gmpk2moleculespermito=50;

(*cmpk2 molecules in each mitochondrion*)
cmpk2moleculespermito=50;

(*ndpk molecules in each mitochondrion*)
ndpkmoleculespermito=300;

(*the factor that the reverse reaction is faster than the forward reaction for NMPK*)
factorMD=0.1;(*AMP/ADP*)
```

(*the factor that the reverse reaction is faster than the forward reaction for NDPK*)
factorDT=0.1;(*ADP/ATP*)

(*ent molecules per mitochondrion Life Sciences Camins 96, Escubedo 00*)
transportermoleculespermito=38;

(*adenylate kinase molecules per mitochondrion Eur. J. Biochem. 93, 263 1979 Tomaselli*)
akmoleculespermito=450;

(*number of total proteins in a mitochondrion assuming average MW of 30 kD and 5x10^10 mito/mg mito protein*)
(*proteinspermito=400000;*)

(*transporter Vmax converting from micromoles substrate/mg enzyme/minute to molecules substrate/mitochondrion/minute refer base model constants, camins 95, jimenez 00*)
transportervmax=0.000086/0.0000021*transportermoleculespermito;

(*agreement between kcat from gerth 07 for tk2 at least and the Vmax values - so ok*)

(*Vmax of the first phosphorylation of dT in the forward direction converting from micromoles substrate/mg enzyme/minute to molecules substrate/mitochondrion/minute Wang 03 DOI 10.1074/jbc.M206143200*)
Vmax1PfdT=1.288*tk2MW*tk2moleculespermito;

(*Vmax of the first phosphorylation of dC in the forward direction converting from micromoles substrate/mg enzyme/minute to molecules substrate/mitochondrion/minute Wang 03 DOI 10.1074/jbc.M206143200*)
Vmax1PfdC=0.789*tk2MW*tk2moleculespermito;

(*Vmax of dC with dgk converting from micromoles substrate/mg enzyme/minute to molecules substrate/mitochondrion/minute Sjoberg 98 Molecular Pharmacology*)
Vmax1PfdCdgk=0.059*dgkMW*dgkmoleculespermito;

(*Vmax of the first phosphorylation of dA in the forward direction converting from micromoles substrate/mg enzyme/minute to molecules substrate/mitochondrion/minute Sjoberg 98 Molecular Pharmacology*)
Vmax1PfdA=0.429*dgkMW*dgkmoleculespermito;

(*Vmax of the first phosphorylation of dG in the forward direction converting from micromoles substrate/mg enzyme/minute to molecules substrate/mitochondrion/minute Sjoberg 98 Molecular Pharmacology*)
Vmax1PfdG=0.043*dgkMW*dgkmoleculespermito;

(*turnover numbers for cytosolic nucleotidases from Brenda seem to match Vmax below*)

(*Vmax of the first phosphorylation of dT in the reverse direction converting from micromoles substrate/mg enzyme/minute to molecules substrate/mitochondrion/minute Mazzon 03 Biochemical Pharmacology*)
Vmax1PrdT=74*dnt2MW*dnt2moleculespermito;

(*Various sources, Spychala 89 for Vmax 45 for AMP so setting lower here, also refer Hunsucker 05*)

(*Ectonucleotidase Vmax of the first phosphorylation of dT in the reverse direction converting from micromoles substrate/mg enzyme/minute to molecules substrate/mitochondrion/minute*)
Vmax1PrdTen=4.5*enMW*enmoleculespermito;

(*Vmax of the first phosphorylation of dC in the reverse direction converting from micromoles substrate/mg enzyme/minute to molecules substrate/mitochondrion/minute*)
Vmax1PrdC=4.5*enMW*enmoleculespermito;

(*Vmax of the first phosphorylation of dA in the reverse direction converting from micromoles substrate/mg enzyme/minute to molecules substrate/mitochondrion/minute*)
Vmax1PrdA=4.5*enMW*enmoleculespermito;

(*Vmax of the first phosphorylation of dG in the reverse direction converting from micromoles substrate/mg enzyme/minute to molecules substrate/mitochondrion/minute*)
Vmax1PrdG=4.5*enMW*enmoleculespermito;

(*Vmax of the second phosphorylation of dT in the forward direction converting from micromoles substrate/mg enzyme/minute to molecules substrate/mitochondrion/minute Brenda, also refer Pasti 03 Kcat value for cytoplasmic enzyme is 1 per second*)
Vmax2PfdT=0.821*tmpk2MW*tmpk2moleculespermito;

(*Vmax of the second phosphorylation of dC in the forward direction converting from micromoles substrate/mg enzyme/minute to molecules substrate/mitochondrion/minute Xu 08 JBC*)
Vmax2PfdC=1.77*cmpk2MW*cmpk2moleculespermito;

(*Vmax of the second phosphorylation of dA in the forward direction converting from micromoles substrate/mg enzyme/minute to molecules substrate/mitochondrion/minute Alexandre 07 Nucleic Acids Research*)
Vmax2PfdA=272.8*akMW*akmoleculespermito;

(*Vmax of the second phosphorylation of dG in the forward direction converting from micromoles substrate/mg enzyme/minute to molecules substrate/mitochondrion/minute from Brenda mouse and rat unreliable values* Hall 86 Eur J Biochem unreliable value*)
Vmax2PfdG=1.54*gmpk2MW*gmpk2moleculespermito;

(*Vmax of the second phosphorylation of dT in the reverse direction*)
Vmax2PrdT=Vmax2PfdT*factorMD;

(*Vmax of the second phosphorylation of dC in the reverse direction*)
Vmax2PrdC=Vmax2PfdC*factorMD;

(*Vmax of the second phosphorylation of dA in the reverse direction*)
Vmax2PrdA=Vmax2PfdA*factorMD;

(*Vmax of the second phosphorylation of dG in the reverse direction*)
Vmax2PrdG=Vmax2PfdG*factorMD;

(*Milon 00 human and Lambeth 97 pigeon both have data but Lambeth 97 has more, and there is overlap between dTDP values - so using Lambeth 97 for all nme4 data*)

(*Vmax of the third phosphorylation of dT in the forward direction converting from micromoles substrate/mg enzyme/minute to molecules substrate/mitochondrion/minute Lambeth 97 JBC*)
Vmax3PfdT=140*ndpkMW*ndpkmoleculespermito;

(*Vmax of the third phosphorylation of dC in the forward direction converting from micromoles substrate/mg enzyme/minute to molecules substrate/mitochondrion/minute Lambeth 97 JBC*)
Vmax3PfdC=50*ndpkMW*ndpkmoleculespermito;(*author statement: dNDPs are slower than rNDPs, so taking dCDP Vmax=CDP*)

(*Vmax of the third phosphorylation of dA in the forward direction converting from micromoles substrate/mg enzyme/minute to molecules substrate/mitochondrion/minute Milon 00 JBC*)
Vmax3PfdA=225*ndpkMW*ndpkmoleculespermito;(*set equal to dGDP Vmax*)

(*Vmax of the third phosphorylation of dG in the forward direction converting from micromoles substrate/mg enzyme/minute to molecules substrate/mitochondrion/minute Lambeth 97 JBC*)
Vmax3PfdG=225*ndpkMW*ndpkmoleculespermito;

(*Vmax of the third phosphorylation of dT in the reverse direction*)
Vmax3PrdT=Vmax3PfdT*factorDT;

```
(*Vmax of the third phosphorylation of dC in the reverse direction*)
Vmax3PrdC=Vmax3PfdC*factorDT;

(*Vmax of the third phosphorylation of dA in the reverse direction*)
Vmax3PrdA=Vmax3PfdA*factorDT;

(*Vmax of the third phosphorylation of dG in the reverse direction*)
Vmax3PrdG=Vmax3PfdG*factorDT;

(*transporter Km Escubedo 00*)
transporterkm=2*conversion;

(*Km of the first phosphorylation of dT in the forward direction Wang 03 DOI 10.1074/jbc.M206143200*)
km1PfdT=13*conversion;

(*Km of the first phosphorylation of dC in the forward direction Wang 03 DOI 10.1074/jbc.M206143200*)
km1PfdC=11*conversion;

(*Km of dC with dgk Sjoberg 98 Molecular Pharmacology*)
km1PfdCdgk=336*conversion;

(*Km of the first phosphorylation of dA in the forward direction Sjoberg 98 Molecular Pharmacology*)
km1PfdA=467*conversion;

(*Km of the first phosphorylation of dG in the forward direction Sjoberg 98 Molecular Pharmacology*)
km1PfdG=4*conversion;

(*Km of the first phosphorylation of dT, dU in the reverse direction Rampazzo 00 PNAS*)
km1PrdT=200*conversion;
km1PrdU=100*conversion;
km1PrrU=1.5*km1PrdT;

(*Ectonucleotidase data from Hunsucker 05 or Brenda*)
(*Geometric means for substrate Kms, higher Kms plugged for inhibitions to be conservative*)

(*Ectonucleotidase Km of the first phosphorylation of dT, dU, rU in the reverse direction*)
km1PrdTen=22.5*conversion;
```

```
km1PrdUen=110*conversion;(*set equal to UMP Km*)
km1PrrUen=110*conversion;(*set equal to Km*)

(*Ectonucleotidase Km of the first phosphorylation of dC, rC in the reverse direction*)
km1PrdC=290*conversion;
km1PrrC=360*conversion;

(*Ectonucleotidase Km of the first phosphorylation of da, rA in the reverse direction*)
km1PrdA=62*conversion;
km1PrrA=19*conversion;(*set equal to Km*)

kiadpen=17*conversion;
kiatpen=15*conversion;

(*Ectonucleotidase Km of the first phosphorylation of dG, rG in the reverse direction*)
km1PrdG=48*conversion;
km1PrrG=59*conversion;(*set equal to Km*)

(*Ectonucleotidase Km of the first phosphorylation of dI, rI in the reverse direction*)
km1PrdI=100*conversion;(*set equal to Km of IMP*)
km1PrrI=100*conversion;(*set equal to Km*)

(*Km of the second phosphorylation of dT in the forward direction Alexandre 07,misc*)
km2PfdT=20*conversion;
km2PfdUtmpk2=2600*conversion;(*Km is 170, but Ki is 2600*)

(*miscellaneous inhibitions Brenda*)
(*deoxythymidine inhibition excluded because even at 770 uM only 27% inhibition observed*)
kidttptmpk2=700*conversion;
kidttmpk2=180*conversion;

(*Km of the second phosphorylation of dC in the forward direction Xu 08*)
km2PfdC=1310*conversion;
km2PfrC=3090*conversion;
km2PfrU=6300*conversion;
km2PfdUcmpk2=100*conversion;
```

```
(*Refer VanRompay 99 Molecular Pharmacology cmpk1 can phosphorylate AMP and dAMP*)
km2PfrAcmpk2=km2PrrAcmpk2=km2PfdAcmpk2=km2PrdAcmpk2=100*500*conversion; (*km of CMP is 500 uM*)

(*Km of the second phosphorylation of dA in the forward direction Alexandre 07 Nucleic Acids Research*)
km2PfdA=210*conversion;
km2PfrA=80*conversion;(*Km is 80, Ki is 500 - but this gives the incorrect impression that dAMP is a better substrate*)

(*Refer Alexandre 07 Nucleic Acids Research 07 - CMP and UMP have some reactivity with ak2 - included as inhibitions*)
km2PfrCak2=6000*conversion;
km2PfrUak2=9000*conversion;

(*Km of the second phosphorylation of dG in the forward direction, Brenda*)
km2PfdG=112*conversion;
km2PfrG=18*conversion;

(*Km of the second phosphorylation of dT in the reverse direction*)
km2PrdT=km2PfdT;
km2PrdUtmpk2=km2PfdUtmpk2;

(*Km of the second phosphorylation of dC in the reverse direction*)
km2PrdC=km2PfdC;
km2PrrC=km2PfrC;
km2PrrU=km2PfrU;
km2PrdUcmpk2=km2PfdUcmpk2;

(*Km of the second phosphorylation of dA in the reverse direction*)
km2PrdA=km2PfdA;
km2PrrA=km2PfrA;

km2PrrCak2=km2PfrCak2;
km2PrrUak2=km2PfrUak2;

(*Km of the second phosphorylation of dG in the reverse direction*)
km2PrdG=km2PfdG;
km2PrrG=km2PfrG;

(*Reaction is linear for dTDP and UDP until at least 1000 uM Lambeth 97 JBC*)
```

```
(*Km of the third phosphorylation of dT in the forward direction Lambeth 97 JBC*)
km3PfdT=1000*conversion;
km3PfdU=km3PfdT;
km3PfrU=km3PfdT;

(*Km of the third phosphorylation of dC in the forward direction Lambeth 97 JBC*)
km3PfdC=1000*conversion;(*dNDPs are weaker substrates than rNDPs: author statement but data n/a so same value used*)
km3PfrC=1000*conversion;(*Reaction linear until at least 1000 uM*)

(*Km of the third phosphorylation of dA in the forward direction Lambeth 97 JBC*)
km3PfdA=70*conversion;(*Km of ADP is about 70 uM OR Km of dADP set equal to that of dGDP*)
km3PfrA=300*conversion;(*substrate inhibition, Ki*)

(*Km of the third phosphorylation of dG in the forward direction Lambeth 97 JBC*)
km3PfdG=75*conversion;
km3PfrG=100*conversion;(*substrate inhibition,Ki*)

(*inosine inhibitions*)
km3PfrI=km3PrrI=km3PfdI=km3PrdI=1000*conversion;

(*Km of the third phosphorylation of dT in the reverse direction*)
km3PrdT=km3PfdT;
km3PrdU=km3PrdT;
km3PrrU=km3PrdT;

(*Km of the third phosphorylation of dC in the reverse direction*)
km3PrdC=km3PfdC;
km3PrrC=km3PrdC;

(*Km of the third phosphorylation of dA in the reverse direction*)
km3PrdA=km3PfdA;
km3PrrA=km3PrdA;

(*Km of the third phosphorylation of dG in the reverse direction*)
km3PrdG=km3PfdG;
km3PrrG=km3PrdG;
```

```
(*initial concentrations*)

dTcyto=RandomReal[{0.05*conversion, 5*conversion}];
dCcyto=RandomReal[{0.05*conversion, 5*conversion}];
dAcyto=RandomReal[{0.05*conversion, 5*conversion}];
dGcyto=RandomReal[{0.05*conversion, 5*conversion}];

dT0=dTcyto;
dC0=dCcyto;
dA0=dAcyto;
dG0=dGcyto;

(*initial dNTP levels*)

(*for transport model, have set these to be chosen randomly*)

If[celltype==1,dTTPcyto=RandomReal[{0.1*conversion, 10*conversion}]];
If[celltype==1,dCTPcyto=RandomReal[{0.1*conversion, 10*conversion}]];
If[celltype==1,dATPcyto=RandomReal[{0.1*conversion, 10*conversion}]];
If[celltype==1,dGTPcyto=RandomReal[{0.1*conversion, 10*conversion}]];

dTMP0=RandomReal[{0.1*conversion, 10*conversion}];
dTDP0=RandomReal[{0.1*conversion, 10*conversion}];
dTTP0=dTTPcyto;

dCMP0=RandomReal[{0.1*conversion, 10*conversion}];
dCDP0=RandomReal[{0.1*conversion, 10*conversion}];
dCTP0=dCTPcyto;

dAMP0=RandomReal[{0.1*conversion, 10*conversion}];
dADP0=RandomReal[{0.1*conversion, 10*conversion}];
dATP0=dATPcyto;

dGMP0=RandomReal[{0.1*conversion, 10*conversion}];
dGDP0=RandomReal[{0.1*conversion, 10*conversion}];
dGTP0=dGTPcyto;
```

```
dU=dUcyto=dTcyto;
rU=rUcyto=dTcyto;
dI=dIcyto=0.1*dAcyto;
rI=rIcyto=0.1*dAcyto;
rC=rCcyto=dCcyto;
rA=rAcyto=dAcyto;
rG=rGcyto=dGcyto;

dUMP=0.1*dTMP0;
rUMP=10*dTMP0;
dIMP=0.1*dAMP0;
rIMP=0.1*dAMP0;
rCMP=10*dCMP0;
rAMP=10*dAMP0;
rGMP=10*dGMP0;

dUDP=0.1*dTDP0;
rUDP=10*dTDP0;
dIDP=0.1*dADP0;
rIDP=0.1*dADP0;
rCDP=10*dCDP0;
rADP=10*dADP0;
rGDP=10*dGDP0;

dUTP=0.1*dTTP0;
rUTP=10*dTTP0;
dITP=0.1*dATP0;
rITP=0.1*dATP0;
rCTP=10*dCTP0;
rATP=10*dATP0;
rGTP=10*dGTP0;

DNA0=0;
LDNA0=0;
HDNA0=0;

(*end file*)
```

REFERENCES

1. Pfanner, N. and A. Chacinska, *The mitochondrial import machinery: preprotein-conducting channels with binding sites for presequences.* Biochimica Et Biophysica Acta-Molecular Cell Research, 2002. **1592**(1): p. 15-24.
2. Lill, R., et al., *Why are mitochondria essential for life?* Iubmb Life, 2005. **57**(10): p. 701-703.
3. Wallace, D.C., *Mitochondrial diseases in man and mouse.* Science, 1999. **283**(5407): p. 1482-1488.
4. Reichard, P., *Interactions between deoxyribonucleotide and DNA-synthesis.* Annual Review of Biochemistry, 1988. **57**: p. 349-374.
5. Young, P., et al., *Ribonucleotide Reductase: Evidence for Specific Association with HeLa-Cell Mitochondria.* Biochemical and Biophysical Research Communications, 1994. **203**(1): p. 46-52.
6. Munch-Petersen, B., et al., *Diverging substrate specificity of pure human thymidine kinases 1 and 2 against antiviral dideoxynucleosides.* J. Biol. Chem., 1991. **266**(14): p. 9032-9038.
7. Gandhi, V.V. and D.C. Samuels, *Enzyme Kinetics of the Mitochondrial Deoxyribonucleoside Salvage Pathway Are Not Sufficient to Support Rapid mtDNA Replication.* PLoS Comput Biol, 2011. **7**(8): p. e1002078.
8. Xu, Y.J., M. Johansson, and A. Karlsson, *Human UMP-CMP kinase 2, a novel nucleoside monophosphate kinase localized in mitochondria.* Journal of Biological Chemistry, 2008. **283**(3): p. 1563-1571.
9. Chen, Y.-L., D.-W. Lin, and Z.-F. Chang, *Identification of a putative human mitochondrial thymidine monophosphate kinase associated with monocytic/macrophage terminal differentiation.* Genes to Cells, 2008. **13**(7): p. 679-689.
10. Nobumoto, M., et al., *Mechanism of mitochondrial import of adenylate kinase isozymes.* Journal of Biochemistry, 1998. **123**(1): p. 128-135.
11. Tokarska-Schlattner, M., et al., *The nucleoside diphosphate kinase D (NM23-H4) binds the inner mitochondrial membrane with high affinity to cardiolipin and couples nucleotide transfer with respiration.* Journal of Biological Chemistry, 2008. **283**(38): p. 26198-26207.
12. Wang, L. and S. Eriksson, *Tissue Specific Distribution of Pyrimidine Deoxynucleoside Salvage Enzymes Shed Light on the Mechanism of Mitochondrial DNA Depletion.* Nucleosides, Nucleotides and Nucleic Acids, 2010. **29**(4): p. 400 - 403.
13. Berk, A.J. and D.A. Clayton, *A Genetically Distinct Thymidine Kinase in Mammalian Mitochondria. Exclusive Labeling of Mitochondrial Deoxyribonucleic Acid.* J. Biol. Chem., 1973. **248**(8): p. 2722-2729.
14. Bridges, E.G., Z.L. Jiang, and Y.C. Cheng, *Characterization of a dCTP transport activity reconstituted from human mitochondria.* Journal of Biological Chemistry, 1999. **274**(8): p. 4620-4625.
15. Ferraro, P., et al., *Mitochondrial deoxynucleotide pool sizes in mouse liver and evidence for a transport mechanism for thymidine monophosphate.* Proceedings of the National Academy of Sciences of the United States of America, 2006. **103**(49): p. 18586-18591.

16. Floyd, S., et al., *The Insulin-like Growth Factor-I mTOR Signaling Pathway Induces the Mitochondrial Pyrimidine Nucleotide Carrier to Promote Cell Growth.* Mol. Biol. Cell, 2007. **18**(9): p. 3545-3555.
17. Leanza, L., et al., *Metabolic interrelations within guanine deoxynucleotide pools for mitochondrial and nuclear DNA maintenance.* Journal of Biological Chemistry, 2008. **283**(24): p. 16437-16445.
18. Rampazzo, C., et al., *Mitochondrial thymidine kinase and the enzymatic network regulating thymidine triphosphate pools in cultured human cells.* Journal of Biological Chemistry, 2007. **282**(48): p. 34758-34769.
19. Gandhi, V.V. and D.C. Samuels, *A Review Comparing Deoxyribonucleoside Triphosphate (dNTP) Concentrations in the Mitochondrial and Cytoplasmic Compartments of Normal and Transformed Cells.* Nucleosides, Nucleotides and Nucleic Acids, 2011. **30**(5): p. 317-339.
20. Wang, L., *Deoxynucleoside Salvage Enzymes and Tissue Specific Mitochondrial DNA Depletion.* Nucleosides Nucleotides & Nucleic Acids, 2010. **29**(4-6): p. 370-381.
21. Copeland, W.C., *Inherited Mitochondrial Diseases of DNA Replication*.* Annual Review of Medicine, 2008. **59**(1): p. 131-146.
22. Hudson, G. and P.F. Chinnery, *Mitochondrial DNA polymerase-Î³ and human disease.* Human Molecular Genetics, 2006. **15**(suppl 2): p. R244-R252.
23. Suomalainen, A. and P. Isohanni, *Mitochondrial DNA depletion syndromes - Many genes, common mechanisms.* Neuromuscular Disorders, 2010. **20**(7): p. 429-437.
24. Sarzi, E., et al., *Mitochondrial DNA Depletion is a Prevalent Cause of Multiple Respiratory Chain Deficiency in Childhood.* The Journal of Pediatrics, 2007. **150**(5): p. 531-534.e6.
25. Bourdon, A., et al., *Mutation of RRM2B, encoding p53-controlled ribonucleotide reductase (p53R2), causes severe mitochondrial DNA depletion.* Nature Genetics, 2007. **39**(6): p. 776-780.
26. Nishino, I., A. Spinazzola, and M. Hirano, *Thymidine phosphorylase gene mutations in MNGIE, a human mitochondrial disorder.* Science, 1999. **283**(5402): p. 689-692.
27. Saada, A., *Mitochondrial deoxyribonucleotide pools in deoxyguanosine kinase deficiency.* Molecular Genetics and Metabolism, 2008. **95**(3): p. 169-173.
28. Saada, A., et al., *Mitochondrial deoxyribonucleoside triphosphate pools in thymidine kinase 2 deficiency.* Biochemical and Biophysical Research Communications, 2003. **310**(3): p. 963-966.
29. Bulst, S., et al., *In vitro supplementation with dAMP/dGMP leads to partial restoration of mtDNA levels in mitochondrial depletion syndromes.* Human Molecular Genetics, 2009. **18**(9): p. 1590-1599.
30. Taanman, J.W., J.R. Muddle, and A.C. Muntau, *Mitochondrial DNA depletion can be prevented by dGMP and dAMP supplementation in a resting culture of deoxyguanosine kinase-deficient fibroblasts.* Human Molecular Genetics, 2003. **12**(15): p. 1839-1845.
31. Akman, H.O., et al., *Thymidine kinase 2 (H126N) knockin mice show the essential role of balanced deoxynucleotide pools for mitochondrial DNA maintenance.* Human Molecular Genetics, 2008. **17**(16): p. 2433-2440.
32. Pontarin, G., et al., *Mitochondrial DNA depletion and thymidine phosphate pool dynamics in a cellular model of mitochondrial neurogastrointestinal encephalomyopathy.* Journal of Biological Chemistry, 2006. **281**(32): p. 22720-22728.
33. Song, S.W., L.J. Wheeler, and C.K. Mathews, *Deoxyribonucleotide pool imbalance stimulates deletions in HeLa cell mitochondrial DNA.* Journal of Biological Chemistry, 2003. **278**(45): p. 43893-43896.

34. Mathews, C.K., *DNA precursor metabolism and genomic stability.* FASEB J, 2006. **20**(9): p. 1300-14.
35. Dalakas, M.C., et al., *Mitochondrial Myopathy Caused by Long-Term Zidovudine Therapy.* New England Journal of Medicine, 1990. **322**(16): p. 1098-1105.
36. Nolan, D. and S. Mallal, *Complications associated with NRTI therapy: update on clinical features, and possible pathogenic mechanisms.* Antiviral Therapy, 2004. **9**(6): p. 849-863.
37. Lee, H., J. Hanes, and K.A. Johnson, *Toxicity of nucleoside analogues used to treat AIDS and the selectivity of the mitochondrial DNA polymerase.* Biochemistry, 2003. **42**(50): p. 14711-14719.
38. Lynx, M.D. and E.E. McKee, *3 '-azido-3 '-deoxythymidine (AZT) is a competitive inhibitor of thymidine phosphorylation in isolated rat heart and liver mitochondria.* Biochemical Pharmacology, 2006. **72**(2): p. 239-243.
39. Samuels, D.C., *Mitochondrial AZT metabolism.* Iubmb Life, 2006. **58**(7): p. 403-408.
40. Wendelsdorf, K.V., et al., *An Analysis of Enzyme Kinetics Data for Mitochondrial DNA Strand Termination by Nucleoside Reverse Transcription Inhibitors.* Plos Computational Biology, 2009. **5**(1).
41. Khaidakov, M., et al., *Accumulation of point mutations in mitochondrial DNA of aging mice.* Mutation Research-Fundamental and Molecular Mechanisms of Mutagenesis, 2003. **526**(1-2): p. 1-7.
42. Linnane, A.W., et al., *Mitochondrial-DNA Mutations as an Important Contributor to Aging and Degenerative Diseases.* Lancet, 1989. **1**(8639): p. 642-645.
43. Michikawa, Y., et al., *Aging-dependent large accumulation of point mutations in the human mtDNA control region for replication.* Science, 1999. **286**(5440): p. 774-779.
44. Penta, J.S., et al., *Mitochondrial DNA in human malignancy.* Mutation Research-Reviews in Mutation Research, 2001. **488**(2): p. 119-133.
45. Trifunovic, A., et al., *Premature ageing in mice expressing defective mitochondrial DNA polymerase.* Nature, 2004. **429**(6990): p. 417-423.
46. Wang, Y., et al., *Muscle-specific mutations accumulate with aging in critical human mtDNA control sites for replication.* Proceedings of the National Academy of Sciences of the United States of America, 2001. **98**(7): p. 4022-4027.
47. Kunz, B.A., et al., *Deoxyribonucleoside Triphosphate Levels - a Critical Factor in the Maintenance of Genetic Stability.* Mutation Research-Reviews in Genetic Toxicology, 1994. **318**(1): p. 1-64.
48. Arner, E.S.J. and S. Eriksson, *Mammalian Deoxyribonucleoside Kinases.* Pharmacology & Therapeutics, 1995. **67**(2): p. 155-186.
49. Spyrou, G. and P. Reichard, *Dynamics of the Thymidine Triphosphate Pool During the Cell-Cycle of Synchronized 3t3 Mouse Fibroblasts.* Mutation Research, 1988. **200**(1-2): p. 37-43.
50. Shao, J., et al., *Ribonucleotide reductase inhibitors and future drug design.* Curr Cancer Drug Targets, 2006. **6**(5): p. 409-31.
51. Bester, Assaf C., et al., *Nucleotide Deficiency Promotes Genomic Instability in Early Stages of Cancer Development.* Cell, 2011. **145**(3): p. 435-446.
52. Favre, C., et al., *Mitochondrial pyrimidine nucleotide carrier (PNC1) regulates mitochondrial biogenesis and the invasive phenotype of cancer cells.* Oncogene, 2010. **29**(27): p. 3964-3976.
53. Bogenhagen, D. and D.A. Clayton, *Mouse L-Cell Mitochondrial-DNA Molecules Are Selected Randomly for Replication Throughout Cell-Cycle.* Cell, 1977. **11**(4): p. 719-727.

54. Gross, N.J., G.S. Getz, and M. Rabinowitz, *Apparent Turnover of Mitochondrial Deoxyribonucleic Acid and Mitochondrial Phospholipids in the Tissues of the Rat.* Journal of Biological Chemistry, 1969. **244**(6): p. 1552-1562.
55. Bestwick, R.K., G.L. Moffett, and C.K. Mathews, *Selective Expansion of Mitochondrial Nucleoside Triphosphate Pools in Antimetabolite-Treated Hela-Cells.* Journal of Biological Chemistry, 1982. **257**(16): p. 9300-9304.
56. Desler, C., B. Munch-Petersen, and L.J. Rasmussen, *The role of mitochondrial dNTP levels in cells with reduced TK2 activity.* Nucleosides Nucleotides & Nucleic Acids, 2006. **25**(9-11): p. 1171-1175.
57. Ferraro, P., et al., *Mitochondrial deoxynucleotide pools in quiescent fibroblasts - A possible model for mitochondrial neurogastrointestinal encephalomyopathy (MNGIE).* Journal of Biological Chemistry, 2005. **280**(26): p. 24472-24480.
58. Frangini, M., et al., *Unchanged thymidine triphosphate pools and thymidine metabolism in two lines of thymidine kinase 2-mutated fibroblasts.* Febs Journal, 2009. **276**(4): p. 1104-1113.
59. Rampazzo, C., et al., *Mitochondrial deoxyribonucleotides, pool sizes, synthesis, and regulation.* Journal of Biological Chemistry, 2004. **279**(17): p. 17019-17026.
60. Posakony, J.W., J.M. England, and G. Attardi, *Mitochondrial Growth and Division During Cell-Cycle in Hela-Cells.* Journal of Cell Biology, 1977. **74**(2): p. 468-491.
61. Vinnakota, K.C. and J.B. Bassingthwaighte, *Myocardial density and composition: a basis for calculating intracellular metabolite concentrations.* American Journal of Physiology-Heart and Circulatory Physiology, 2004. **286**(5): p. H1742-H1749.
62. Ross, D.W. and H.C. Mel, *Growth dynamics of mitochondria in synchronized Chinese hamster cells.* Biophysical Journal, 1972. **12**(11): p. 1562-72.
63. Tupper, J.T. and F. Zorgniotti, *Calcium Content and Distribution as a Function of Growth and Transformation in Mouse 3t3-Cell.* Journal of Cell Biology, 1977. **75**(1): p. 12-22.
64. Imaizumi, T., et al., *Effect of human basic fibroblast growth factor on fibroblast proliferation, cell volume, collagen lattice contraction: In comparison with acidic type.* Journal of Dermatological Science, 1996. **11**(2): p. 134-141.
65. Lindhurst, M.J., et al., *Knockout of Slc25a19 causes mitochondrial thiamine pyrophosphate depletion, embryonic lethality, CNS malformations, and anemia.* Proceedings of the National Academy of Sciences, 2006. **103**(43): p. 15927-15932.
66. Pursell, Z.F., et al., *Trace amounts of 8-oxo-dGTP in mitochondrial dNTP pools reduce DNA polymerase gamma replication fidelity.* Nucleic Acids Research, 2008. **36**(7): p. 2174-2181.
67. Song, S., et al., *DNA precursor asymmetries in mammalian tissue mitochondria and possible contribution to mutagenesis through reduced replication fidelity.* Proceedings of the National Academy of Sciences of the United States of America, 2005. **102**(14): p. 4990-4995.
68. Ferraro, P., et al., *Quantitation of cellular deoxynucleoside triphosphates.* Nucleic Acids Research, 2010. **38**(6): p. 7.
69. Warburg, O., *On the origin of cancer cells.* Science, 1956. **123**(3191): p. 309-14.
70. Heiden, M.G.V., L.C. Cantley, and C.B. Thompson, *Understanding the Warburg Effect: The Metabolic Requirements of Cell Proliferation.* Science, 2009. **324**(5930): p. 1029-1033.
71. Matthews, L., et al., *Reactome knowledgebase of human biological pathways and processes.* Nucleic Acids Res, 2009. **37**(Database issue): p. D619-22.

72. Murray, D., et al., *In silico gene expression analysis - an overview.* Molecular Cancer, 2007. **6**: p. 10.
73. Kai, Y., et al., *Rapid and random turnover of mitochondrial DNA in rat hepatocytes of primary culture.* Mitochondrion, 2006. **6**(6): p. 299-304.
74. Saada, A., *Deoxyribonucleotides and disorders of mitochondrial DNA integrity.* DNA and Cell Biology, 2004. **23**(12): p. 797-806.
75. Franco, M., M. Johansson, and A. Karlsson, *Depletion of mitochondrial DNA by down-regulation of deoxyguanosine kinase expression in non-proliferating HeLa cells.* Experimental Cell Research, 2007. **313**(12): p. 2687-2694.
76. Mandel, H., et al., *The deoxyguanosine kinase gene is mutated in individuals with depleted hepatocerebral mitochondrial DNA.* Nature Genetics, 2001. **29**(3): p. 337-341.
77. Singh, K.K., et al., *Inter-genomic cross talk between mitochondria and the nucleus plays an important role in tumorigenesis.* Gene, 2005. **354**: p. 140-146.
78. Singh, K.K., et al., *Mutations in mitochondrial DNA polymerase-[gamma] promote breast tumorigenesis.* J Hum Genet, 2009. **54**(9): p. 516-524.
79. Vander Heiden, M.G., L.C. Cantley, and C.B. Thompson, *Understanding the Warburg effect: the metabolic requirements of cell proliferation.* Science, 2009. **324**(5930): p. 1029-33.
80. Clayton, D.A., *Replication of Animal Mitochondrial-DNA.* Cell, 1982. **28**(4): p. 693-705.
81. Alexandre, J.A.C., et al., *Enantioselectivity of human AMP, dTMP and UMP-CMP kinases.* Nucleic Acids Research, 2007. **35**(14): p. 4895-4904.
82. Dolce, V., et al., *The human mitochondrial deoxynucleotide carrier and its role in the toxicity of nucleoside antivirals.* Proceedings of the National Academy of Sciences of the United States of America, 2001. **98**(5): p. 2284-2288.
83. Johnson, A.A. and K.A. Johnson, *Fidelity of nucleotide incorporation by human mitochondrial DNA polymerase.* Journal of Biological Chemistry, 2001. **276**(41): p. 38090-38096.
84. Lam, W., et al., *Expression of deoxynucleotide carrier is not associated with the mitochondrial DNA depletion caused by anti-HIV dideoxynucleoside analogs and mitochondrial dNTP uptake.* Molecular Pharmacology, 2005. **67**(2): p. 408-416.
85. Mazzon, C., et al., *Cytosolic and mitochondrial deoxyribonucleotidases: activity with substrate analogs, inhibitors and implications for therapy.* Biochemical Pharmacology, 2003. **66**(3): p. 471-479.
86. Milon, L., et al., *The Human nm23-H4 Gene Product Is a Mitochondrial Nucleoside Diphosphate Kinase.* J. Biol. Chem., 2000. **275**(19): p. 14264-14272.
87. Murakami, E., et al., *Characterization of novel reverse transcriptase and other RNA-associated catalytic activities by human DNA polymerase gamma - Importance in mitochondrial DNA replication.* Journal of Biological Chemistry, 2003. **278**(38): p. 36403-36409.
88. Rampazzo, C., et al., *A deoxyribonucleotidase in mitochondria: Involvement in regulation of dNTP pools and possible link to genetic disease.* Proceedings of the National Academy of Sciences of the United States of America, 2000. **97**(15): p. 8239-8244.
89. Sjoberg, A.H., L. Wang, and S. Eriksson, *Substrate Specificity of Human Recombinant Mitochondrial Deoxyguanosine Kinase with Cytostatic and Antiviral Purine and Pyrimidine Analogs.* Mol Pharmacol, 1998. **53**(2): p. 270-273.
90. Wang, L.Y., A. Saada, and S. Eriksson, *Kinetic properties of mutant human thymidine kinase 2 suggest a mechanism for mitochondrial DNA depletion myopathy.* Journal of Biological Chemistry, 2003. **278**(9): p. 6963-6968.

91. Chang, A., et al., *BRENDA, AMENDA and FRENDA the enzyme information system: new content and tools in 2009.* Nucleic Acids Research, 2009. **37**: p. D588-D592.
92. Hunsucker, S.A., B.S. Mitchell, and J. Spychala, *The 5 '-nucleotidases as regulators of nucleotide and drug metabolism.* Pharmacology & Therapeutics, 2005. **107**(1): p. 1-30.
93. Bradshaw, P.C. and D.C. Samuels, *A computational model of mitochondrial deoxynucleotide metabolism and DNA replication.* American Journal of Physiology-Cell Physiology, 2005. **288**(5): p. C989-C1002.
94. Traut, T.W., *Physiological concentrations of purines and pyrimidines.* Mol Cell Biochem, 1994. **140**(1): p. 1-22.
95. Honeywell, R., et al., *Analysis of deoxycytidine accumulation in gemcitabine treated patients.* Nucleosides Nucleotides Nucleic Acids, 2006. **25**(9-11): p. 1225-32.
96. Li, K.M., et al., *Altered deoxyuridine and thymidine in plasma following capecitabine treatment in colorectal cancer patients.* British Journal of Clinical Pharmacology, 2007. **63**(1): p. 67-74.
97. Sjoberg, A.H., L.Y. Wang, and S. Eriksson, *Antiviral guanosine analogs as substrates for deoxyguanosine kinase: Implications for chemotherapy.* Antimicrobial Agents and Chemotherapy, 2001. **45**(3): p. 739-742.
98. Jimenez, A., et al., *Further characterization of an adenosine transport system in the mitochondrial fraction of rat testis.* European Journal of Pharmacology, 2000. **398**(1): p. 31-39.
99. Lambeth, D.O., et al., *Characterization and Cloning of a Nucleoside-diphosphate Kinase Targeted to Matrix of Mitochondria in Pigeon.* J. Biol. Chem., 1997. **272**(39): p. 24604-24611.
100. Van Rompay, A.R., M. Johansson, and A. Karlsson, *Phosphorylation of deoxycytidine analog monophosphates by UMP-CMP kinase: Molecular characterization of the human enzyme.* Molecular Pharmacology, 1999. **56**(3): p. 562-569.
101. Wang, L., et al., *Human thymidine kinase 2: molecular cloning and characterisation of the enzyme activity with antiviral and cytostatic nucleoside substrates.* FEBS Letters, 1999. **443**(2): p. 170-174.
102. Watkins, L.F. and R.A. Lewis, *The metabolism of deoxyguanosine in mitochondria - characterization of the uptake process.* Molecular and Cellular Biochemistry, 1987. **77**(1): p. 71-77.
103. Andrews, R.M., et al., *Reanalysis and revision of the Cambridge reference sequence for human mitochondrial DNA.* Nat Genet, 1999. **23**(2): p. 147-147.
104. Samson, R. and J.M. Deutch, *Diffusion-controlled reaction rate to a buried active site.* The Journal of Chemical Physics, 1978. **68**(1): p. 285-290.
105. Kang, J. and D.C. Samuels, *The evidence that the DNC (SLC25A19) is not the mitochondrial deoxyribonucleotide carrier.* Mitochondrion, 2008. **8**(2): p. 103-108.
106. Yasukawa, T., et al., *Replication of vertebrate mitochondrial DNA entails transient ribonucleotide incorporation throughout the lagging strand.* Embo Journal, 2006. **25**(22): p. 5358-5371.
107. Van Rompay, A.R., M. Johansson, and A. Karlsson, *Phosphorylation of nucleosides and nucleoside analogs by mammalian nucleoside monophosphate kinases.* Pharmacology & Therapeutics, 2000. **87**(2-3): p. 189-198.
108. Gallois-Montbrun, S., M. Veron, and D. Deville-Bonne, *Antiviral nucleoside analogs phosphorylation by nucleoside diphosphate kinase.* Mini-Reviews in Medicinal Chemistry, 2004. **4**(4): p. 361-369.

109. Hu, C.M. and Z.F. Chang, *Mitotic control of dTTP pool: a necessity or coincidence?* Journal of Biomedical Science, 2007. **14**(4): p. 491-497.
110. Ylikallio, E., et al., *Ribonucleotide reductase is not limiting for mitochondrial DNA copy number in mice.* Nucleic Acids Research, 2010. **38**: p. 8208-8218.
111. Saada-Reisch, A., *Deoxyribonucleoside kinases in mitochondrial DNA depletion.* Nucleosides Nucleotides & Nucleic Acids, 2004. **23**(8-9): p. 1205-1215.
112. Morris, G.W., et al., *Origin of pyrimidine deoxyribonucleotide pools in perfused rat heart: implications for 3 '-azido-3 '-deoxythymidine-dependent cardiotoxicity.* Biochemical Journal, 2009. **422**: p. 513-520.
113. Dorado, B., et al., *Onset and organ specificity of Tk2 deficiency depends on Tk1 down-regulation and transcriptional compensation.* Human Molecular Genetics, 2011. **20**(1): p. 155-164.
114. Bartesaghi, S., et al., *Loss of thymidine kinase 2 alters neuronal bioenergetics and leads to neurodegeneration.* Human Molecular Genetics, 2010. **19**(9): p. 1669-1677.
115. Gotz, A., et al., *Thymidine kinase 2 defects can cause multi-tissue mtDNA depletion syndrome.* Brain, 2008. **131**: p. 2841-2850.